UNIVERSITÀ DEGLI STUDI DI VERONA

Department of Biotechnology
Graduate School of Natural Sciences and Engineering

Doctoral program in Biotechnology
XXXII Cycle/2016-2019

Title of the PhD Thesis

The tomato serotonin pathway: unravelling the puzzling biological roles of plant indolamines

S.S.D. BIO/01 - Botanica Generale

Coordinator: Prof. Matteo Ballottari

Tutor: Prof.Flavia Guzzo

Doctoral student: Stefano Negri

Stefano Negri

The tomato serotonin pathway:

unravelling the puzzling biological roles of plant indolamines

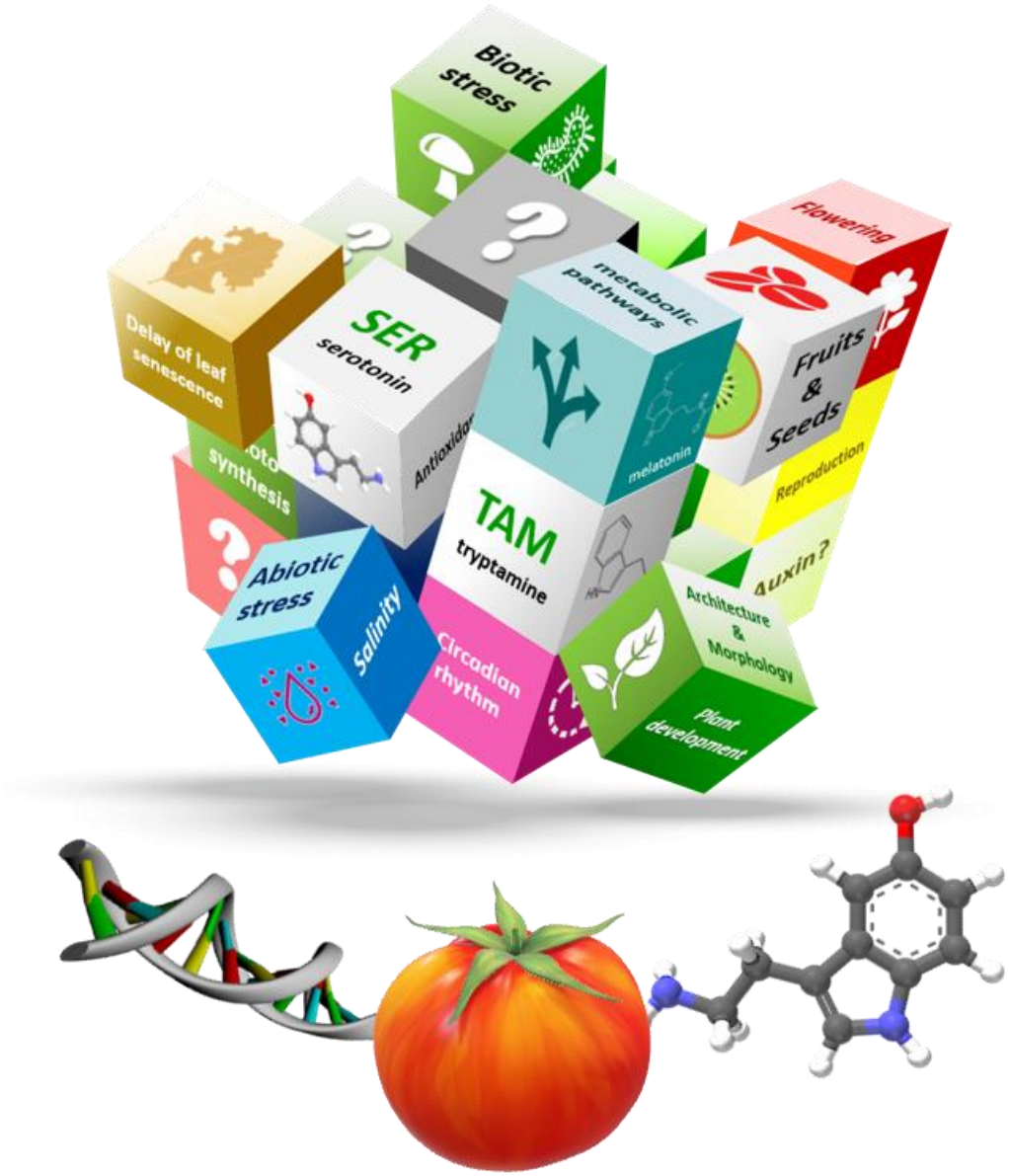

PhD Thesis

Verona, April 2020

Table of Contents

List of abbreviations

5-HT – 5-Hydroxytryptamine (serotonin)
5-MT – 5-Methoxytryptamine
5-OH-Trp – 5-Hydroxytryptophan
AADC – Aromatic L-Amino Acid Decarboxylase
AAO – Aldehyde oxidase
Abs – Absorbance
AMI – Amidase
ANOVA – Analysis of Variance
ASDAC – Acetylserotonin Deacetylase
ASMT – Acetylserotonin Methyltransferase
AU – Arbitrary Units
bp – Base pair
BPC – Base Peak Chromatogram
cDNA – Complementary DNA
c-PCR – Colony PCR
CDS – Coding Sequence
COMT – Caffeic acid-O-methyltransferase
CS – N-(Coumaroyl)-Serotonin
cv - Cultivar
CYP – Cytochrome P450 monooxygenase
db – Database
DPA – Days Post-Anthesis
dpi – Days Post-Infection
dw – Dry weight
EIC – Extracted Ion Chromatogram
ER – Endoplasmic Reticulum
ESI – ElectroSpray Ionization
for – Forward primer
FS – N-(Feruloyl)-Serotonin
fw – Fresh weight
gDNA – Genomic DNA
GFP – Green Fluorescent Protein
GoI – Gene of Interest
HIOMT – Hydroxyindole-O-methyltransferase
HPLC – High Performance Liquid Chromatography
HT – Hydroxycinnamoyl transferase
IAA – Indole-3-acetic acid
IAAld – Indole-3-acetaldehyde
IAM – Indole-3-acetamine
IAN – Indole-3-acetonitrile
IAOx – Indole-3-acetaldoxime
IPA – Indole-3-pyruvate
Kb - Kilobases
LB – Luria Bertani
LC – Liquid Chromatography
m/z – Mass over Charge ratio
MIAs – Monoterpenoid indole-alkaloids
MNE – Mean Normalized Expression
MS – Mass Spectrometry
NAS – N-acetylserotonin
NCBI – National Center for Biotechnology Information
NIT – Nitrilase
NMT – N-methyltryptamine
OD – Optical Density
OPLS-DA – Orthogonal Projections to Latent Structures Discriminant Analysis
PCA – Principal Component Analysis
PCR – Polymerase Chain Reaction
PLS-DA – Projections to Latent Structures Discriminant Analysis
PLP – Pyridoxal-5'-phosphate
QC – Quality Control
rev – Reverse primer
RT – Reverse Transcriptase
SGN – Sol Genomics Network
SHT – Serotonin N-hydroxycinnamoyl Transferase
Sl – Solanum lycopersicum
SM – Secondary Metabolites
SNAT – Serotonin N-acetyltransferase
SOC – Super Optimal broth with Catabolite repression
spp. – species plures
SSS - Strictosidine Synthase
T5H – Tryptamine-5-Hydroxylase
TAA – Tryptophan aminotransferase
TAM - Tryptamine
TDC – Tryptophan decarboxylase
TPH – Tryptophan-5-hydroxylase
Trp – Tryptophan
TyDC – Tyramine Decarboxylase
UPLC – Ultra Performance Liquid Chromatography
UTR – Untranslated Region
VAS – Pyridoxal Phosphate-dependent Aminotransferase
YUC – YUCCA Flavin-containing Monooxygenase

Summary

Tryptamine and serotonin are specialized metabolites belonging to the group of tryptophan-derived indolamines that have been demonstrated to be widespread among all the living kingdoms, in which evolution shaped very different distributions and functional versatility. First discovered in humans, these metabolites were later detected in plants in which, despite their wide occurrence in several plant families, the study of their biological roles has been largely neglected. Tryptamine, due to its central position as a precursor of many plant specialized metabolites, including serotonin, has long been considered a mere metabolic intermediate; on the other hand, the increasing awareness of the many medical issues of serotonin (e.g. neurotransmission and hormonal activity), triggered the botanical research towards the elucidation of its biosynthetic pathway and functions also in plants, leading to a huge number of experimental evidences that, yet often controversial, suggest its putative involvement in many different plant physiological processes (e.g. development, stress response and reproduction).

This PhD thesis proposed to shed a light on the biological roles of plant tryptamine and serotonin, with a particular focus on an aspect that has never been investigated in plants, i.e. the high level of accumulation of these metabolites within the reproductive organs, such as the fruit, observed in many edible species, which, given the high costs to plant metabolism, can be reasonably hypothesized to reflect an important plant physiological function. To fulfil this aim, this PhD project relied on the use of *Solanum lycopersicum*, a tryptamine and serotonin accumulator that is a model plant for fruit-bearing crops. The first step consisted in the genetic characterization of the tomato tryptamine and serotonin biosynthetic pathway: a three-member gene family and one single gene codifying for the enzymes of the 2-step pathway that leads to the production of serotonin from tryptophan via tryptamine (i.e. tryptophan decarboxylase, TDC and tryptamine-5-hydroxylase, T5H) were respectively identified and functionally characterized as *bona-fide SlTDCs* and *SlT5H*. The expression analysis of these genes and the investigation of tryptamine and serotonin distribution revealed organ and developmental-specific expression and accumulation patterns in tomato, confirming the complementary but not redundant activity of the three *SlTDC* genes in the plant and the presence of notable amounts of the two indolamines in the fruit, which accumulated with a characteristic trend during development and ripening. Moreover, it was revealed the fruit-specific nature of the *SlTDC1* gene that, as a preliminary point in the elucidation of the biological roles of plant tryptamine and serotonin, was targeted by a metabolic engineering approach in order to look for the effects resulting from altered levels of these metabolites on the plant phenotype. Transgenic plants overexpressing this gene resulted in deep modifications of plant metabolome presenting in one case altered morphology of younger leaves. This evidence, together with the observation along the main axis of

the wild type plant of complex expression and accumulation gradients of *SlTDCs*/*SlT5H* genes and related products, i.e. tryptamine and serotonin, leads to hypothesize the possible interference with the hormonal cross-talk.

On the other hand, *SlTDC1* knock-out fruits did non exhibit obvious phenotype but further characterization of their metabolome are needed to speculate on the biological roles of tryptamine and serotonin in this organ.

In summary, this work provided useful information and details to the biosynthesis, regulation and putative biological roles of plant indolamines in the model plant of tomato and highlighted the putative involvement of the actors of the plant serotonin pathway in important physiological functions, which deserve, thus, future deeper investigation.

Keywords

Tryptamine, serotonin, specialized metabolome, plant indolamines, *Solanum lycopersicum*, fruit biology, gene functional characterization, metabolite accumulation, metabolic engineering.

Graphical summary

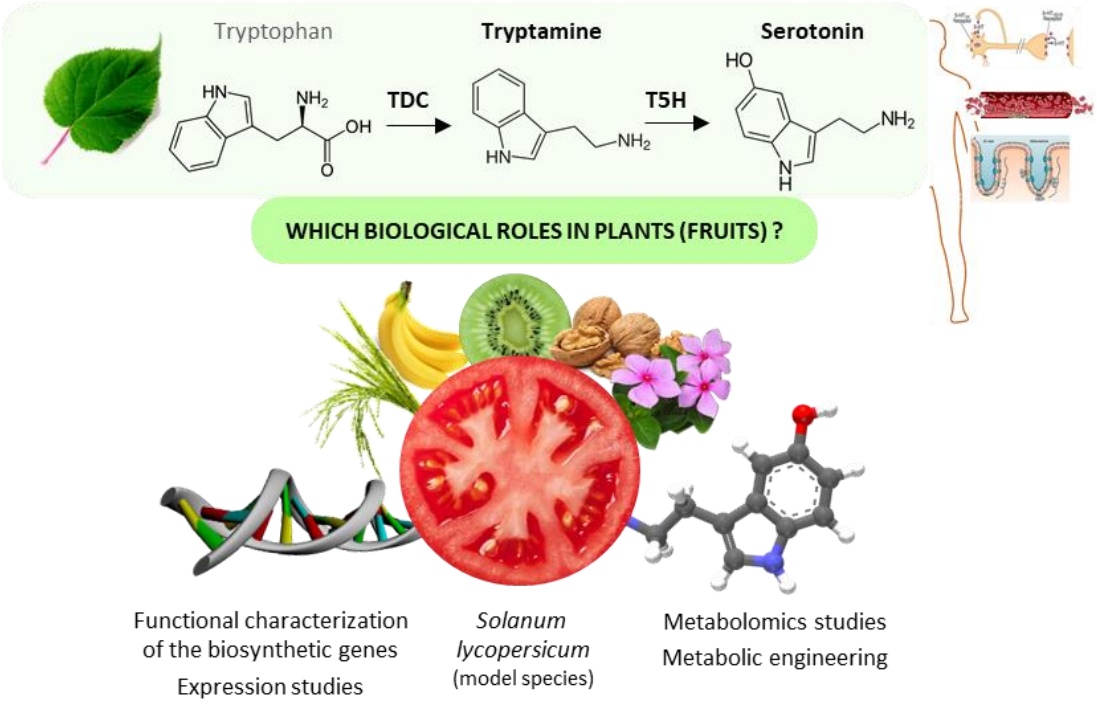

Aim and outline of the PhD thesis

The aim of this PhD thesis is to contribute to shed a light on the *in-planta* biological roles of tryptamine and serotonin, two indolamines that, being wides pread in all the living kingdoms, have always attracted the attention of many researches from different scientific backgrounds, but whose study in plants still presents many missing gaps. One of these issues concerns the extremely scarce information about the functions of these metabolites in the reproductive organs, such as the fruit, in which the highest levels of accumulation have been observed.

In order to investigate the biosynthetic mechanisms and the accumulation dynamics responsible for the biological functions of plant/fruit tryptamine and serotonin, this PhD work relied on *Solanum lycopersicum* L. (cv. Micro-Tom), the model species for fleshy fruit-bearing crops. Tomato presents several characteristics that perfectly suits the purposes of this thesis, such as a simple genome, the availability of open-access genomics and transcriptomics resources, consolidated methods that allow its stable genetic transformation and, most importantly, the fact that it is one of the major tryptamine and serotonin accumulator fruits described in the literature.

The work presented in this PhD thesis is organized as follows:

- **Chapter 1** - *General introduction*
  a preface on plant secondary metabolism and on the tools of modern *omics* sciences for its study introduces the following paragraph, in which the current state of the art on plant indolamines research is reviewed.

- **Chapter 2** - *Identification and functional characterization of Solanum lycopersicum genes involved in tryptamine and serotonin biosynthesis*
  Despite the occurrence of tryptamine indolamines is not a novelty in tomato, the biosynthetic pathway responsible for their production in this species has never been characterized and thus, its elucidation represents the focus of this chapter.

- **Chapter 3** - *Development of a gene expression and metabolite accumulation atlas for the preliminary investigation of the biological roles of the tomato serotonin pathway*
  The distribution of tryptamine and serotonin, as well as the evaluation of the expression patterns of their biosynthetic genes identified in the previous chapter, are here investigated in the whole Micro-Tom plant in order to provide preliminary information about their putative involvement in specific physiological functions.

- **Chapter 4** – *Preliminary results in the metabolic engineering and promoter study of the tomato fruit-specific SlTDC1 gene*

  Different metabolic engineering approaches are exploited in this chapter with the aim of: i) modifying the levels of tryptamine in the plant in order to look for visible effects resulting from the hyperaccumulation or depletion of plant indolamines; ii) studying the spatio-temporal promoter activity of a fruit-specific gene responsible for tryptamine accumulation in the berry.

- **Chapter 5** – *Concluding remarks*

  A final resume of the work and the results achieved in this PhD thesis are presented together with the discussion of the possible directions and objectives that this research might address in the future.

- **Appendice**

  A list of past and ongoing research products derived from this PhD project is here enclosed together with the description of the contributions from the co-authors involved.

To those marvellous, diverse interconnections that shape our world

… in science, as they do in people

Chapter 1

General introduction

Plant secondary metabolism: a long history of wise balance between costs and benefits

Nowhere in the living kingdoms do evolution, ecology, and human affairs meet as fascinatingly and intricately as in the biology of plant secondary metabolism, an engaging story that lasts from over 500 million of years.

During the mid-Palaeozoic era plants started their own colonization of the mainland and they had to cope, from the outset, with novel living conditions respect to those of their photosynthetic aquatic predecessors, i.e. exposure to direct sunlight, lack of mechanical anchoring and support, drought and varying temperature, higher oxidative damage, the constant presence of pathogens and, later during their evolution, of herbivores (Delwiche & Cooper, 2015). Given their sessile nature, the only ways plants had to face these new challenges passed through the adoption of several physiological innovations together with a deep evolution of a real "biochemical arsenal" known as secondary metabolome or, in more recent years, specialized metabolome, which allowed adaptation to biotic and abiotic stress and a more efficient interaction with other plant communities and the rest of the living kingdoms (Wink, 2003).

The term *metabolome* (Oliver et al., 1998) refers to all low molecular weight (< 1500 Da) metabolites, i.e. intermediates and end products of enzymatic reactions, which occur as part of biological pathways in living organisms. Secondary metabolites (SM) represent a typical trait of plants, bacteria and fungi and largely exceed in terms of number, structural diversity, functions and distribution primary metabolites (i.e. nucleosides, amino acids, sugars, organic acids). The latter are the actors of the central carbon metabolism, and constitute, together with their polymers, the construction bricks of each organism in which they drive growth, developmental and reproductive processes, being thus ubiquitous in all living systems (Wink, 2010). On the other hand, the presence and distribution of specific SM within the plant kingdom is neither ubiquitous nor does it follow a ruled phylogenetic pattern, although some classes of SM, which group compounds with close related structures, might be more characteristic of specific taxa (Weng et al., 2012).

For these reasons, at the very early beginning of modern science, plant SM were long considered as mere waste products of primary metabolism, but this theory was gradually confuted upon

experimental evidences witnessing their active involvement in chemical defence and environmental adaptation.

Nowadays, with the huge amount in the literature of reports that demonstrate the biological roles of many SM, the distinction between primary and secondary metabolism have become blurred and considering them as biochemical supporters of plant *fitness* (i.e. the ability of a species to survive and reproduce in an environment) is a legitimate and shared idea. Several classes of SM play in fact vital functions in plants ecophysiology: phenylpropanoids, for instance, are not only the precursors of lignin, which is essential to provide mechanical support in vascular plants, but also protect the tissues from the harmful UV-component of the sunlight and, by acting together with other SM and primary metabolites, are fundamentals to the reproductive phase in the interaction with insects and animals for pollen transport and seed dispersal, thus ensuring the survival of the species (Rensing, 2018). Moreover, some derivatives of pathways involved in SM production are important for plant development as they constitute phytohormones (e.g. cytokinins, auxins, gibberellins) or photosystem-related compounds such as the phytoene tail of chlorophyll and carotenoids (Böttger et al., 2018).

The maintenance of the plant biochemical machinery to produce, transport (H^+-ATPase, ABC transporters) or activate SM and to regulate their biosynthetic genes as well as the development of specialized store compartments (e.g. resin ducts, laticifers, trichomes) is energetically costly, demanding ATP or reduction equivalents. Since the resources allocated to these functions cannot be addressed to plant growth or progeny creation, careful consideration has to be given whether the synthesis of specialized metabolites occurs at a certain time or ontogenetic stage and in specific plant sites. The presence of many secondary metabolites is restricted to organs or tissues that are, for instance, potential targets of an attack or dedicated to specific interactions with other organisms (e.g. plant growth-promoting rhizobacteria). Depending on the grade and nature of stress occurrence in specific environments and the biosynthetic cost of a secondary metabolite, the plant "chooses" among its constitutive production, induced production or storage of a pro-active form of the substance that will be activated upon enzymatic or chemical intervention whenever required (Delgoda & Murray, 2017).

Based on a limited number of principal molecular scaffolds from primary metabolome, plants produce a wide variety of SM with very different biological functions. Metabolites deriving from photosynthesis, glycolysis and Krebs cycle (mainly acetyl coenzyme A, shikimic acid, mevalonic acid and 1-deoxy-xylulose 5-phosphate) are tapped off from these energy-generating processes by key enzymes which regulate the metabolic flux into the secondary metabolome to provide biosynthetic intermediates. Products of the carbon and nitrogen metabolism form the basic structures of the three major classes, the terpenoids (isoprenoids), alkaloids and phenylpropanoids, but also the polyketides, quinones and cyanogenic glycosides, whereas the alkyl-amides are derivatives of fatty acids and the glucosinolates derive from sulphur metabolism (Böttger et al., 2018). Plant secondary metabolome has been estimated to contain more than 200˙000 molecules (Yonekura-Sakakibara & Saito, 2009) but,

despite the huge structural diversity, the number of enzymes involved in their biosynthesis does not reflect such abundance. This is rather the consequence of two distinct strategies of plant SM biosynthetic enzymes: first, scaffold-generating transformations that utilize distinct but closely related substrates, and second, differential tailoring of a specific scaffold (Anarat-Cappillino & Sattely, 2014). Genes encoding secondary metabolism enzymes have often evolved from those of primary metabolism, with the most important mechanisms driving the SM biosynthesis diversification being whole-genome and local-gene duplication (Moore et al., 2014). Then, accumulated mutations in structural biosynthetic genes might give rise to loss of function, resulting in pseudogenes (Zhang et al., 2003) or, by determining different substrate preferences or catalytic activity, to neofunctionalization, resulting in a wide novel product range (Schwab 2003). This genetic variability might be an advantage in dealing with a changing and/or demanding environment and is shaped by evolution (Kliebenstein & Osbourn, 2012). In this way, there are many examples of convergent evolution in which different plants have independently acquired the ability to make compounds already present in other plant lineages or to produce different compounds covering same biological roles (Pichersky & Lewinsohn, 2011).

The study of plant secondary metabolites in the *omics* era

Despite deciphering the diversity, the evolution and the biological roles of plant SM, as well as exploiting their chemical potential for human applications, have always represented attractive topics to scientists, our knowledge about the mechanisms by which these are synthesized and the functions they cover in plants is far from being complete. At the beginning of the new millennium it was estimated that less than 10% of the plant secondary metabolome from identified species was revealed (Wink, 1999).

Nowadays, as with other branches of biological sciences, the study of plant metabolism has significantly improved since the quick advent of powerful technological tools for the functional characterization of genes and metabolites in all living beings. The mining and exploitation of the data obtained from classical (e.g. genomics, transcriptomics, proteomics and metabolomics) as well as new-born omics sciences restricted to specific topics (e.g. secretomics, regulomics, epigenomics, glycomics, phenomics) brought us into a new era of understanding of biological systems (Oksman-Caldentey et al., 2004; Isaacson & Rose, 2018; Yadav et al., 2018; Ran et al., 2019).

To date, the advancements in genomics led to the deposition of about 600 complete plant genome assemblies in public repositories (Kersey, 2019) providing important information that aided to overcome major challenges to the study of genes involved in secondary metabolism in plants, e.g. the complexity of the plant genome, large genome size and genetic redundancy (Nascimento & Fett-Neto; 2010). From the transcriptomics and regulomics perspective, the exponential increase of works relying on cutting-edge approaches, e.g. RNA-seq-based transcriptome profiling and gene co-expression analysis, provided remarkably useful insights in the identification of genes involved in the production of plant SM and of regulatory elements and factors (e.g transcription factors, epigenetic factors, cis-elements) driving their biosynthetic pathways (Rai et al., 2017; Ran et al., 2019).

Regarding metabolic channelling and SM compartmentalization, proteomics has identified and cleared the role of new metabolons, i.e. supramolecular enzymatic complexes allowing the direct passage of a product from one enzymatic reaction to a consecutive enzyme in a metabolic pathway (Møller, 2010). Such an organization is effective under many levels, allowing to maintain separate pools of intermediates, facilitating turnover or exclusion of labile or toxic intermediates, and likely preventing undesired crosstalk between different metabolic pathways (Martínez-Esteso et al., 2015; Dastmalchi & Facchini, 2016).

Finally, and most importantly to the study of SM, the burst in the development of high-resolution metabolomics techniques based on mass-spectrometry (MS), allowed to establish high accurate and sensitive untargeted methods for the separation and detection of SM present in trace amounts, e.g at the femtograms scale, in complex mixtures (Breitling et al., 2013; Wang et al., 2019$_a$). Since the spread

of ultra performance liquid chromatography-MS (UPLC-MS) platforms, which can produce about 20% more metabolite detection than that of high-performance liquid chromatography-MS (HPLC-MS; Nordstromet al., 2006) several technological innovations triggered plant SM research. The latest upgrade in plant metabolomics consists in high-spatial resolution MS imaging, which allows precise metabolite localizations in plant tissues and whose next challenge is to achieve single-cell resolution (Hansen & Lee, 2018).

State of the art concerning indolamines research in plants

Biosynthetic and functional versatility of tryptamine and serotonin in the living kingdoms

Tryptamine and serotonin (5-hydroxytryptamine) are secondary metabolites belonging to the class of indole-alkaloids and, more specifically, they are indolamines formed by an indole backbone with an ethylamine side chain, both deriving from the amino acid tryptophan. These compounds have been found to be widespread among all the living kingdoms, from bacteria to higher eukaryotes, in which evolution shaped very different distributions and functions, representing a fascinating yet still largely unravelled issue of biology (Mohammad-Zadeh et al., 2008; Ramakrishna et al., 2011).

The history of serotonin research has long dealt with issues related to animal biology, due to its numerous physiological roles (e.g. neurotransmission) which were gradually discovered in humans and vertebrates in the last century. Later, the discovery of serotonin in plants and bacteria and the evidence that serotonin, in some organisms, shared strict biosynthetic relations with tryptamine, which is also an animal indolamine yet working at a different functional level respect to serotonin, triggered the research on these indolamines also in the botanical and microbiological sciences.

In most organisms, including plants but not humans, tryptamine originates from the decarboxylation of L-tryptophan through the activity of Tryptophan Decarboxylase (TDC) enzymes (Kumar et al., 2016). These are a subgroup of Aromatic L-Amino Acid Decarboxylases (AADCs) that operate at the interface between primary and secondary metabolism by catalysing the production of biogenic amines able to enter secondary biosynthetic pathways (Facchini et al, 2000).

Although AADCs are present in many bacteria, only few of them rely on tryptophan, being tyrosine or L-DOPA (3,4-dihydroxyphenyl-L-alanine) the preferred substrates (Koyanagi et al., 2012). TDC activity has been earlier found in *Bacillus cereus* and *Micrococcus percitreus* (Perley & Stove, 1966; Nakazawa et al., 1974) and later also in dairy strains from the genera *Lactococcus* and *Leuconostoc* (De Llano; 1998) but, in general, it is not widely distributed within the prokaryotes.

Interestingly, in contrast with the general rarity of *TDC* genes and activity in this kingdom, TDCs are much more represented in the human microbiota bacteria, where the product, tryptamine, is a signal perceived by a specific receptor by the human guest and results in acceleration of whole-gut transit (Williams et al., 2014; Bhattarai et al., 2018). Beside the perception of food and microbiota tryptamine, tryptophan decarboxylation by AADC is probably exploited by humans to produce their own tryptamine into the brain in trace amounts, where it might work as minor neuromodulator rather than a neurotransmitter (Khan & Nawaz, 2016).

TDC activity was demonstrated also in some basidiomycetes fungi, such as *Psilocybe carpophores* in which tryptamine is canalised, as well as in some plant species, to downstream substituted

tryptamines, such as psilocybin, which is however an exclusive metabolite of psychedelic mushrooms (Fricke et al., 2017). The latter, by primarily acting on the serotonergic system as agonists of serotonin receptors in the brain (Greene, 2013), have long been used as recreational drugs and have inspired the synthesis of modern hallucinogenic and psychotropic compounds (Araújo et al., 2015).
Within plants the *TDC* genes, although not ubiquitous, are probably more recurring then in the other kingdoms. Plants use TDC enzymes in the first step of the pathway that ends up with serotonin and/or melatonin production (Ramakrishna et al., 2011; Arnao and Hernández-Ruiz, 2019; Figure 1.1).

Serotonin is above all famous for its role as major neurotransmitter in humans in which its ability to regulate mood, and to induce the onset of depression when depleted, earned itself the epithet of "hormone of happiness" (Loonen & Ivanova, 2016; Baixauli, 2017). Nonetheless, this indolamine, which is ubiquitous in the animal kingdom, is involved in other important physiological functions in our body acting, moreover, as a hormone and a mitogen being able to regulate, beyond mood, also sleep, appetite, blood pressure, platelet aggregation, vasoconstriction and intestinal peristalsis (Veenstra-VanderWeele et al. 2000; Mohammad-Zadeh et al., 2008; Olivier, 2015).
Although enteramine, namely serotonin, was first isolated in 1937 from gut enterochromaffin cells (Erspamer & Vialli; 1937) and only a few decades later in plants, evolutionarily, it is an ancient molecule, existing in bacteria, fungi and plants even before the appearance of animals (Azmitia 2001). Several authors suggest that serotonin was useful to microbial life forms in dealing with the oxygenated atmosphere developed by early photosynthetic organisms due to its strong antioxidant properties which could protect the cell from the threat of excessive oxidation (Azmitia, 2010; Manchester et al., 2015). In fungi serotonin occurs mainly in the fruiting body of edible and non-edible mushrooms, sometimes connected to the metabolism of psychotropic tryptamines, and in a few yeast species, in which, however, there is no exhaustive information about its functions (Sprenger et al., 1999; Muszyńska et al., 2011). Another interesting point in the evolutive comparison of serotonin across the kingdoms is that plants and animals do not share the same pathway for its biosynthesis (Figure 1.1). In animals this occurs from tryptophan via the formation, through tryptophan hydroxylase (TPH), of the 5-hydroxytryptophan (5-OH-Trp) intermediate, which is in turn decarboxylated by human AADC. Contrarily, in the plant pathway these reactions are reversed, so that tryptophan is firstly decarboxylated to form tryptamine by TDC which is then hydroxylated by tryptamine-5-hydroxylase (T5H) to give serotonin (Erland et al., 2015, 2016). Interestingly, the animal and plant pathways merge in the further downstream enzymatic steps that, from serotonin, lead to the production of melatonin (N-acetyl-5-methoxytryptamine), another indolamine that represents a major hormone in animals in which it regulates many relevant physiological functions including circadian rhythms linked to sleep-wake cycles (Brzezinski, 1997; Reiter et al., 2010; Drăgoi & Nicolae, 2018).

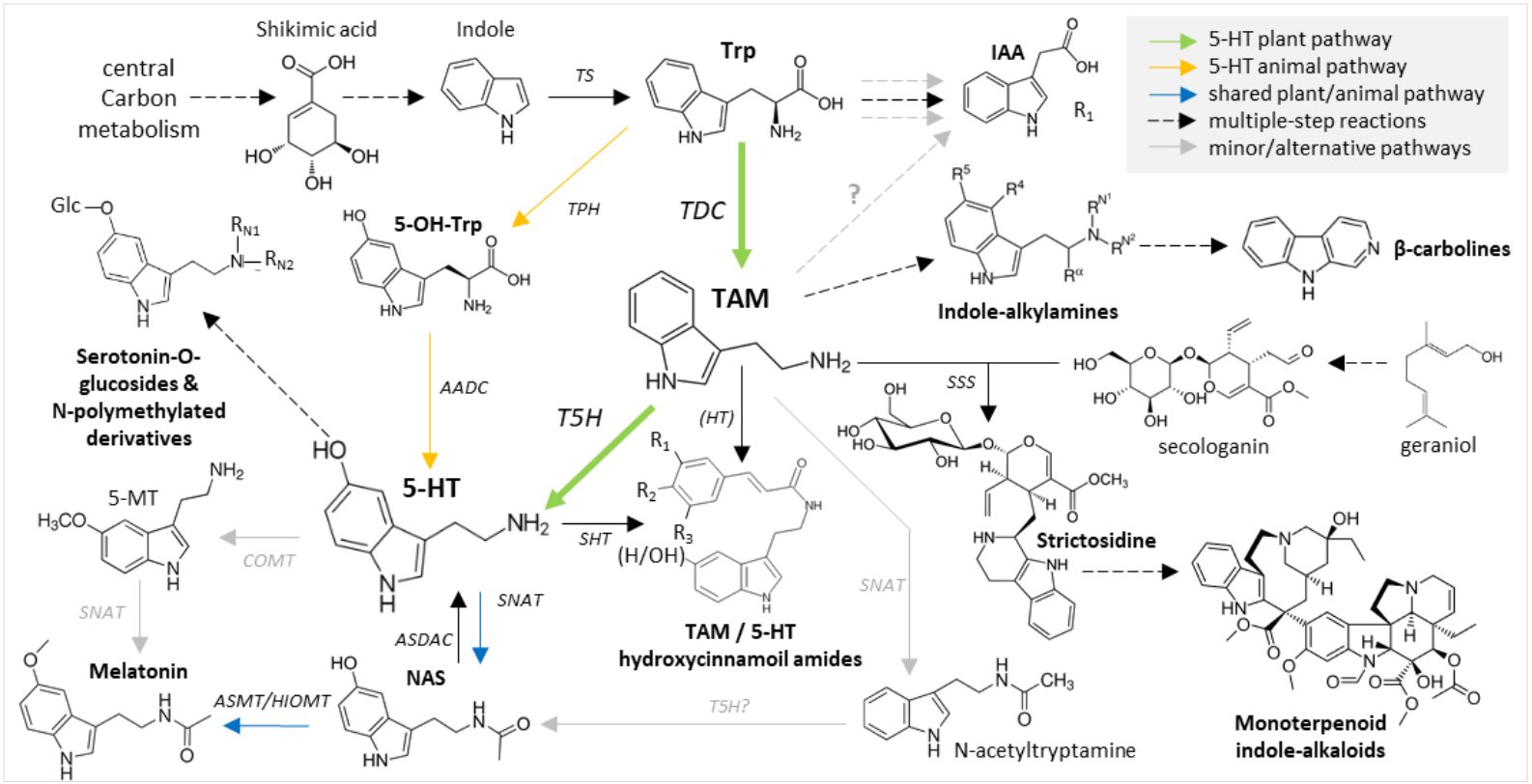

Figure 1.1 Known biosynthetic trails of plant tryptamine and serotonin and of their derivatives (modified from Erland et al., 2015-2016 and Arnao & Hernández-Ruiz, 2014). Enzymes legend: AADC, aromatic L-amino acid decarboxylase; ASDAC, acetylserotonin deacetylase; ASMT, acetylserotonin methyltransferase; COMT, caffeic acid-O-methyltransferase; HIOMT, hydroxyindole-O-methyltransferase; HT, hydroxycinnamoyl transferase; SHT, serotonin N-hydroxycinnamoyl transferase; SNAT, serotonin N-acetyltransferase; SSS, strictosidine synthase; SSS, strictosidine synthase; T5H, tryptamine-5-hydroxylase; TDC, tryptophan decarboxylase; TPH, tryptophan-5-hydroxylase; TS, tryptophan synthase. Metabolites legend: 5-HT, 5-hydroxytryptamine (serotonin); 5-OH-Trp, 5-hydroxytryptophan; 5-MT, 5-methoxytryptamine; IAA, indole-3-acetic acid; NAS, N-acetylserotonin; NMT, N-methyltryptamine; TAM, tryptamine; Trp, tryptophan.

It is exactly for the great interest in such attractive compound that, following its discovery in plants in the mid-1990s (Hattori et al., 1995; Dubbels et al., 1995), the study of both plant melatonin and serotonin received a great burst from functional, biotechnological, nutraceutical and evolutionary perspectives. However, discussing the many faces of melatonin metabolism and functions in plants, which have been extensively, and redundantly, reviewed in the last ten years, is out of the aims of this PhD thesis (Tan et al., 2011, 2014; Nawaz et al., 2016; Hardeland, 2016; Erland et al., 2015-2019; Arnao & Hernández-Ruiz, 2014, 2018, 2019).

Plant tryptamine: biochemical fates and suggested biological roles

The history of plant tryptamine and of its biosynthetic enzyme, TDC, is a lights and shadows novel: great emphasis has been given to both the occurrence of antitumoral indole-alkaloids and the functions of serotonin and melatonin in plants but, despite the key position of tryptamine in their biosynthetic pathways (Figure 1.1), its quantification and biological roles have been largely neglected so far. On the other hand, the willing of increasing the levels of the above-mentioned phytochemicals through metabolic engineering strategies had to pass first through the identification of plant *TDC* genes, with the earliest step being done in the Madagascar periwinkle (*Catharanthus roseus*; De Luca et al., 1989), together with deep *in-vitro* characterizations of their enzymatic properties (Facchini et al, 2000; Torrens-Spence, 2013). By homology-based research, various *TDC*s were in turn identified and functionally characterized, or just postulated to exist in different species on the basis of the presence of tryptamine-derived metabolites and orthologous TDC sequences, as recently reported in the genera *Malus* and *Citrus* (Lei et al., 2013; De Masi et al., 2017). A list of well characterized plant TDCs is presented in the Table 2.1 from chapter 2.

The biosynthesis of plant tryptamine occurs in the cytosol (Back et al., 2016) and, once produced, it meets the following possible fates:

i) to be canalised into the indolamines pathway;
ii) to give rise to a myriad of specialized metabolites possessing the indolyl moiety;
iii) to be an intermediate in one of the putative tryptophan-dependent alternative pathways for indole-3-acetic acid (IAA) biosynthesis;
iv) to be accumulated.

The precursor of plant indolamines

The large abundance of TDCs together with the evidence of tryptamine-5-hydroxilase activity in plants, first observed in 1971 in *Piptadenia peregrina* (Fellows & Bell), raised the hypothesis for the existence of a tryptamine pathway involved in serotonin production, thus overcoming the initial idea that plants rely, to this purpose, on the 5-OH-Trp intermediate as animals do (Stowe, 1959). While from one side the existence of *TPH* genes responsible for the production of 5-OH-Trp, which in some species might

reach high amounts fare exceeding those of tryptamine (Diamante et al., 2019), has still to be proven in plants, from the other side, the identification and characterization of the first plant *T5H* gene, codifying for an endoplasmic reticulum cytochrome P450 having high specificity towards tryptamine (Fujiwara et al., 2010), was achieved in 2007 while elucidating the genes involved in melatonin production in rice (Kang et al., 2007$_a$).

Tryptamine formation is an obliged step in the biosynthesis of melatonin, which is the final product of the indolamine pathway. This has been demonstrated to occur from tryptamine mainly through serotonin production which is in turn acetylated to N-acetylserotonin (NAS) and methylated by, respectively, chloroplastic Serotonin-N-AcetylTransferase (SNAT) and cytosolic N-AcetylSerotonin-O-MethylTransferase (ASMT) enzymes (Kang et al., 2013; Byeon et al., 2014$_a$; Back et al., 2016; Figure 1.1). However, minor alternative pathways leading to melatonin have also been hypothesized to exist in plants by converting tryptamine to an N-acetyltryptamine intermediate that is then hydroxylated to NAS (Arnao, M. B., & Hernández-Ruiz, 2014), thus by-passing the serotonin intermediate.

A bridge between essential and specialized metabolites

TDC represents one of the major entry points of carbon and nitrogen sources into plant secondary metabolism. The great interest towards tryptamine lies in the fact that a large number of tryptamine-derived specialized metabolites, that occur in various plant families and medicinal plants exploited worldwide in traditional medicine, possess a wide plethora of biological activities in animals, such as powerful antitumoral or psychotropic properties (Sakarkar & Deshmukh, 2011; Negi et al., 2014; Kousar et al., 2017); a great effort, driven by pharmaceutical purposes, triggered thus the research towards the understanding of tryptamine downstream biosynthetic pathways as well as the isolation, characterization, artificial scaffold-modification and metabolic engineering of the natural tryptamine-derived specialized metabolites for drug development (Kutchan et al., 1995; Pasquali et al., 2006; Mizoguchi et al., 2014). Despite their huge structural variety, the latter can be summarized into the following classes:

i) Monoterpenoid indole-alkaloids (MIAs): the first committed step to this pathway is represented by strictosidine synthase (SSS), which joins the indole structure of tryptamine to the geraniol-derived iridoid-monoterpene nucleus of secologanin. Further enzymatic reactions tailor indeed this scaffold with several functional groups originating the diversified architecture of thousands of MIAs, which are particularly represented in the families of Apocynaceae, Loganiaceae and Rubiaceae (O-Connor & Maresh, 2006). However, both the intricated biosynthetic networks of MIAs and their complex genetic regulation still put notable challenges to the desirable increase in the content of these compounds through biotechnological approaches, which besides targeting downstream structural and regulatory genes have to properly tune the activity of TDC to provide the tryptamine precursor to the pathway without falling into negative-feedback regulation drawbacks (Mujib et al., 2012; De Luca et al., 2014; Zhu et al., 2015).

ii) Indole-alkylamines: this is a fascinating group of substituted tryptamines in which botany meets neurobiology, comprising compounds that are often agonists of the 5-HT_{2A} animal receptors, thus acting as classical or serotonergic hallucinogens (Araújo et al. 2015). N,N-dimethyltryptamine is the most represented in plants, occurring in several species from tropical and subtropical regions. Recently, N-polymethylated tryptamines and their 5-hydroxylated forms, likely produced from tryptamine through several N-methylation/hydroxylation steps, have been identified at relatively high levels in the seeds and leaves of some *Citrus* species, including bergamot and, given their nicotine-like activity towards acetylcholine receptor, they have been hypothesized to be involved in plant defence (Servillo et al., 2012-2013).

iii) β-carbolines (harman alkaloids): this group of tricyclic indole-pyridines derives from the cyclization of tryptamine-alkylamines via the formation of tetrahydro-β-carbolines intermediates. They have been shown to possess good antimicrobial properties and might represent a chemical weapon towards bacteria and fungi (Olmedo et al., 2017). Coffee is the major dietary source of harman and norharman, two neuroactive β-carbolines that might be implicated to the health benefits related to its consumption (Rodrigues & Casal, 2019; Piechowska et al., 2019). The simultaneous association of N-dimethyltryptamine from *Psychotria viridis* and the β-carboline harmine from *Banisteriopsis caapi* in the brew known as the "vine of the souls", namely Ayahuasca, is responsible for the hallucinogenic effects, following its oral consumption, exploited in sacred rituals by shamans from South America (McKenna et al.; 1998). By acting as a reversible inhibitor of monoamine oxidase-A (MAO-A), harmine prevents the catabolism of the tryptamines in the gut, thus allowing them to be active orally and prolonging their psychedelic effects in the brain (Dos Santos et al., 2017).

iv) Tryptamine amides: this group comprises tryptamines that are N-conjugated to the phenylpropanoid moieties of different hydroxycinnamates, mainly p-coumaric and ferulic acids, and, to a lesser extent, to long-chain unsaturated fatty acids deriving from isovalerate (Kumar et al., 2018). N-p-(coumaroyl)-tryptamine and N-(feruloyl)-tryptamine were identified in maize kernels, green onion, safflower seeds and in various species from the Lauraceae, Piperaceae and Rutaceae families as well as in the *Croton* genus (Ehman, 1974; Novello et al., 2016; Lee et al., 2017). They are supposed to be involved in defence as well as in plant reproduction, given their antimicrobial in vitro properties and the fact that genes for plant hydroxycinnamoyl-amines biosynthesis are induced by wounding or expressed during flower development (Facchini et al., 2002; Lee et al., 2017).

The IAA-alternative pathway hypothesis

Due to its high structural similarity to the hormone IAA and given the common precursor, i.e. tryptophan, the occurrence of tryptamine in plants has long been associated to auxin-like activities or to the biosynthesis/catabolism of auxin phytohormones (Fawcett, 1961). Since then, evidences of the

existence of multiple tryptophan-dependent auxin biosynthetic pathways in plants have been reported (Di et al., 2016). The genetic complexity behind the mechanisms of auxin biosynthesis long prevented researchers from uncover a clear biosynthetic route, till the elucidation of the *Arabidopsis thaliana* TAA/YUC (Tryptophan Aminotransferase of Arabidopsis/YUCCA) pathway, which converts tryptophan to auxin in two consecutive steps: first tryptophan is deaminated to produce indole-3-pyruvate (IPA) by the TAA family of aminotransferases, then IPA is oxidized and decarboxylated to IAA by the YUC family of flavin-containing monooxygenases (Zhao et al., 2018). The other supposed tryptophan-dependent pathways would involve, respectively, indole-3-acetaldoxime (IAOx), indole-3-acetamine (IAM) and tryptamine (Kasahara et al., 2016; Figure 1.2). However, the IAOx pathway is not completely elucidated while the IAM pathway, despite this compound is present in various plant species, is rather characteristic of rhizosphere bacteria (Mohite, 2013). The existence of a tryptamine pathway has been suggested only following the observation of deuterium incorporation into tryptamine and indole-3-acetaldehyde (IAAld) upon treatment with deuterated tryptophan in the roots of pea (Quittenden et al., 2009). However, given the fact that various transgenic plants overexpressing *TDC* did not show increased IAA levels (Songstad et al., 1990; Facchini et al., 2000), this enzyme is rather likely dedicated to channelling tryptophan into the indolamines or indole-alkaloids. Some authors hypothesized, thus, a YUC-dependent decarboxylation of tryptophan to tryptamine that could occur in a few species, and within specific organs, but in general this idea is not well supported (Tivendale et al., 2014; Di et al., 2016).

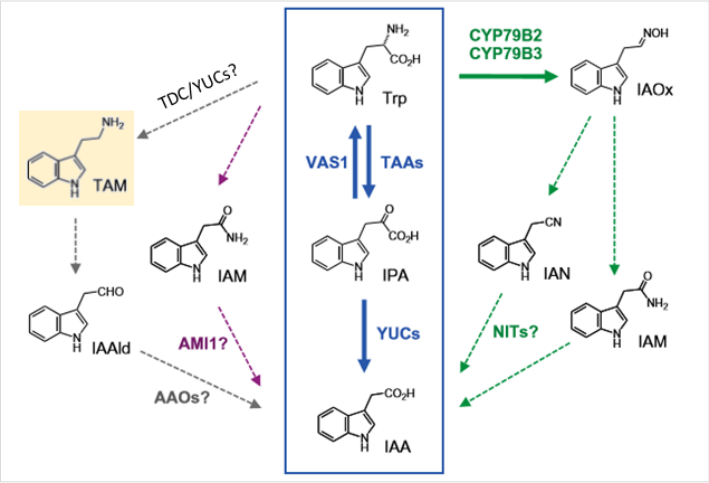

Figure 1.2 Hypothesized and confirmed (blue box) tryptophan-dependent pathways for IAA biosynthesis in plants (modified from Kasahara et al., 2016). Enzymes legend: AMI, amidase; AAO, aldehyde oxidase; CYP, cytochrome P450 monooxygenase; NIT, nitrilase; TAA, tryptophan aminotransferase; TDC, tryptophan decarboxylase; VAS, pyridoxal phosphate-dependent aminotransferase; YUC, YUCCA flavin-containing monooxygenase. Metabolites legend: IAA, indole-3-acetic acid; IAAld, indole-3-acetaldehyde; IAM, indole-3-acetamine; IAN, indole-3-acetonitrile; IAOx, indole-3-acetaldoxime; IPA, indole-3-pyruvate; TAM, tryptamine; Trp, tryptophan.

Accumulation issues

When not addressing the tryptophan plant resources into the huge variety of specialized metabolites just described, tryptamine can be accumulated at almost bulk amounts in the reproductive organs of some plant species (as also serotonin does). Tryptamine quantification in plant organs have long been a poorly represented topic in the literature of plant indolamines, being not comparable to the amount of data available for serotonin and melatonin. However, since the early reports following tryptamine isolation from leaves and flowers of *Acacia* spp. (White, 1944), it was evident that some edible fruits were able to accumulate moderate to high levels of this metabolite (Udenfriend et al., 1959; West, 1959). More recently, by relying on modern metabolomics techniques, various authors determined the tryptamine content of many other plant edible species including fruits and vegetables commonly consumed in our diet (Ly et al., 2008; Islam et al., 2016; Badria et al., 2002; Table 1.1). Green kiwifruit is the greatest tryptamine accumulator so far, with high levels being observed also in tomato, plums, peach, bell pepper and okra fruits. Interestingly, Commisso and co-workers (2019) recently carried out an investigation of the levels of this indolamine throughout berry development in the berry of green kiwifruit and observed that this indolamine peaks in the early stages following anthesis, then gradually decreasing till the end of the developmental process. The fact that tryptamine accumulates more frequently in fruits rather than within the vegetative parts of the plant, e.g. leaves and underground organs, suggests that this compound might be involved in some unknown yet important function during the early plant reproductive phases. In addition, to enhance this hypothesis, huge amounts of tryptamine were also detected in the pollen of *Prosopis juliflora* (Al-Soqeer et al., 2017).

Despite these evidences, a deeper investigation of the putative involvement of tryptamine in functions related to fruit metabolisms or plant reproduction still represents an unexplored issue of plant biology.

Biological roles of tryptamine suggested by transgenic studies targeting plant TDC genes

The intricated yet pharmaceutically-attractive networks of tryptamine-derived indole-alkaloids has always puzzled the mind of scientists trying to manipulate the amounts of specialized metabolites by triggering TDC activity through constitutive overexpression. While overlooking the effects of this approach *in vitro,* which represent, however, a great amount of data in the literature (Pan et al., 2016_a), the most important hints to suppose a biological role for accumulated tryptamine come from *in-planta* experiments. In most cases, *TDC* overexpression resulting in high levels of tryptamine was not reflected into any phenotype alteration, as observed in transgenic tobacco, even though a 260-times accumulation was measured (Songstad et al., 1990). Nonetheless, while evaluating the response of both transgenic tobacco and poplar ectopically expressing *TDC* to herbivory threats, it was observed a significative suppression of the growth of insect pests feeding on tryptamine hyperaccumulating leaves (Gill et al, 2003; 2006).

Species	common name	organ	µg/g	References
Fleshy fruits				
Abelmoschus esculentus	okra	berry	2.93 ± 0.51	Islam et al.,2016
Actinidia deliciosa	green kiwifruit	berry	6.38 ± 1.24	Islam et al.,2016
		early developing berry	16.0 ± 0.5	Commisso et al. 2019
		developed berry	4.8 ± 0.4	Commisso et al. 2019
Ananas comosus	pineapple	infructescence	1.24 ± 0.15	Islam et al.,2016
			6.2 (dw)	Badria, 2002
Capsicum annuum	bell pepper	berry	2.29 ± 0.16	Islam et al.,2016
	hot pepper	berry	16.2 ± 1.6 (dw)	Ly et al., 2008
	paprika	berry	6.8 ± 0.5 (dw)	Ly et al., 2008
Citrullus lanatus	watermelon	fleshy fruit	0.74 ± 0.16	Islam et al.,2016
Citrus paradisi	grapefruit	berry	1.33 ± 1.0	Islam et al.,2016
Citrus x sinensis	orange	berry	0.1	Udenfriend et al., 1959
Citrus unshiu	mikan	berry	1.61 ± 0.42	Islam et al.,2016
Cucumis sativus	cucumber	berry	0.44 ± 0.02	Islam et al.,2016
			12.8 (dw)	Badria, 2002
Diospyros kaki	kaki	berry	0.08 ± 0.01	Islam et al.,2016
Fragaria x ananassa	strawberry	false fruit	57.0 ± 5.9 (dw)	Ly et al., 2008
Fragaria magna	strawberry	false fruit	4.7 (dw)	Badria, 2002
Malus domestica	apple	false fruit	5.3 (dw)	Badria, 2002
Malus pumila	apple	false fruit	0.84 ± 0.40	Islam et al.,2016
Momordica charantia	bitter melon	berry	0.37 ± 0.04	Islam et al.,2016
Musa acuminata	banana	berry	0.96 ± 0.28	Islam et al.,2016
Musa ensete	banana	berry	11.3 (dw)	Badria, 2002
Persea americana	avocado	berry	1.70 ± 0.52	Islam et al.,2016
Prunus avium	cherry	stone fruit	0.67 ± 0.06	Islam et al.,2016
Prunus persica	peach	stone fruit	3.75 ± 0.35	Islam et al.,2016
Prunus subg. *Prunus*	plum	stone fruit	2 - 5	Udenfriend et al., 1959
Punica granatum	pomegranate	berry	4.7 (dw)	Badria, 2002
Pyrus nivalis Jacq.	pears	fleshy fruit	0.32 ± 0.08	Islam et al.,2016
Solanum melongena	eggplant	berry	0.22 ± 0.06	Islam et al.,2016
			0.5 - 3.0	Udenfriend et al., 1959
Solanum lycopersycum	tomato	berry	4	Udenfriend et al., 1959
			1 - 4.8	West, 1959
			147.1 ± 7.5 (dw)	Ly et al., 2008
			2.8 ± 0.1	Islam et al.,2016
	cherry tomato	berry	140.3 ± 3.7 (dw)	Ly et al., 2008
			3.1 ± 0.1	Islam et al.,2016
Solanum pimpinellifolium	currant tomato	berry	9.3 (dw)	Badria, 2002
Grains				
Hordeum vulgare	barley	seed	25.4 (dw)	Badria, 2002
Oryza sativa (var. japonica)	rice	seed	40.1 (dw)	Badria, 2002
Zea mays	corn	kernel	61.7 (dw)	Badria, 2002
Flowers and flowers vegetables				
Brassica oleracea (var.italica)	broccoli	inflorescence	0.94 ± 0.54	Islam et al.,2016
Brassica oleracea (var. botrytis)	cauliflower	inflorescence	1.46 ± 0.14	Islam et al.,2016
			4.69 - 9.00 (dw)	Diamante et al., 2019
			19.8 (dw)	Badria, 2002
Prosopis juliflora	mesquite	pollen	3.4 - 143.3 (dw)	Al-Soqeer et al., 2017
Leafy vegetables				
Brassica oleracea (var capitata)	cabbage	leaves	0.62 ± 0.20	Islam et al.,2016
			7.7 (dw)	Badria, 2002
Brassica rapa (ssp.pekinensis)	chinese cabbage	leaves	0.71 ± 0.21	Islam et al.,2016
			14.5 ± 4.9 (dw)	Ly et al., 2008
Brassica rapa	turnip		21.2 (dw)	Badria, 2002
Cichorium intybus	chicory	leaves	0.8 ± 0.2 (dw)	Ly et al., 2008
Lactuca sativa	lettuce	leaves	0.35 ± 0.08	Islam et al.,2016
Lactuca serriola	lettuce	leaves	24.5 ± 2.4 (dw)	Ly et al., 2008

Spinacia oleracea	spinach	leaves	0.26 ± 0.09 6.5 ± 1.6 (dw)	Islam et al.,2016 Ly et al., 2008
Shoot and root vegetables				
Allium cepa	onion	bulb	1.33 ± 0.06 9.2 (dw)	Islam et al.,2016 Badria, 2002
Allium fistulosum	green onion	bulb	3.9 ± 2.8 (dw)	Ly et al., 2008
Allium sativum	garlic	bulb	13.9 (dw)	Badria, 2002
Allium wakegi	spring onion	bulb	2.77 ± 1.07	Islam et al.,2016
Asparagus officinalis	asparagus	shoots	0.79 ± 0.41	Islam et al.,2016
Daucus carota	carrot	root	1.72 ± 0.63 15.8 (dw)	Islam et al.,2016 Badria, 2002
Ipomoea batatas	sweet potato	tuber	0.63 ± 0.34	Islam et al.,2016
Raphanus sativus	daikon radish	root	0.20 ± 0.05	Islam et al.,2016
Raphanus sativus	radish	root	14.7 (dw)	Badria, 2002
Solanum tuberosum	potato	tuber	0.40 ± 0.24	Islam et al.,2016
Zingiber officinale	ginger	rhizome	0.11 ± 0.04	Islam et al.,2016

Table 1.1 Tryptamine content expressed as µg/g of fresh weight (when not specified as dw, dry weight) in various plant species available in the literature so far.

These evidences, together with the earlier observation that tryptamine administration through artificial assay was able to negatively affect the reproduction rate in *Drosophila melanogaster* (Thomas et al., 1998) by likely depression-induced anti-oviposition effects, strongly suggest that tryptamine might act as an anti-attractant or antifeedant in plants. On the other hand, it has been demonstrated, more recently, a strong induction of *TDC* expression and serotonin accumulation in response to insect feeding in the green foxtail millet (*Setaria viridis*; Dangol et al., 2019), thus rising the doubt about which one of the two indolamines is really involved in protective effects. This recalls the need of further experimental investigations in order to discriminate between tryptamine and serotonin functions in plants.

Further details concerning the tuning of tryptamine levels, and related effects in the plant, by metabolic engineering approaches are reviewed in the introductive paragraph of Chapter 4.

Plant serotonin: a multi-active compound involved in the regulation of many plant processes

Serotonin was discovered in plants in the mid-1950s in the stinging hairs of cowhage (*Mucuna pruriens*; Bowden et al., 1954) and nettle (*Urtica dioica*; Collier & Chesher; 1956). Since then, serotonin has been found in more than 70 plant families so far, in which it is produced in wide range amounts (Erland et al., 2019). The main pathway for serotonin biosynthesis in plants occurs as previously described through the tryptamine intermediate, even though an early report from Fellows & Bell (1970) proposed the 5-OH-Trp intermediate route in the seeds of *Griffonia simplicifolia*, but this and other eventual pathways, whose existence might not be excluded, should be rather considered a rarity in plants.

Catabolic trails of serotonin in plants

One of the possible and most characterized biochemical fates of serotonin is to be addressed to melatonin biosynthesis. The elucidated pathway that passes through the synthesis of the NAS intermediate, as previously described, seems to be the main way by which plants produce melatonin in standard growing conditions, however, some authors proposed the existence of an alternative pathway which may occur when plants produce large amounts of serotonin, as during senescence (Kang et al., 2009$_a$). The latter involves the activity of a Caffeic acid-O-MethylTransferase (COMT) able to convert serotonin to 5-methoxy-tryptamine (5-MT), which is in turn acetylated by SNAT (Figure 1.1; Back et al., 2016; Choi et al., 2017). The melatonin and serotonin pathways seems to be under strict enzymatic control and the at least three-order of magnitude difference in the accumulation between this two indolamines in favour of serotonin (μ/g versus ng/g of fresh weight) commonly observed in plants, is reasonably ascribable to the very low catalytic efficiencies demonstrated for SNAT and ASMT melatonin biosynthetic enzymes respect to the serotonin TDC and T5H ones (Back et al., 2016).

Serotonin is addressed in many plants towards the production of phenylpropanoid derivatives through conjugation with hydroxycinnamoyl-CoA thioesters from the pool of phenylpropanoids mediated by Serotonin-N-Hydroxycinnamoyl Transferases (SHT; Park et al. 2008). The two most common serotonin amides N-(feruloyl)-serotonin (FS) and N-(p)-coumaroyl-serotonin (CS) were first identified in safflower seeds (*Carthamus tinctorius*; Sakamura et al., 1978) and, while generally present in traces in plants, they accumulate at huge levels in the seeds of various Asteraceae species (225-740 μg/g of fresh weight; Kang et al.,2009$_a$). Although still little information is available on this group of metabolites, they are likely involved in response to wounding and pathogen attack (Macoy et al.,2015). While the pool of hydroxycinnamates comprises also caffeic, sinapic and cinnamic acid, there is no exhaustive information about the distribution of the corresponding serotonin amides in plants. Since both FS and CS seem to exhibit strong antioxidant, anti-inflammatory and anti-atherogenic activities, thus making them valuable for both nutritional and pharmacological use in humans, the production of the minor represented serotonin amides constitute rather the target of recent biotechnological applications (Kang et al., 2009$_a$; Takahashi & Miyazawa, 2012; Lee et al., 2017).

Other downstream biosynthetic pathways starting from serotonin, which might share the same methyltransferases active towards tryptamine (Servillo et al., 2013), end up in indole-alkylamines such as the 5-hydroxy-N,N-dimethyl-tryptamine (bufotenine) which is accumulated in the seeds of plants from *Piptadenia* genus (Ramakrishna et al., 2011). Interestingly, it has been recently demonstrated the presence of serotonin 5-O-β-glucoside in green coffee beans and of its N-polymethylated forms in plants from the *Citrus* genus (Servillo et al., 2015,2016) but their function has not been elucidated.

Serotonin accumulation within the reproductive organs: an unsolved issue

Serotonin has been found to be present in all parts of plants, occurring in a very wide range of amounts (Erland et al., 2016). Nonetheless, some reproductive organs of species from different families are able to accumulate serotonin up to a few hundreds of µg/g of fresh weight, such as the seeds of the Juglandaceae, far exceeding the quantities of this indolamine commonly present in plants (300-400 µg/g of fresh weight). In *Juglans regia* it has been proposed that serotonin accumulation in the seed might represent a nitrogen sink in which storing free toxic ammonium that originates from the proteolysis and deamination of amino acids during fruit abscisic period, thus reflecting a protective activity towards the embryo (Grosse et al., 1982).

Moreover, as reported for tryptamine, also several common fruits, such as banana, kiwifruit, pineapple, tomato, grape and the berry of coffee present moderate to high levels of serotonin, often showing peculiar accumulation trends throughout fruit development and ripening and within different parts of the pericarp which do not follow a general accumulation rule in this organ (Rayne, 2010; Ramakrishna et al., 2012;). However, despite serotonin accumulation, which often occurs at very crucial stages of fruit formation and development such as the fruit set - or even during flower bud maturation as in *Datura metel* - and the switch towards the ripening phase, strongly suggests an involvement of this indolamine in the reproductive phase, there are no study to date that have investigated the functions *in loco* of fruit serotonin (Murch et al., 2009-2010; Hano et al., 2017; Commisso et al., 2019).

An eclectic metabolite: the functional yet puzzling versatility of plant serotonin

Similar to the multiple roles played in animal and prokaryotic cells (Roschina, 2010), serotonin has also been suggested to be involved in several physiological functions in plants, which have been deeply reviewed in the last ten years (Arnao & Hernández-Ruiz, 2014, 2018-2019; Erland et al., 2015-2019; Ravishankar & Ramakrishna, 2016; Figure 1.3). A brief summary of the resumes proposed by the authors is here described:

i) Biotic stress response: this role of serotonin is the most represented in the literature. To date the best demonstration of serotonin involvement in pant protection comes from experiments on rice, in whose leaves, the accumulation of serotonin is related to the protection against *Bipolaris oryzae* and the oxidative damages following hypersensitive response induced by biotic stress. Moreover, huge deposit of serotonin in the plant cell wall at the pathogen lesion site seems to play an important role in control of the strength of the cell wall for the mechanical barrier against fungal pathogens (Ishihara et al., 2008; Hayashi et al., 2016). Serotonin production has been demonstrated to occur under different threatening conditions, coupled mostly to a burst in *TDC* expression rather than *T5H* but, however, its strict connection to melatonin or its channelling to other derivatives such as the hydroxycinnamoyls amides, whose levels where not always assessed in metabolic engineering approaches intervening on the pathway, makes it difficult to attribute the

putative protective effects against pathogens or herbivores to a molecule rather than another. In fact, it is rising the idea that these activities might be more efficiently exerted by the serotonin amides derivatives, that, thanks to their phenylpropanoid-deriving structure show high antioxidant and ROS-scavenging abilities.

ii) Abiotic stress response: serotonin might be involved in mitigating the effect of salt stress, a hypothesis that arose following the observation of root serotonin accumulation in sunflower plants threatened with high saline growing conditions and the fact that growth of sunflower seedlings in the presence of saline stress was improved following serotonin supplementations (Mukherjee et al., 2014). This protective mechanism of serotonin might likely occur through regulation of the osmotic pressure in plants in the presence of salt stress by modulating ion mobility into the roots.

iii) Plant growth regulator: serotonin is, moreover, suggested to be a mediator of plant development by having cytokinin-like activities. It was demonstrated to be able to increase both size and number of shoots when supplied to *in-vitro* cultured plants of *Hypericum perforatum* and *Mimosa pudica* (Murch et al., 2001; Giridhar & Ravishankar; 2009). This evidence together with other morphogenic-like effects of serotonin are thought to be modulated by calcium signalling (Ramakrishn et al., 2016) as well as by the cross-talk with melatonin, which rather shows auxin-like activities *in vitro*. Some authors thus proposed that a serotonin/melatonin balance might mime the cytkonins/auxin relationships in orchestrating plant morphogenesis and architecture at minor levels. Nonetheless, examining the role of a metabolite *in-vitro* without respecting a real physiological context may often lead to confounding results. Early reports suggesting auxin-like effects were confuted upon the evidence of serotonin by acting as an auxin-inhibitor, likely by interfering with the auxin receptors given their high structural similarity (Pelagio-Flores et al., 2011; Arnao & Hernández-Ruiz 2019).

iv) Many other roles of serotonin are currently under debate and they include its involvement in the photosynthesis process, bud dormancy and flowering, gamete compatibility, regulation of plant rhythms and signalling (Erland et al., 2019).

Chapter 2

Identification and functional characterization of *Solanum lycopersicum* genes involved in tryptamine and serotonin biosynthesis

Abstract

Several species from different plant families are able to synthesize serotonin from L-tryptophan by subsequent decarboxylation and hydroxylation reactions involving the activity of tryptophan decarboxylase (TDC), which produces the tryptamine intermediate, and tryptamine-5-hydroxylase (T5H) enzymes (Kang et al., 2007_b). This represents the sole pathway for the biosynthesis of these indolamines characterized so far in plants (Erland et al., 2016). The existence of *TDC* and *T5H* genes can be reasonably postulated also in *Solanum lycopersicum* (Hano et al., 2017) given the high amounts of serotonin reported in its fruit. Plant TDCs as well as other pyridoxal-5'-phosphate dependent aromatic L-amino acid decarboxylases (AADCs), e.g. tyrosine decarboxylases (TyDCs), have been extensively investigated from a genetic and enzymatic perspective whereas only a plant T5H from *Oryza sativa* was characterized so far (Fujiwara et al., 2010). This information was therefore exploited to fulfil the first aim of this chapter, i.e. the homology-based identification of putative tomato genes involved in tryptamine and serotonin production. This allowed to select four TDCs and one T5H candidate proteins in tomato whose putative activities were indeed tested in an *in vivo* functional assay by coupling their transient heterologous expression in an indolamine non-accumulator species (*Nicotiana benthamiana)* to an untargeted metabolomics approach. The application of such robust functional characterization method resulted in the observation of tryptamine and serotonin production, revealed by HPLC-ESI-MS, in plants transiently expressing the coding sequences of three *SlTDCs* and *SlT5H*, thus proving the existence of a 3-member *TDC* gene family and one *T5H* gene in *Solanum lycopersicum*.

Introduction

Since the discovery, in the fifties, that some plant species were able to produce tryptamine and serotonin and the evidence, a few decades later, of their role as metabolic intermediates in the production of high-valuable secondary metabolites (e.g. antitumoral indole-alkaloids and melatonin), these two indolamines have puzzled the mind of botanists and biotechnologists, which put great interest in the elucidation of the mechanisms responsible for their biosynthesis. The identification in 1989 (De Luca et al.) of a tryptophan decarboxylase (TDC) gene from *Catharanthus roseus*, codifying for a pyridoxal-5'-phosphate (PLP) dependent enzyme able to catalyse the biosynthesis of tryptamine through L-tryptophan decarboxylation, paved the way for the characterization of tryptamine and serotonin biosynthetic pathway in plants. Since that moment, indeed, several other plant *TDC* genes were in turn functionally identified in the plant kingdom by homology-based research and then expressed as heterologous proteins in *Escherichia coli* for the characterization of their enzymatic features. Depending on the species, only single gene or small *TDC* gene families have been identified so far. The well characterized *TDC* of *C. roseus* is a single copy gene (Goddijn et al., 1994) whereas in other species such as *Camptotheca acuminata* and *Capsicum annuum* 2-member *TDC* gene families were identified (López-Meyer & Nessler, 1997; Park et al., 2009) arriving up to 3 members in *Oryza sativa* (Kang et al., 2007[b]).

Plant TDCs, operate at the interface in between primary and secondary metabolism, being thus crucial enzymes for the synthesis of a wide range of secondary metabolites, as well as other evolutionary-close plant aromatic L-amino acids decarboxylases (AADCs), e.g. tyrosine decarboxylases (TyDCs), with whom they share extensive structural similarities, often showing more than 50% identity (Facchini et al., 2000). For these reasons it is not straightforward to distinguish TyDCs from TDC-like proteins by relying only on sequence homology findings. Functional characterization of many plant TDCs and TyDCs mostly demonstrated exclusive preference towards either indole or phenol structures, respectively, but not both together (Sáenz-de-Miera & Ayala, 2004), with the former being active towards tryptophan (and in a less extent to its indolic analogous, e.g. 5-hydroxytryptophan) and the latter accepting both tyrosine and L-Dopa (3,4-dyhidroxy-L-phenylalanine). Nonetheless, Kumar (2016), as recently revising the evolutionary trails of plant PLP-dependent decarboxylases and the challenges associated to their functional annotation, underlined that the elucidation of their preferred substrate specificities as well as their catalytic activities do not always match the expectations. Torrens-Spence et al. (2013), for instance, recently re-annotated a characterized TyDC from parsley (Kawalleck et al., 1993) as aromatic aldehyde synthase (AAS), a catalytic promiscuous enzyme able to carry out both decarboxylation and subsequent oxidative deamination reactions. The same researchers in 2014 further investigated this aspect and found out that even the replacement of single

amino acid residues in the sequence of annotated enzymes determinates the switch between decarboxylation and decarboxylation/oxidative deamination as demonstrated also for a mutagenized version of *C. roseus* TDC. These evidences further complicated the formerly complex scenario of plant AADCs but provided very useful information to be considered while looking for new putative decarboxylase enzymes.

Plant tryptophan decarboxylases act in coordination with other enzymes from secondary metabolism in a species-specific way. In some species, for instance, the product of the decarboxylation reaction, tryptamine, is subsequently hydroxylated on 5' carbon of its indole-backbone to give serotonin. The enzyme responsible for this conversion, a ER-membrane cytochrome P450 annotated as tryptamine 5'-hydroxylase (T5H), has been characterized only in rice so far, thanks to *sl*-mutants presenting strong tryptamine accumulation linked to a deficit in the expression of this gene (Kang et al., 2007_a, Fujiwara et al., 2010). The subsequent intervention of TDC followed by T5H represents, at present, the only way by which plants produce tryptamine and, in turn, serotonin (Ramakrishna et al., 2011; Erland et al., 2016).

Evidences of tryptophan decarboxylase activity in *Solanum lycopersicum* date back to the seventies, when Gibson and colleagues purified and described the enzymatic properties of a TDC from the tomato cultivar Big Boy (1972). Since then, scientist have not made any more efforts to investigate the molecular mechanisms involved in the biosynthesis of tryptamine and serotonin, until the onset of recent interest towards the valuable and attractive melatonin. After that, two putative TDCs and one T5H were postulated to exist in tomato based on protein sequence analysis (Hano et al., 2017), arriving to propose up to five putative *TDC* genes (Pang et al., 2018), without ever characterizing them from a functional perspective.

In this first chapter it is therefore reported the identification of putative tomato TDC and T5H proteins (carried out prior to the publication of the former reports) and their functional characterization performed by transient expression in a heterologous plant system associated to untargeted metabolomics, a powerful approach to link gene expression to enzymatic activity and metabolite production.

Materials and methods

Bioinformatics

The amino acid sequences of functionally characterized plant TDC and T5H proteins (Table 2.1) were downloaded from NCBI (https://www.ncbi.nlm.nih.gov; accession numbers reported in Table 2.1) and used as query in the Blastp tool of the Sol Genomics Network database (https://solgenomics.net/tools/blast/) to launch an homology research towards the deposited *Solanum lycopersicum* proteins (ITAG release 3.20).

All alignments of nucleotide and amino acid sequences were carried out by Clustal Omega (ClustalO, https://www.ebi.ac.uk/Tools/msa/clustalo/) using default parameters. *In-silico* translation of gene CDS was performed through the translation tool from the ExPASy Bioinformatics resource portal (https://web.expasy.org/translate/).

To profile the sequence divergence-based evolutionary position of putative tomato SlTDCs towards other plant aromatic L-amino acid decarboxylases (AADCs; Table 2.1), all the protein sequences were submitted to an online tool for phylogeny analysis (http://www.phylogeny.fr/phylogeny.cgi). MUSCLE alignement was used and a phylogenetic tree was generated by applying the neighbour-joining method and bootstrap analysis (100 iterations); tree rendering was obtained through TreeDyn.

Microbiology

The following culture media were used for bacteria culture and manipulation:

- LB (Luria-Bertani) broth pH 7.5 (Bertani, 1951); for solid medium preparation, 15g/L of bacteriological agar were added.
- SOC (Super Optimal broth with Catabolite repression) pH 7.0: it is obtained by the addition of 20 mM glucose and 10 mM $MgCl_2$ to SOB (Hanahan, 1983);

One Shot® Top10 Chemically Competent *Escherichia coli* (Thermo Fisher, Waltham, USA) is a kanamycin-resistant strain that was used for plasmids propagation in molecular cloning. Strain features and heat-shock transformation procedure are reported in the product information provided by the manufacturer. Rifampicin-resistant *Agrobacterium tumefaciens* EHA105 (Hellens et al., 2000) was used as high-virulence strain to deliver the T-DNA from assembled plant expressions vectors into the *Nicotiana benthamiana* host in transient expression experiments. Bacterial transformation of EHA105 electro-competent cells stored in glycerol 10% (v/v) was carried out by the electroporation method (Wise et al., 2006).

	Annotation	Organism	NCBI code	Reference
Functionally characterized TDCs	AcTDC	*Actinidia chinensis*	Achn173261[1]	Commisso et al., 2019
	AdTDC	*Actinidia deliciosa*	QBK17431	Commisso et al., 2019
	CacTDC1	*Camptotheca acuminata*	AAB39708	López-Meyer et al., 1997
	CacTDC2		AAB39709	
	CrTDC	*Catharanthus roseus*	AAA33109	De Luca et al., 1989
	MsTDC	*Mytragina speciosa*	AEQ01059	Charoonratana et al., 2013
	OpuTDC	*Ophiorrhiza pumila*	BAC41515	Yamazaki et al., 2003
	OsTDC1	*Oryza sativa*	BAG91223	Kang et al.,2007_b
	OsTDC2		BAG95977	
	OsTDC3		NP_001060969	Byeon et al.,2014_b
	RvTDC	*Rauvolfia verticillata*	ADL28270	Liu et al., 2012
	PepTDC1	*Capsicum annuum*	NP_001312016	Park et al., 2009
	PepTDC2		ACN62126	
	WcTDC	*Withania coagulans*	not deposited	Jadaun et al., 2017
Putative TDCs	ArTDC	*Actaea racemosa*	CCO62221	Spiering et al., 2011
	HvTDC	*Hordeum vulgare*	BAD11769	Li et al., 2016
	OprTDC	*Ophiorrhiza prostrata*	ABU40982	De Masi et al., 2017
	PlTDC	*Paeonia lactiflora*	ART46241	Zhao et al., 2018
	TeTDC	*Tabernaemontana elegans*	AEY82396	De Masi et al., 2017
	TuTDC1	*Triticum urartu*	EMS51668	Li et al., 2016
	TuTDC2		EMS68447	
	VmTDC	*Vinca minor*	AEY82397	De Masi et al., 2017
Functionally characterized TyDCs	AtTyDC	*Arabidopsis thaliana*	Q8RY79	Lehmann & Pollmann, 2009
	BdTyDC1	*Brachypodium distachyon*	KQK09947	Noda et al., 2015
	BdTyDC2		KQK09953	
	CreTyDC	*Citrus reshni*	ACX29991	Bartley et al., 2010
	OsTyDC	*Oryza sativa*	BAG89694	Park et al., 2012
	PcTyDC2	*Petroselinum crispum*	AAA33860	Kawalleck et al., 1993
	PcTyDC4		AAA33863	
	PsTyDC1	*Papaver somniferum*	AAA62346	Facchini & De Luca, 1995
	PsTyDC2		AAA62347	
	RcTyDC	*Rhodiola crenulata*	AFN89854	Lan et al., 2013
	RsTyDC	*Rhodiola sachalinensi*	ABF06560	Zhang et al., 2011

Table 2.1 List of all plant AADCs used in SlTDCs computational analysis and respective NCBI accession numbers ([1]accession number from Kiwifruit Genome Database; http://bioinfo.bti.cornell.edu/cgi-bin/kiwi/home.cgi).

Molecular biology

Plant material and growth conditions

Plants of *Solanum lycopersicum* cultivar Micro-Tom were grown in a greenhouse at 21-30°C and 32-50% RH with a 15h/9h light/dark photoperiod. Plants subjected to these environmental conditions were able to bloom in about 1 month from the germination and to complete the life cycle in about 4 months.

Wild-type plants of *Nicotiana benthamiana* were grown in a growth chamber at 25°C with 13h/11h light/dark photoperiod till they reached about 30 cm in height and then used for transient expression experiments.

Molecular cloning of the genes of interest into the pK7WG2 plant expression vector

The genetic source for *SlTDCs* and *SlT5H* cloning consisted of leaves, flowers at the anthesis and mature-green fruits (20 days post anthesis) sampled from 2-months old Micro-Tom plants.

Total RNA was extracted from 100 mg frozen plant material using the Spectrum Plant Total RNA Kit (Sigma-Aldrich, St. Louis, USA), followed by removal of genomic DNA through Ambion® TURBO DNA-free™ DNase Treatment and Removal Reagents (Life Technologies, Carlsbad, USA). SuperScriptIII Reverse Transcriptase (Thermo Fisher) was used to synthesize cDNA from 2 µg total RNA from each sample by oligo(dT) transcription initiation. Specific primers designed on the coding sequences (CDS) and 5'-3' untranslated regions (UTRs) of the genes of interest (GoI) were used to amplify total cDNA by high-fidelity KAPA HiFi-DNA polymerase (Kapa Biosystems, Wilmington, USA) in PCR reaction. All primers and PCR cycles used in this step are reported in Table 2.2 and 2.3 respectively. Following nucleic acid electrophoresis, the PCR products were checked on agarose gel and purified through the Wizard® SV Gel and PCR Clean-UP System (Promega, Madison, USA). The purified amplicons were thus ligated into the pENTR™/D-TOPO™ (Thermo Fisher, Figure 2.1) vector by mean of the pENTR/D-TOPO cloning kit (Thermo Fisher) using a 2:1 insert/vector ratio. The directional cloning into this entry vector was allowed by a 5'-CACC-3' tag inserted at the beginning of the forward primer that couples to the sticky 5'-GTGG-3' overhang present in the vector. One Shot TOP10®*E.coli* cells were transformed by heat-shock with the pENTR.GoI and plated on LB solid medium containing 100 mg/L kanamycin. To verify the success of the ligation reaction, 15 colonies were screened by colony-PCR (c-PCR) and positive colonies were grown to amplify the plasmids. These were extracted from the bacterial suspensions through the E.Z.N.A.® Plasmid Mini Kit I (Omega Bio-Tek, Norcross, USA) and re-checked by PCR. Several aliquots for each plasmid sample were air-dried together with M13 primers pairing to cloning site side-regions and sent to BMR Genomics laboratories (Padova, Italy) for sequencing analysis. Evaluation of sequencing data was performed by visualization in Chromas (https://technelysium.com.au/wp/chromas/). Once confirmed the exactness of the inserts, these were cloned from the pENTR entry vector into the pK7WG2 destination vector (Karimi et al., 2002;

Figure 2.1), which is suitable for in-plant expression, by Gateway™ LR Clonase™ II Enzyme mix (Thermo Fisher). The pK7WG2.GoI reaction products were transformed into One Shot TOP10®*E.coli* and c-PCR-verified colonies growing on LB solid medium with 75 mg/L spectinomycin served to propagate and extract the plasmids as described above. Following PCR check, these were used to transform *Agrobacterium tumefaciens* EHA105 electrocompetent cells by electroporation. Colonies growing on solid LB medium containing 50 mg/L rifampicin and 100 mg/L spectinomycin were tested through c-PCR to assess the presence of GoI in the T-DNA.

Proper assembly of pENTR.GoI and pK7WG2.GoI vectors were checked throughout the whole cloning procedure by performing PCRs and c-PCRs with GoTaq® DNA Polymerase (Promega) which shared the same PCR conditions reported in table 2.3, except for the denaturation steps (94°C, 5 min for initial denaturation; 94°C, 30 sec for cycle denaturation).

Primer name	**5'-3' sequence**
SlTDC1-for	CACCATGGGAAGCCTTGATTCCA
SlTDC1-rev	TTAAAACACACTTTTTCTCAGCAAAC
SlTDC2-for	CACCAACTACCAATACTTAGTCTTTCCCCC
SlTDC2-rev	AACAATCACAAATGCCTATACATAAAT
SlTDC3-for	CACCATGGAAGGGGGATTGAAG
SlTDC3-rev	TTAACATTTACTTAACAATGTAGCAGC
SlTDC4-for	CACCGCTAACCATTTATTTTTCTTTCAAGG
SlTDC4-rev	TTGATTTAGCAGGGCATTGG
SlT5H-for	CACCATGGAAGCATCAATTCTACAGCTAC
SlT5H-rev	TTACAACTTGTTGATGGTTGGAAC
M13-for*	GTAAAACGACGGCCAG
M13-rev*	CAGGAAACAGCTATGAC

Table 2.2 List of all primers used in molecular cloning of Sl*TDCs* and *T5H* genes (*primers used for DNA sequencing of the cloned inserts from pENTR.GoI)

		SlTDC1	***SlTDC2***	***SlTDC3***
	SGN ID	*Solyc07g054860*	*Solyc07g054280*	*Solyc09g064430*
	Source	cDNA	cDNA	cDNA
	Primer design	5'-CDS/3'-CDS	5'-UTR/3'-UTR	5'-UTR/3'-CDS
	Lenght (bp)[1]	1519	1705	1468
	Initial denaturation	95°C, 3 min		
x 5	Denaturation	98°C, 20 sec		
	Annealing	60°C, 45 sec	59°C, 45 sec	60°C, 45 sec
	Extension	72°C, 1 min 32 sec	72°C, 1 min 42 sec	72°C, 1 min 28 sec
x 25	Denaturation	98°C, 20 sec		
	Annealing	65°C, 45 sec	61°C, 45 sec	64°C, 45 sec
	Extension	72°C, 1 min 32 sec	72°C, 1 min 42 sec	72°C, 1 min 28 sec
	Final extension	72°C, 5 min		

		SlTDC4	
	SGN ID	*Solyc03g044120*	
	Source	cDNA	genomic DNA
	Primer design	5'-UTR/3'-UTR	5'-UTR/3'-UTR
	Lenght (bp)[1]	1525	1577
	Initial denaturation	95°C, 3 min	
x 5	Denaturation	98°C, 20 sec	
	Annealing	54°C, 45 sec	54°C, 60 sec
	Extension	72°C, 1 min 32 sec	72°C, 1 min 32 sec
x 25	Denaturation	98°C, 20 sec	
	Annealing	59°C, 45 sec	59°C, 60 sec
	Extension	72°C, 1 min 32 sec	72°C, 1 min 32 sec
	Final extension	72°C, 5 min	

		SlT5H
	SGN ID	*Solyc09g014900*
	Source	Synthesize
	Primer design	5'-CDS/3'-CDS
	Lenght (bp)[1]	1492
	Initial denaturation	95°C, 3 min
x 30	Denaturation	98°C, 20 sec
	Annealing	56°C, 45 sec
	Extension	72°C, 1 min 30 sec
	Final Extension	72°C, 5 min

Table 2.3 Cloning details and PCR conditions for the amplification of *SlTDCs* and *SlT5H* from Micro-Tom total cDNA by Kapa HiFi-DNA Polymerase. [1]The presence of the 5'-CACC-3' tag in the forward primer confers 4 extra nucleotides to the cloned sequences. SGN, Sol Genomics Network database.

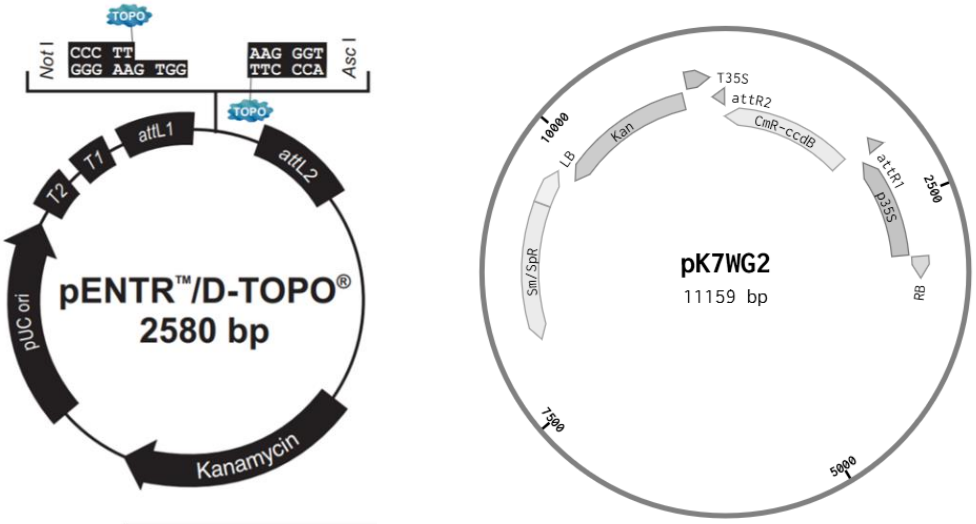

Figure 2.1 Gateway™ entry (left, image provided by Thermo Fisher) and destination (right) vectors used in the molecular cloning of putative *TDC* and *T5H* genes (attL, attR: sites required for the LR recombination reaction; Sm/SpR: streptomycin/spectinomycin resistance; ccdB: negative selection gene; LB and RB: Left and right T-DNA borders; p35S and T35S: promoter and terminator regions from Cawliflower Mosaic Virus; Kan: kanamycin resistance).

Agroinfiltration of Nicotiana benthamiana leaves for transient heterologous expression experiments

A. tumefaciens EHA105 colonies carrying the pK7WG2.GoI were grown in LB liquid medium containing 50 mg/L rifampicin and 100 mg/L spectinomycin for two days, pelleted by centrifugation at 4000 *g* and resuspended in infiltration buffer to an OD_{600} of 0.9-1.0. Following 2 hours-incubation at room temperature, bacterial suspensions were syringe-infiltrated into the leaves of 5-weeks old plants of *N. benthamiana* as described by Gecchele et al. (2015). Three plants for each construct to be tested were used and three leaves were infected for each plant. Each plant represented a biological replicate and starting from the third day after the infiltration (dpi) leaves were daily sampled till the fifth dpi (Figure 2.2). Sampled leaves were independently homogenized in liquid nitrogen and the powder stored at -80°C. A bacterial suspension carrying the pK7WG2.*GFP* was used to infect plants that represented the negative control group. Other two bacterial suspensions carrying pK7WG2.*AcTDC* and pK7WG2.*OsT5H* were used to generate positive control plants when testing *SlTDCs* and *SlT5H* functions respectively.

pK7WG2.GFP and pK7WG2.AcTDC were previously assembled in this laboratory and transferred into *A. tumefaciens* EHA105. *OsT5H* CDS (Genbank accession: AK071599) was synthesized *de-novo* (including the 5'-CACC-3' tag) through the GeneArt Gene Synthesis service (Thermo Fisher) and was directly cloned into the pENTR™/D-TOPO™. The rest of the cloning procedure to produce pK7WG2.*OsT5H* and *A. tumefaciens* EHA105 transformation were carried out as described in the previous paragraph.

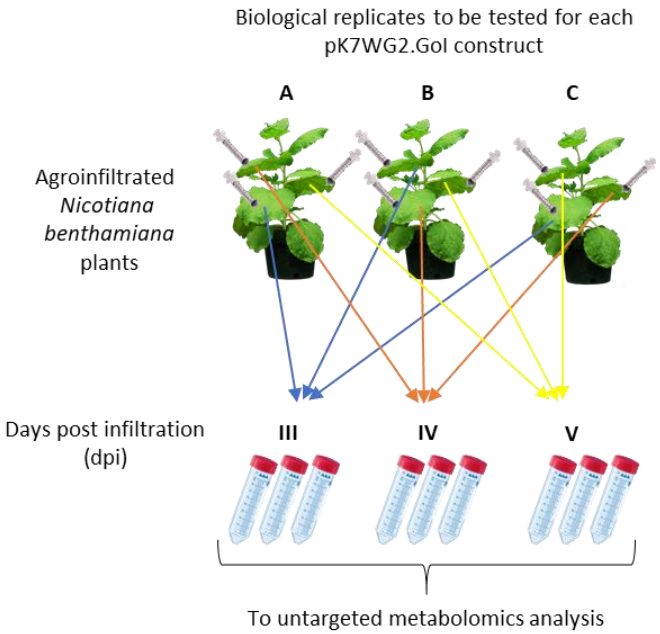

Figure 2.2 Schematic representation of the experimental design for *SlTDCs* and *SlT5H* in-vivo functional assays in *Nicotiana benthamiana* plants (GoI, gene of interest).

Metabolomics

Metabolites extraction from Nicotiana benthamiana leaves and untargeted metabolomics analysis

To extract polar and medium polar metabolites from leaf material, laves were collected, nitrogen-frozen and powdered. 150 mg of powder was dissolved in 10 volumes (1.5 mL) of LC-MS grade methanol (Honeywell, Seezle, Germany). The mixture was vortexed for 30 sec and sonicated at 40 kHz in a Sonica Ultrasonic Cleaner ultrasonic bath (Soltec, Milano, Italy) in ice for 10 min before two rounds of centrifugation at 14,000× g and 4°C for 15 min each. For the untargeted metabolomics analysis, the methanol extracts were diluted 1:2 (v/v) with LC-MS grade water (Honeywell), passed through Minisart RC4 filters with 0.2 µm pores (Sartorius, Göttingen, Germany) and 20 µL was injected into the HPLC device.

The instrument consisted of a Gold 508 Autosampler (Beckman Coulter) set at 4 °C in front of a Gold 127 HPLC system (Beckman Coulter) equipped with a reversed phase (RP) Alltima HP C18 column (150 × 2.1 mm, particle size 3 µm) protected with a C18 guard column (7.5 × 2.1 mm, particle size 5 µm). The flow rate was set at 0.2 mL/min and the two mobile phases consisted of 0.05% formic acid in water (A) and 0.05% formic acid in acetonitrile (B). The initial conditions were 98% A and 2% B, and the following elution profile was applied: 0–2 min, 2% B; 2–10 min, 2–10% B; 10–20 min, 10–60% B; 20–30 min, 60–90% B; 30–35 min, 90% B; 35–36 min, 2–90% B (initial conditions). Subsequently, the

system was equilibrated in 98% A and the method was complete in 60 min. Sample analysis were randomized. The metabolites were detected using an Esquire 6000 ion trap mass spectrometer (Bruker Daltonics GmbH, Bremen, Germany) performing a scan range of 50–1500 *m/z* with a target mass of 200 *m/z*. MS/MS and MS3 mass spectra were recorded in positive and negative ionization modes in the range 50–1500 *m/z* with a fragmentation amplitude of 1 V. The ESI source operated in alternate positive mode, exploiting nitrogen as both nebulizing (50 psi and 350 °C) and drying gas (10 L/min). The vacuum pressure was 1.4 × 10−8 bar. Additional parameters were: capillary source 4500 V; end plate offset –500 V; skimmer: 40 V; cap exit 121 V. The chromatographic data files were recorded with the Esquire v5.2 Control software (Bruker Daltonik GmbH, Bremen, Germany).

LC-MS data processing and multivariate statistical analysis

The generated HPLC-ESI-MS chromatograms were processed using Data Analysis v3.2 software (Bruker Daltonik GmbH). The presence of tryptamine and serotonin signals in the chromatograms was assessed by checking three key parameters, i.e. *m/z*, retention time and MS/MS fragmentation pattern, with those recorded in the laboratory *in-house* library for the respective commercial authentic standards (Sigma-Aldrich). Specifically, to measure the relative levels of the two indolamines, peak areas relative to the signals of tryptamine and serotonin diagnostic ions (144 *m/z* and 160 *m/z* respectively) were manually extrapolated from the chromatograms. These ions corresponded to the highest in-source generated fragments detected in positive ionization mode. The presence of low-abundant molecular ions was also considered (161 *m/z* for tryptamine and 177 *m/z* for serotonin).

LC-MS chromatograms were converted to netCDf files for peak alignment and area extraction using MZmine (http://mzmine.sourceforge.net/). The resulting feature quantification matrix was analysed using SIMCA v.13.0 (Umetrix AB, Umea, Sweden). Pareto scaling was applied to all analytical methods. Unsupervised PCA was used to identify the major clusters defined by the samples prior to supervised partial least squares discriminant analysis (PLS-DA) and orthogonal partial least squares discriminant analysis (OPLS-DA and O2PLS-DA). PLS-DA models were validated using a permutation test (200 permutations) and the corresponding OPLS-DA/O2PLS-DA models were cross-validated by analysis of variance (ANOVA) with a threshold of $p < 0.01$.

Results

Identification and functional characterization of the tomato *TDC* gene family

Identification and computational analysis of putative tomato TDC proteins

Tryptophan decarboxylase (TDC) is the enzyme responsible for the decarboxylation of tryptophan leading to the production of tryptamine and it represents the entry step for the synthesis of serotonin and other indole-alkaloids in plants.

In order to search for TDC candidate genes of *Solanum lycopersycum* a homology research approach was adopted by relying on functionally characterized plant TDCs already described in literature. The amino acid sequences of TDCs from *Catharanthus roseus* (CrTDC) *Oryza sativa* (OsTDCs) and *Capsicum annuum* (PepTDCs) were thus used as queries in the Blastp tool of the Sol Genomics Network (SGN) database, https://solgenomics.net). Each research gave as output a list of several tomato gene products (the CrTDC output is reported in Figure 2.3 that were selected as putative TDC candidates when the following parameters were met: high identity percentage (>50%) and good coverage of the protein used as a query, the presence of the protein candidates in the output list of all the launched queries and a high alignment score.

SubjectId	id%	Aln	evalue	Score	Description
Solyc07g054860.1	69.40	338/487	0.0	747	Aromatic amino acid decarboxylase IPR010977 Aromatic-L-amino-acid decarboxylase Length = 504
Solyc07g054280.1	67.56	327/484	0.0	726	Aromatic amino acid decarboxylase IPR010977 Aromatic-L-amino-acid decarboxylase Length = 504
Solyc09g064430.2	53.75	251/467	0.0	561	Aromatic L-amino acid decarboxylase IPR010977 Aromatic-L-amino-acid decarboxylase Length = 468
Solyc03g044120.1	52.97	250/472	0.0	538	Aromatic L-amino acid decarboxylase IPR010977 Aromatic-L-amino-acid decarboxylase Length = 476
Solyc03g045020.2	57.62	208/361	e-151	439	Aromatic L-amino acid decarboxylase IPR010977 Aromatic-L-amino-acid decarboxylase Length = 374
Solyc03g045010.1	49.06	52/106	5e-29	111	Aromatic L-amino acid decarboxylase IPR015422 Pyridoxal phosphate-dependent transferase, major region, subdomain 2 Length = 106
Solyc08g068630.2	23.48	77/328	3e-12	68.2	Decarboxylase family protein IPR002129 Pyridoxal phosphate-dependent decarboxylase Length = 476

Figure 2.3 Blastp homology research output showing the list of matched *Solanum lycopersicum* proteins from the SGN database towards the *Catharantus roseus* functionally characterized TDC (CrTDC).

Four tomato proteins ranging in size from 476 to 504 amino acid residues and sharing more than 50% sequence identity towards the above-mentioned characterized plant TDCs were selected as putative *Solanum lycopersicum* TDC candidates and annotated as SlTDC1 (Solyc07g054860), SlTDC2 (Solyc07g054280), SlTDC3 (Solyc09g064430) and SlTDC4 (Solyc03g044120). Table 2.4 summarizes the identity percentages of the four putative tomato TDCs towards the above-mentioned characterized plant TDCs used in the homology research. The highest identity percentages were observed for SlTDC1, SlTDC2 and SlTDC3 towards the two TDCs from pepper (PepTDC1 and PepTDC2), another species from the family Solanaceae. SlTDC1 and SlTDC2 had also high identity percentage towards CrTDC as well as SlTDC3 towards OsTDC2. On the other hand, SlTDC4 presented the lowest identity percentages towards all plant TDCs.

	CrTDC	OsTDC1	OsTDC2	OsTDC3	PepTDC1	PepTDC2
SlTDC1	68.33	51.94	52.67	53.03	86.23	55.37
SlTDC2	66.07	50.68	53.50	50.97	84.00	55.37
SlTDC3	50.98	45.26	68.76	46.15	52.95	90.41
SlTDC4	51.32	43.83	50.63	43.34	53.52	51.80

Table 2.4 Identity percentages among the amino acid sequences of the four identified *Solanum lycopersicum* TDC candidate proteins (SlTDC) and the functionally characterized TDCs of *Catharantus roseus* (CrTDC), *Oryza sativa* (OsTDC) and *Capsicum annuum* (PepTDC).

Comparative analysis of the sole putative tomato candidates revealed that SlTDC1 and SlTDC2 differed only by 10.71% among them whereas SlTDC3 and SlTDC4 displayed the lowest sequence identity towards all SlTDCs (Table 2.5).

	SlTDC2	SlTDC3	SlTDC4
SlTDC1	89.29	55.34	54.38
SlTDC2		55.77	53.97
SlTDC3			52.84

Table 2.5 Identity percentages among the amino acid sequences of the putative SlTDCs.

The SGN Blastp tool reported for all the four putative SlTDCs the annotation “aromatic L-amino acid decarboxylase” (Figure 2.3). A recent paper in which different plant Aromatic L-Amino acid Decarboxylases (AADCs) were investigated from a biochemical and structural perspective revealed the existence of conserved residues necessary to the decarboxylation reaction, substrate selectivity and cofactor binding (Torrens-Spence et al., 2018). As a preliminary *in-silico* investigation of these enzymatic features, the comparison of the amino acid sequences of the four putative SlTDCs towards all the functionally characterized plant TDCs so far (Table 2.1) was performed by ClustalO alignment. The information reported by Torrens and colleagues was used to localize the putative key sites required for proper enzymatic activity in the alignment output (Figure 2.4). The histidine and tyrosine residues in the first and second putative catalytic sites, respectively, are considered key elements for the decarboxylation reaction and were highly conserved in SlTDC1, SlTDC2 and SlTDC3 as well as the putative cofactor (pyridoxal phosphate, PLP) binding site. The mentioned tyrosine residue was replaced by phenylalanine in OsTDC2 and SlTDC4 and, moreover, the PLP-binding site in the latter was completely missing. Another point in the structural differentiation of this candidate from the other TDCs was the replacement of glycine, considered a key residue in the putative substrate selection site, with serine.

In order to get further information about the phylogenetic relationships of the putative SlTDCs with other plant AADCs, a phylogenetic tree including functionally annotated TDCs and TyDCs (tyrosine decarboxylases) from various plant species (Table 2.1) was constructed. As reported in Figure 2.5, SlTDC1 and SlTDC2 clustered in the exclusive TDC-family clade, showing the closer relationship with

TDCs from the two Solanaceae *Withania coagulans* (WcTDC) and *Capsicum annuum* (PepTDC1), whereas both SlTDC3 and SlTDC4 did not.

Although SlTDC3 clustered together with PepTDC2 and OsTDC2, this group shared more phylogenetic proximity to functionally characterized TyDCs rather than other TDCs and represented the only case of functionally characterized TDCs excluded from the observed TDC-clade. SlTDC4 clustered in another clade of the TyDC family sharing the closest similarities to TyDCs from the herbaceous species *Petroselinum crispum* (PcTyDCs).

Isolation and structural elucidation of putative Micro-Tom TDCs

The coding sequences (CDS) of SlTDCs candidates were obtained from the SGN database and, since these referred to genes of the tomato cultivar Heinz 1706, they were used as queries on the Kazusa Full-length Tomato cDNA database (KafTom; http://www.pgb.kazusa.or.jp/kaftom/blast.html) to get the corresponding CDS homologs in the cultivar Micro-Tom, which was the model plant used in this PhD project.

The Blastn research (data not shown) revealed that *SlTDC1* and *SlTDC3* CDS matched with two full-length cDNA clones from the KafTom database (LEFL2019I23 and LEFL2001AC09 respectively). *SlTDC2* CDS shared high identity (89.6%) towards the LEFL2019I23 clone but presented many mismatches, including sites in the upstream and downstream regions of the putative CDS. On the other hand, *SlTDC4* CDS did not match with any deposited Micro-Tom cDNA sequence.

These observations imposed different choices for primer design in order to amplify the four *SlTDCs* CDS from Micro-Tom cDNA: for *SlTDC1* and *SlTDC3* the primers were designed on the 5' and 3' CDS extremities whereas for *SlTDC2* and *SlTDC4* the 5' and 3' UTRs were used (Tables 2.2 and 2.3). The starting genetic material for the isolation of *SlTDCs* consisted of total cDNA obtainedfrom the reverse transcription of RNA extracted from different Micro-Tom organs (leaves, flowers and mature-green fruit).

The sequencing analysis of isolated and cloned *SlTDCs* revealed that Micro-Tom *SlTDC1*, *SlTDC2* and *SlTDC3* CDS were identical to those deposited for Heinz 1706 in the SGN database (Table 2.6; Figure 2.6). On the contrary, the amplification of the *SlTDC4* from Micro-Tom total cDNA did not give any PCR product suggesting that this gene might not be expressed in Micro-Tom plants in standard growing conditions. This hypothesis was encouraged by the fact that no expression, or extremely low expression levels, were reported for *SlTDC4* in microarray (Tomato Genome Consortium, 2012) and RNA-seq (TomExpress; http://tomexpress.toulouse.inra.fr/) expression datasets in Heinz 1706 and Micro-Tom cultivars, respectively (Figure 2.7). The *SlTDC4* sequence was therefore amplified from Micro-Tom genomic DNA by using the same primers designed on 5' and 3' UTRs. The nucleotide alignment of the cloned genomic Micro-Tom sequence with the corresponding SGN-deposited *SlTDC4* gene (Solyc03g044120) revealed that 6 nucleotides were differentially substituted, resulting in an identity of 99.58% (Figure 2.8A). These substitutions putatively resulted in 5 different amino acid

residues following the *in-silico* translation of the cloned sequence respect to the Solyc03g044120 protein (Figure 2.8B) but they did not modify the putative sites responsible for Trp-decarboxylase protein activity.

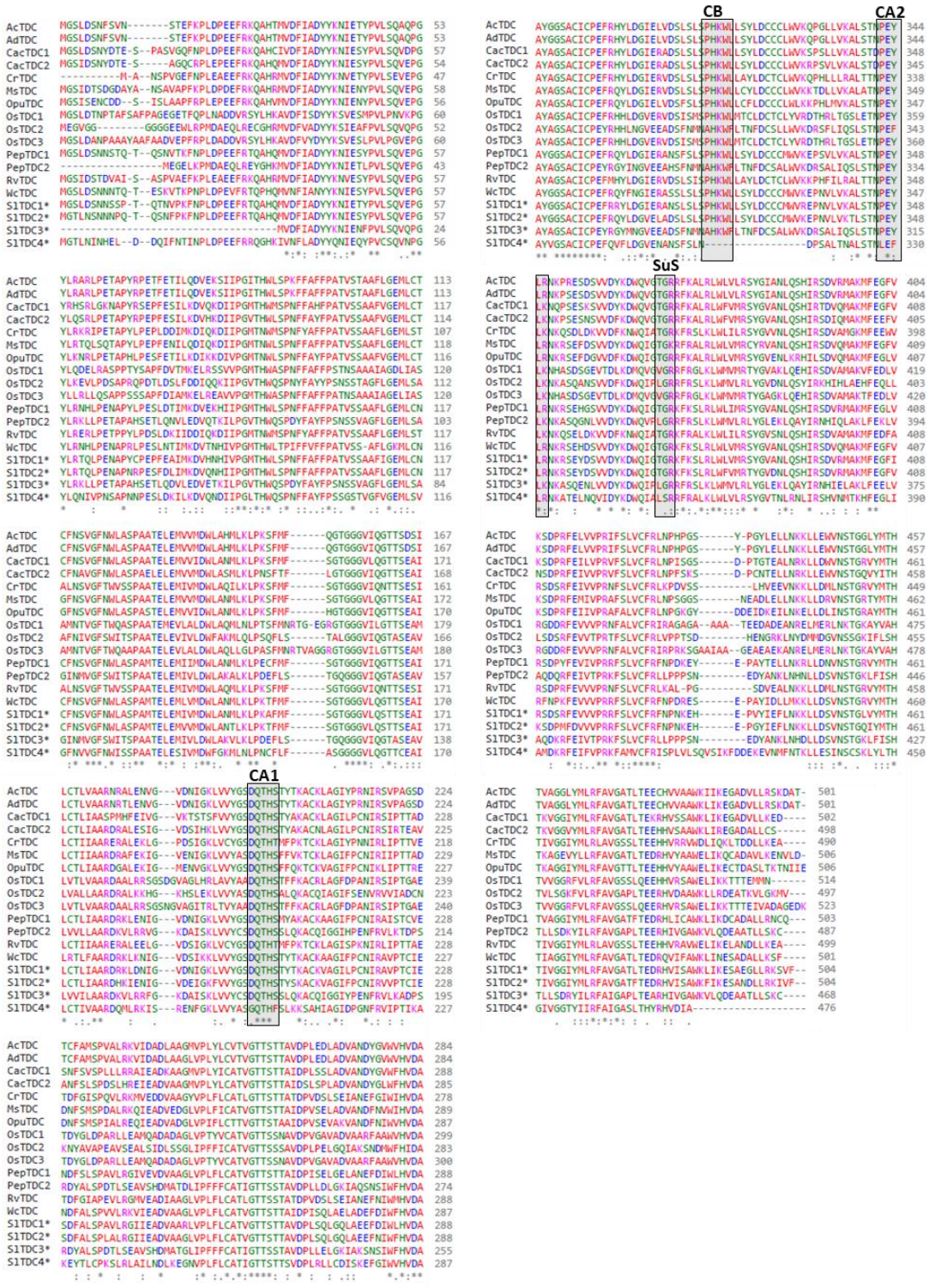

Figure 2.4 Sequence alignment by ClustalO of the amino acid sequences of putative SlTDCs towards all the functionally characterized plant TDCs so far (Table 2.1). Grey boxes highlight the putative sites for: catalytic activity (CA1 and CA2); cofactor binding (CB); substrate selection (SuS).

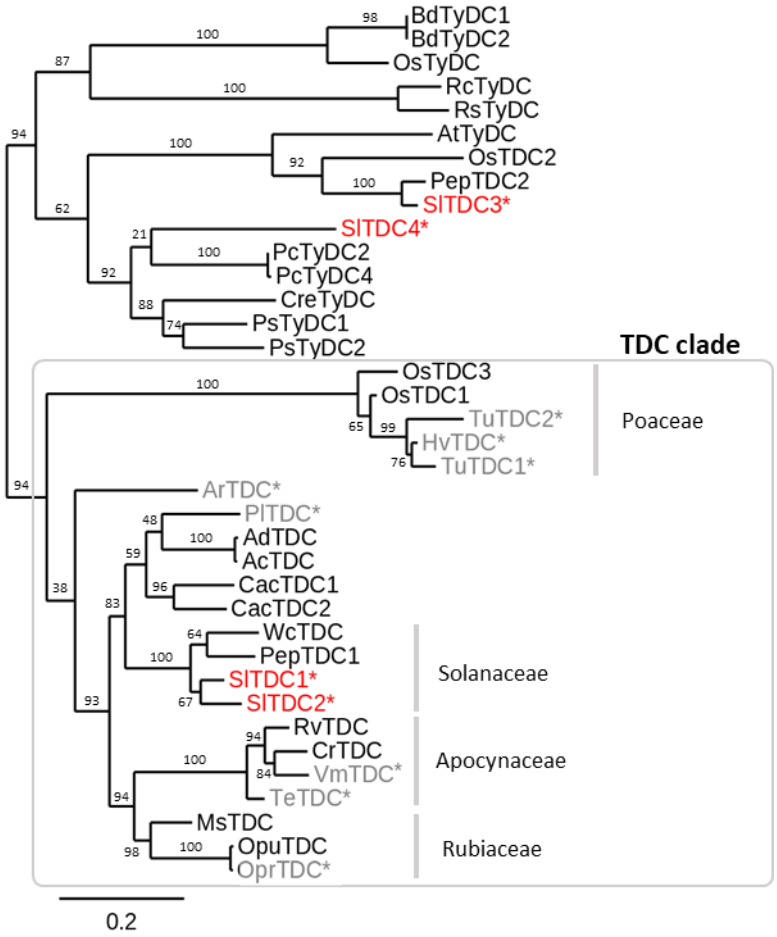

Figure 2.5 Phylogenetic tree showing the relationships among the putative SlTDC proteins and other plant TDCs and TyDCs (tyrosine decarboxylases). Numbers next to the branches indicate the hit iteration percentage calculated using the bootstrap method (100 iterations). Asterisks indicate that putative TDCs were not functionally characterized for Trp-decarboxylase activity but were reported in literature as protein orthologs of characterized plant TDCs. All the details about the proteins reported in this phylogenetic tree are listed in Table 2.1.

Gene	Source	Organ	Putative CDS length (bp)	identity (%)[1]	Putative protein length (aa)
SlTDC1	Total cDNA	Mature-green fruit	1515	100	504
SlTDC2	Total cDNA	Flowers	1515	100	504
SlTDC3	Total cDNA	Leaves	1407	100	468
SlTDC4	Genomic DNA	Leaves	1431	99.58*	476

Table 2.6 Structural features of the Micro-Tom cloned *SlTDCs* (see Figure 2.6). [1] Identities between Micro-Tom sequenced CDS and those deposited in the SGN database. *the identity percentage refers to the cloned Micro-Tom *SlTDC4* gene respect to *Solyc03g044120* gene deposited in the SGN database (Figure 2.8A).

SlTDC1|**CACC**ATGGGAAGCCTTGATTCCAATAACAGCTCTCCAACCCAAACCAACGTTCCAAAATTCAACCCGCTTGACCCGGAAGAATTCCGGACCCAAGCCCATC
AAATGGTGGACTTCATTGCTGATTACTACAAGAATATTGAGACCTACCCGGTTCTAAGCCAAGTCGAACCGGGTTATCTCCGTACTCAATTACCCGAAAATGCCCCCT
ACTGCCCCGAACCATTCGAGGCAATTATGAAAGATGTCCACAACCATATTGTCCCCGGTATGACCCATTGGTTGAGCCCGAATTTCTTCGCATTTTTTCCAGCTACTGT
TAGTTCCGCAGCGTTCATTGGTGAAATGCTTTGCAATTGTTTCAACTCCGTCGGGTTTAACTGGCTGGCTTCGCCGGCCATGACGGAGTTGGAAATGATAGTCATGGA
CTGGCTCGCTAATATGTTGAAATTACCAAAAGCCTTCATGTTTTCTGGCACGGGTGGTGGTGTACTTCAAAGTACAACCAGTGAAGCGATCCTATGCACGTTAATTGC
TGCACGTGATCGTAAACTCGATAACATAGGCGTTGATAACATCGGAAAGCTTGTAGTCTATGGTTCTGATCAAACGCATTCTACGTATACCAAAGCCTGCAAGGTAGC
TGGTATTTTACCATGCAATATTCGTGCGGTGCCAACTTGTATTGAAAGCGATTTCGCTTTATCTCCCGCAGTTCTACGTGGAATTATTGAAGCTGATGTTGCTGCTAGA
CTTGTCCCGCTTTTCCTCTGTGCTACTGTTGGGACCACTTCCACTACAGCCGTCGATCCTCTCAGCCAGCTGGGTCAGCTGGCTGAGGAATTCGACATTTGGCTTCACG
TGGATGCTGCTTATGGAGGGAGCGCATGTATATGTCCAGAGTTTAGACGATACCTCGATGGAATTGAACGAGCTAACTCATTGAGCCTAAGCCCTCATAAGTGGCTA
CTAAGTTACTTAGATTGTTGTTGCATGTGGGTGAGAGAACCAAACGTGTTAGTCAAGGCATTGAGCACGAATCCTGAGTACCTACGAAATAAACGATCCGAATACGA
CTCGGTTGTGGATTACAAGGACTGGCAAATCGGTACGGGACGAAAGTTCAAGTCTCTCCGATTATGGCTCGTCATGCGTAGTTATGGCGTAGCCAATCTTCAGAGTC
ACATCAGGTCCGATGTTCGTATGGCCAAAATGTTTGAAGGGTTCATTAGGTCTGATTCGAGGTTTGAAGTTGTCGTGCCACGACGTTTTTCACTCGTCTGCTTCCGGTT
CAACCCTAATAAGGAACATGAACCGGTGTATATCGAGTTTTTAAACAAGAAATTACTTGATAGTGTTAATTCAACGGGTCTAGTTTACATGACTCACACAATAGTTGG
TGGAATATACATGTTAAGGTTTGCAGTAGGTGCTACTCTCACGGAGGACAGACATGTAATTTCAGCTTGGAAGTTGATTAAGGAGTCGGCAGAAGGTTTGCTGAGAA
AAAGTGTGTTTTAA

SlTDC2|**CACC**AACTACCAATACTTAGTCTTTCCCCCTTTTGCTATAAAATCTCCCTCTCTAATTCCCTTTTTTTCCCTAAACTTAATCCCAAAATTATATTATGGGAACCC
TTAATTCAAATAACAACCCTCAAACCCAATCCAACTTCCCAAAATTCAACCCGCTTGACCCGGAAGAATTCCGTACCCAAGCCCATCAAATGGTGGACTTCATTGCTGA
TTACTACAAGAATATTGAGTCCTACCCGGTTCTAAGTCAAGTCGAACCCGGTTATCTTCGTACCCAATTACCCGAAAACGCCCCTAATCGACCCGAATCATTCGATTTA
ATTATGAAAGATGTCCAAAACCATATTATCCCGGGTATGACCCATTGGCTAAGCCCGAATTTCTTCGCATTTTTTCCAGCTACTGTTAGCTCCGCTGCGTTTCTAGGTGA
AATGCTTTGCAATTGTTTCAACTCCGTCGGATTTAATTGGCTGGCTTCGCCAGCCATGACGGAGTTGGAAATGGTAGTCATGGACTGGCTTGCTAATACGTTGAAATT
ACCAAAAACTTTCATGTTTTCTGGCACGGGTGGTGGTGTACTACAAAGTACAACTAGTGAAGCTATACTGTGTACGTTAATCGCTGCGCGTGATCATAAGATCGAGAA
TATAGGTGTTGATGAGATAGGAAAATTTGTAGTCTACGGTTCTGATCAAACTCACTCTACTTATAGCAAAGCCTGCAAGGTAGCTGGTATTTTCCCATGCAATATTCGT
GTGGTACCAACTTGTATTGAAAGCGATTTCGCTTTATCTCCTCTAGCACTACGTGGAATTATTGAAGCTGATGTTGCTGCTGGACTGGTCCCACTTTTCCTCTGTGCTAC
CGTTGGGACCACTTCCACAACAGCAGTTGATCCTCTCAGCCAGCTGGGTCAGCTGGCTGAGGAATTCAATATTTGGTTCCACGTGGACGCTGCTTATGGAGGTAGCG
CGTGTATATGTCCAGAGTTTAGACAATATCTGGACGGAGTCGAACTAGCGGACTCGTTAAGCCTAAGCCCACATAAGTGGCTATTAAGTTACTTAGATTGTTGTTGTA
TGTGGGTGAAAGAACCAAACGTGTTAGTGAAGACATTGAGCACGAATCCCGAGTACTTACGTAATAAACGATCTGAATACGACTCGGTTGTTGATTATAAAGACTGG
CAAATCGGTACGGGACGAAAGTTCAAGTCTCTCCGATTATGGTTCGTCATGCGTACTTATGGCGTAGACAATCTTCAAAGCCACATTAGGTCCGATGTTCGCATGGCC
AAAATGTTTGAAGGGTTCGTTAAGTCCGATCCCATGTTTGATGTCGTCGTGCCACGACGTTTTTCACTCGTGTGCTTTCGGTTTAACCCGAACAAGGAACATGAACCG
GGCTACATCGAGTTTTTAAACAAGAAATTGCTTGATAGTGTTAACTCGACAGGTCAAATTTACATGACACACACAATAGTGGGTGGAATATACATGTTAAGGTTTGCA
GTAGGTGCGACGTTCACTGAGGATAGACATGTAATTTCAGCTTGGAAGTTTATTAAGGAGTCAGCCAATGATTTGCTCAGAAAAATTGTGTTTTAGAAAATAATATAT
TAATGGAGGATGAAGAAGAAGAAGAGTAAAATAAATGTTTGGATTGTGTGTGTTAAATTTATGTATAGGCATTTGTGATTGTT

SlTDC3|**CACC**ATGGAAGGGGGATTGAAGCCGATGGATGCAGAGCAACTGCGAGAGTATGGTCACAAGATGGTAGATTTCATTGCTGATTACTACAAAAACATTGA
GAATTTCCCCGTTCTCAGTCAAGTCCAGCCTGGTTATCTCCGTAAGCTTTTGCCTGAAACCGCACCTGCTCATTCTGAGACATTGCAAGACGTTCTTGAAGACGTTGAA
ACAAAAATATTACCAGGGGTGACCCACTGGCAGAGCCCAGATTACTTTGCATATTTTCCTTCAAATAGTAGTGTGGCTGGATTTCTGGGGGAAATGCTCAGTGCCGG
GATTAACATGGTGGGCTTTAGTTGGATAACTTCTCCAGCAGCGACAGAACTTGAAATGATCGTTCTGGATTGGCTTGCTAAAGTACTTAAGTTGCCTGATGAATTCCT
TTCAACAGGTCAAGGAGGTGGAGTGATACAGGGAACAGCAAGTGAAGCTGTTCTAGTTGTGATTTTAGCTGCTAGGGATAAGGTTCTGAGAAGATTCGGAAAAGAT
GCAATCAGCAAACTTGTGGTCTATTGTTCTGATCAAACTCATTCTTCTTTACAGAAAGCATGCCAGATCGGAGGCATTTATCCTGAGAACTTTCGGGTGCTGAAAGCA
GACCCATCCAGGGATTATGCTCTTTCTCCTGATACACTTTCAGAAGCTGTATCACATGACATGGCCACTGGTTTAATACCTTTCTTCTTTTGTGCTACTATTGGTACAAC
ATCTTCAACTGCTGTGGATCCTTTGCTCGAACTGGGAAAGATTGCCAAGAGTAATAGCATATGGTTTCATGTGGATGCGGCCTATGCTGGAAGTGCATGTATCTGTCC
AGAATACCGGGGCTATATGAATGGTGTCGAAGAAGCTGATTCGTTCAACATGAATGCACATAAATGGTTCCTGACAAACTTTGACTGTTCCGCTCTCTGGGTCAAGG
ACCGGAGTGCACTCATCCAGTCACTGTCAACAAATCCTGAGTATCTCAAAAACAAAGCCTCTCAAGAAAACTTGGTTGTGGATTATAAAGATTGGCAAATTCCTCTTG
GACGCAGGTTCAGATCACTGAAGCTGTGGATGGTATTGAGACTCTATGGGCTGGAAAAGCTTCAAGCTTACATAAGAAACCATATAGAACTAGCAAAGCTATTTGAG
GAACTTGTTGCTCAAGACAAGAGGTTTGAGATTGTCACCCCTCGGAAGTTCTCATTGGTTTGTTTTCGCCTACTTCCACCCCCGAGTAATGAAGATTATGCCAACAAAC
TGAACCATGACCTGCTAGATTCTGTCAACTCAACTGGAAAACTGTTTATTTCTCACACGCTTCTTTCAGATAGATACATACTACGCTTTGCAATAGGGGCTCCACTGAC
AGAAGCGAGGCACATCGTTGGAGCTTGGAAAGTTTTACAAGATGAGGCTGCTACATTGTTAAGTAAATGTTAA

SlTDC4|**CACC**GCTAACCATTTATTTTTCTTTCAAGGCAACATATACACACAAATTGAAATAATGGGTACCCTCAATATCAACCATGAACTTGATGACCAAATTTTCAAT
ACCATAAGCCCTTTAGACCCTGAAGAATTTAGAAGGCAAGGTCATAAAATTGTGAATTTCCTAGCTGACTACTATCAAAATATTGAACAATATCCTGTTTGTAGTCAAG
TAAATCCAGGGTATCTCCAAAACATTGTACCAAATTCCGCACCTAATAATCCTGAGTCTCTCGATAAAATTCTTAAGGATGTCCAAAATGATATTATTCCAGGGCTAAC
ACATTGGCAAAGTCTTAACTTTTTCGCGTATTTTCCATCTTCAGGAAGTACTGTTGGATTCGTAGGTGAAATGTTAAGTGTTGGATTTAATGTTGTAGGGTTTAATTGG
ATATCATCCCCTGCTGCTACTGAACTTGAGAGTATTGTAATGGATTGGTTTGGGAAAATGTTAAATCTTCCCAATTGTTTTTTGTTCGCGAGTGGTGGTGGAGGTGTAC
TACAAGGTACAACTTGTGAAGCCATATTGTGTACTATAGTTGCAACTAGAGATCAAATGCTGCAAAAAATAAGTAGAGAGAATTTTGGAAAATTGGTTGTATATGCAT
CTGGTCAAACACATTTCTCACTTAAGAAGTCTGCCCACATTGCTGGGATAGACCCTGGAAATTTTCGAGTTATCCCAACAATAAAGGCTAAAGAGTACACCTTGTGTC
CAAAATCGCTACGATTAGCAATTTTGAATGATCTAAAAGAAGGAAATGTTCCTTTGTTCTTGTGCGCGACAATTGGGACAACTCCAACAACTTCTGTTGATCCATTGCG
TCTACTCTGTGATATTTCTAAGGAGTTTGGGATTTGGGTACATGTAGATGCAGCTTATGTAGGAAGTGCTTGTATTTGCCCTGAATTTCAAGTCTTTCTTGATGGTGTT
GAAAATGCAAATTCATTTAGTCTCAACGCGCACAAATGGTTCTTTTCCACTTTTGGATTGTTGTTGTCTTTGGGTTAAGGATCCAAGTGCACTTACTAACGCGTTATCAA
CTAATCTTGAATTTTTGAGAAACAAGGCTACAGAGTTAAATCAAGTGATTGATTATAAGGATTGGCAAATTGCATTGAGTAGGAGGTTTAGAGCATTGAAATTATGG
TTAGTTTTGAGAAGTTATGGGGTAACTAATCTTAGAAACTTGATAAGAAGTCATGTGAACATGACTAAACATTTTGAAGGGCTTATAGCTATGGACAAAAGGTTTGA
AATCTTTGTCCCTAGAAAGTTTGCTATGGTGTGTTTTAGGATCTCTCCGCTAGTACTAAGTCAAGTTTCAATCAAATTTGATGATGAGAAAGAAGTGAACATGTTTAAC
ACTAAGTTGTTGGAGTCTATTAATTCATGTAGCAAACTCTATTTGACTCATGGAATTGTTGGAGGCACTTATATTATTAGATTTGCAATTGGTGCTTCTCTTACACATTA
TAGGCATGTTGACATAGCTTGAAAAGTTATACAAGATCATGCCAATGCCCTGCTAAATCAA

Figure 2.6 5'-3' nucleotide sequences of the Micro-Tom cloned *SlTDCs* including for some of them partial UTRs (light blue nucleotides). Start and stop codons are highlighted in green and red respectively. Attachment sites for forward and reverse primer are underlined. CDS have been cloned for *SlTDC1*, *SlTDC2*, *SlTDC3* whereas *SlTDC4* was cloned from the entire gene, in which the 52-bp intron is highlighted in grey.

A

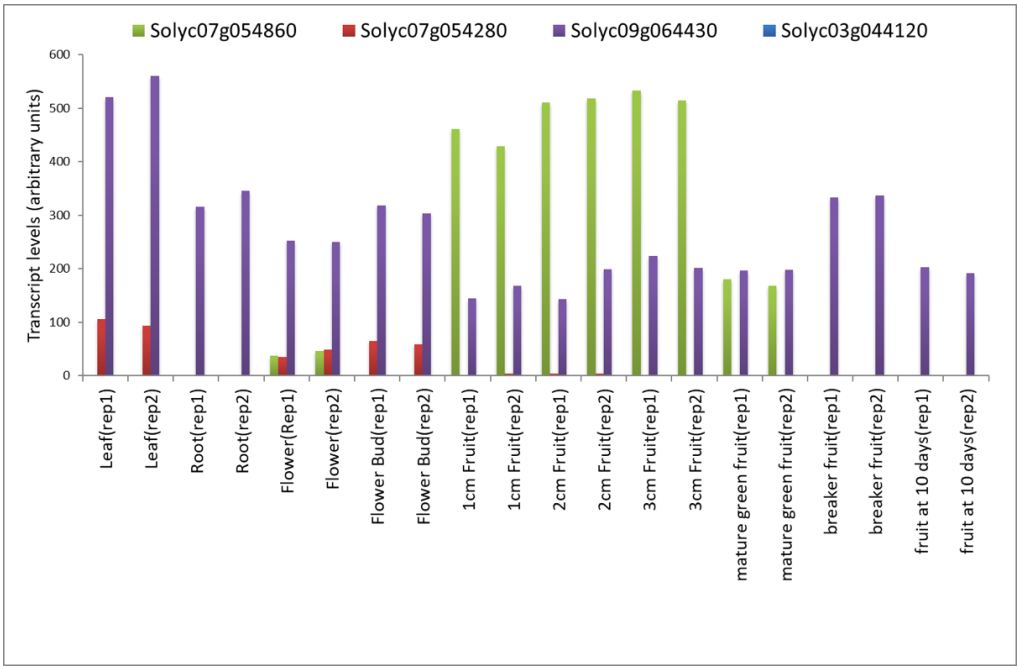

B

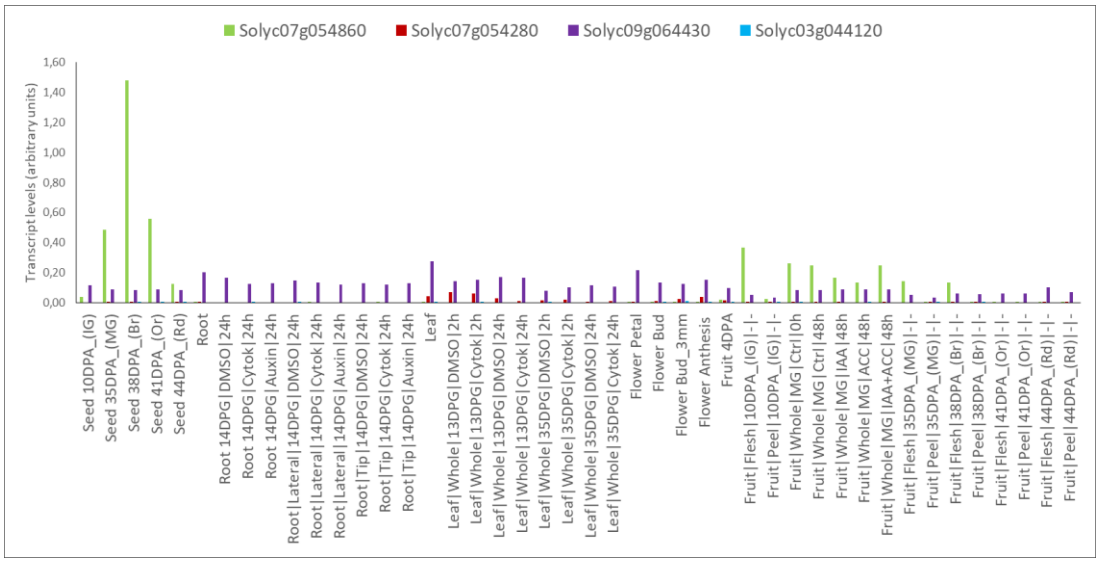

Figure 2.7 Graphic representation of transcript levels of *SlTDC1*, *SlTDC2*, *SlTDC3* and Solyc03044120 in different organs and developmental stages of wild type tomato cultivars Heinz 1706 (A) and Micro-Tom (B) as respectively reported from micro-array (Tomato Genome Consortium. 2012) and RNA-seq expression datasets (Tom-Express). Legend for B: DPA, days post anthesis; DPG, days post germination; MG, mature green.

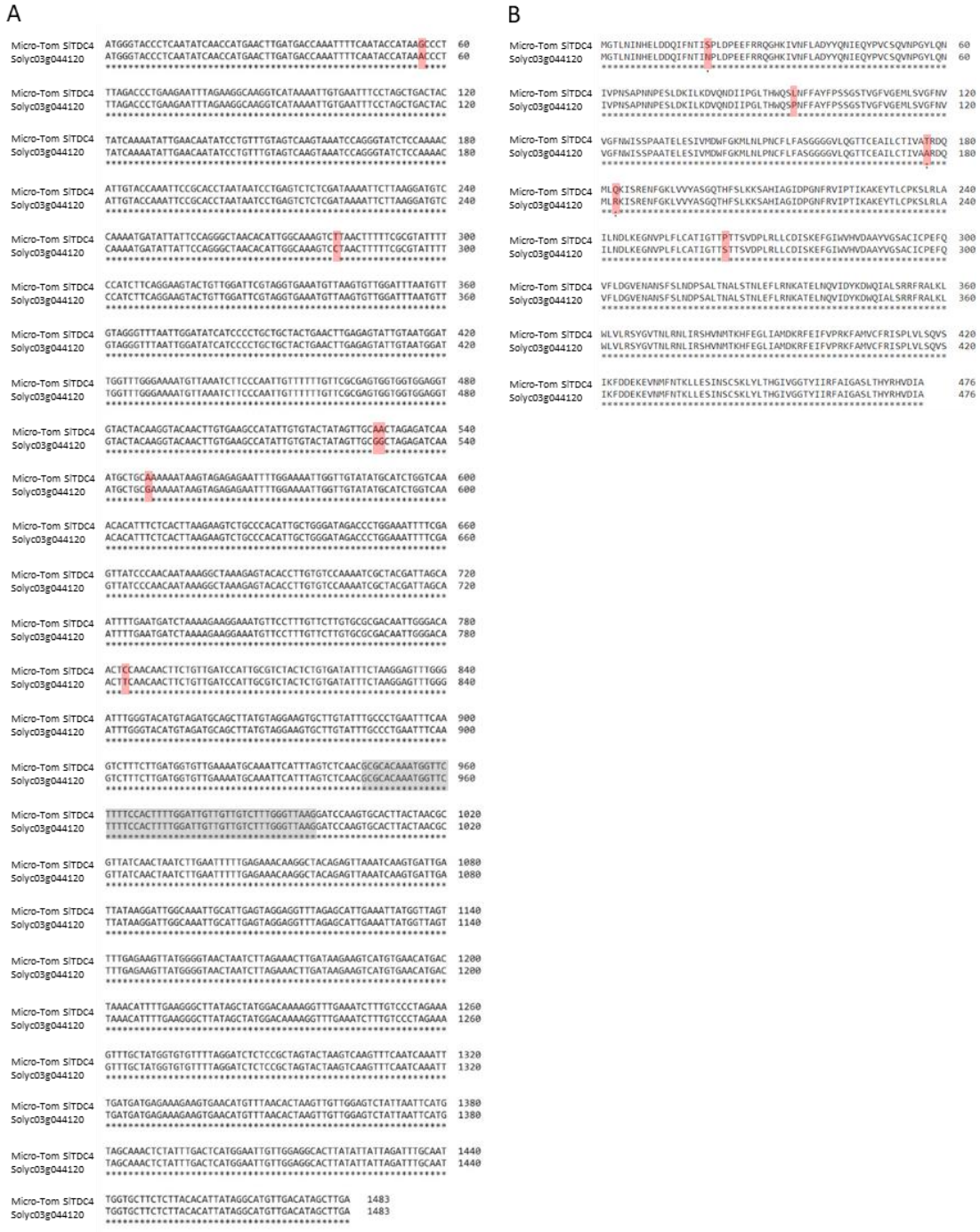

Figure 2.8 Sequence alignments by ClustalO of the genes (A) and the respective protein products (B) of Micro-Tom cloned *SlTDC4* and the SGN-deposited Solyc03g044120. The only one gene intron is highlighted in grey; sites presenting differences in nucleotides or amino acid residues are highlighted in red.

Functional characterization of Micro-Tom SlTDC genes in Nicotiana benthamiana

To assess the function of Micro-Tom SlTDC candidates an *in-vivo* functional assay based on transient heterologous expression of the *SlTDCs* genes was developed. *Nicotiana benthamiana* was chosen as plant host in which performing the assay since, from previous experimental evidences (data not shown), it accumulates tryptophan, the substrate of TDCs, but does not accumulate detectable levels of tryptamine nor serotonin, the products of TDCs, in its aerial organs. Moreover, *N. benthamiana* represents a reliable and robust model for gene heterologous expression and functional characterization in plants (Gecchele et al., 2015).

The *SlTDC1*, *SlTDC2*, *SlTDC3* CDS and *SlTDC4* gene were individually cloned into the binary destination vector pK7WG2 (Karimi et al., 2002), which allows plant heterologous overexpression of the gene of interest driven by the constitutive Cauliflower Mosaic Virus (CaMV) 35S promoter (Figure 2.9).

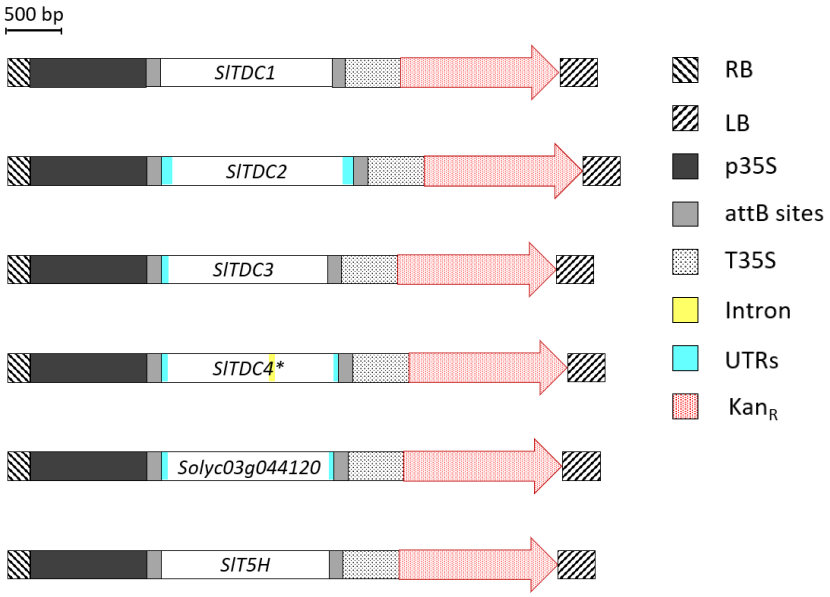

Figure 2.9 Schematic scale representation of the T-DNA regions harbouring the *SlTDCs* and *SlT5H* CDS sequences cloned into pK7WG2 plant expression vector. **SlTDC4* was cloned from Micro-Tom genomic DNA instead of cDNA. Legend: RB and LB, right and left border; p35S, CaMV 35S promoter; attB, GATEWAY® recombination elements; UTRs, untranslated regions, Kan_R, neomycin phosphotransferase (*nptII*) gene conferring kanamycin resistance in plants.

The constructs were individually introduced into *Agrobacterium tumefaciens* and each bacterial suspension was singularly transferred by syringe agroinfiltration into three leaves each of three different *N. benthamiana* plants. Plants transiently expressing the Green Fluorescence Protein (GFP) or the formerly characterized AcTDC (Commisso et al., 2019) represented, respectively, the negative and positive controls. According to previously obtained results concerning time-course recombinant protein accumulation in *N. benthamiana* (data not shown), leaves were collected from 3 to 5 days post-infiltration (dpi).

The leaf methanolic extracts were analysed by HPLC-ESI-MS following an untargeted metabolomics approach. As first step, tryptamine presence was assessed by looking for the signal of the diagnostic tryptamine ion (144 *m/z*) in the recorded chromatogram (Figure 2.10A). The corresponding peak area was measured allowing to determine relative tryptamine levels accumulated by *N. benthamiana* plants (Figure 2.10B).

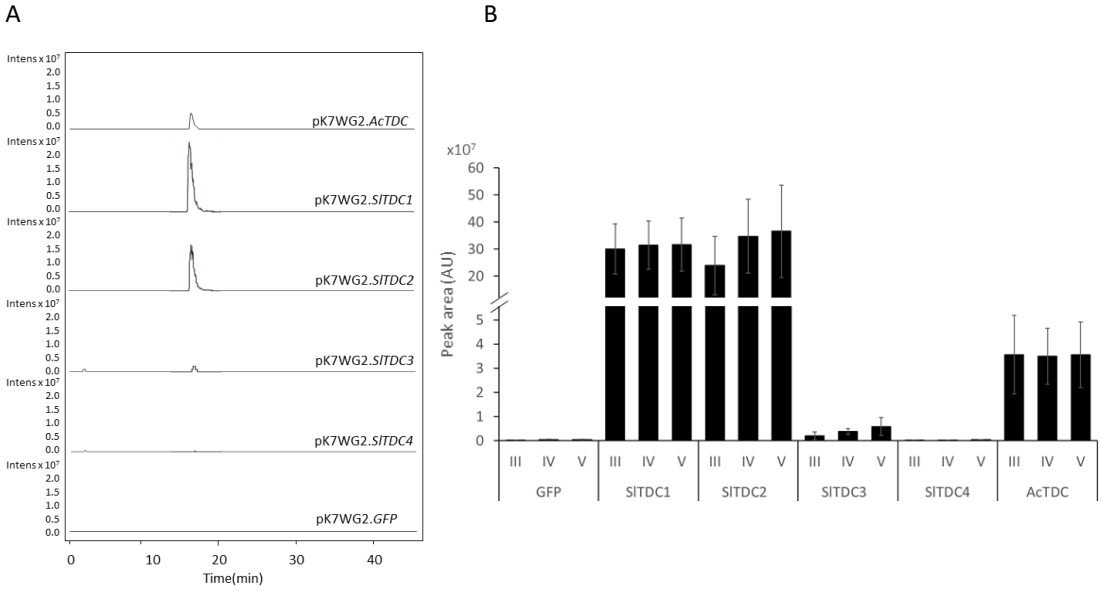

Figure 2.10 HPLC-ESI-MS analysis of leaf methanolic extracts of *N.benthamiana plants* used in *SlTDCs* functional characterization assay. A) Extracted Ion Chromatograms (EICs) of tryptamine diagnostic ion (144 *m/z*; Rt 19.2 min) detected in positive ionization mode. All chromatograms are scaled to the highest signal intensity. B) Relative tryptamine levels expressed as peak area, arbitrary units (AU). Bars indicate standard deviations (n=3).

As expected, in *GFP*-transiently expressing plants no tryptamine production was observed whereas high and constant levels of this indolamine were noticed in both *SlTDC1* and *SlTDC2* plants throughout the 3 days of sampling. *SlTDC3* transformed plants were also able to accumulate tryptamine, although at much lower levels (about 40 times less) whereas *SlTDC4* plants di not accumulate detectable levels of tryptamine, as the negative control plants.

These evidences witness the tryptophan decarboxylase activity of SlTDC1, SlTDC2 and SlTDC3 proteins proving that they are *bona fide* TDCs.

In order to check if other perturbations in *N. benthamiana* metabolome eventually occurred following the transient expression of *SlTDCs*, two datasets, respectively for positive and negative ionization recorded chromatograms, were created and submitted to multivariate statistical analysis. The principal component analysis of the positive data matrix (PCA) showed two distinct groups in which *SlTDC1* and *SlTDC2* plants separated from the negative control that clustered together with *SlTDC3* and *SlTDC4* plants (Figure 2.11A). The corresponding OPLS-DA (orthogonal partial least square-

statistical analysis; Figure 2.11B) highlighted that, beyond tryptamine, there were five more metabolites that highly correlated with the *SlTDC1*/*SlTDC2* group (Figure 2.11C). Among them, it was possible to identify only serotonin that, together with other unidentified metabolites were differentially accumulated respect to *GFP*/*SlTDC3*/*SlTDC4* group (Figure 2.12). On the other hand, the multivariate statistical analysis of the negative dataset highlighted no clustering among the samples in PCA (data not shown).

SlTDC4 agroinfiltrated plants did not accumulate tryptamine, thus suggesting that this gene might not be either expressed or codifying for a tryptophan decarboxylase. Therefore, the presence of *SlTDC4* transcript in *N. benthamiana* agroinfiltrated leaves was investigated by RT-PCR, observing that *SlTDC4* was effectively expressed (data not shown). The sequencing of Micro-Tom *SlTDC4* clone revealed the persistence of the 52-bp intronic region and, thus, to investigate if this still led to the formation of a functional polypeptide, its nucleotide sequence was translated *in silico*. The formation of a truncated protein was observed, suggesting that the possible lack of tryptophan decarboxylase activity might derive from an inactive/incorrectly-folded enzyme. Therefore, the activity of the original SGN-deposited gene, i.e. Heinz 1706 *SlTDC4* (Solyc03g044120), was investigated by cloning the CDS deposited in the SGN database into the pK7WG2 vector and transiently transforming leaves of *N. benthamiana* plants.

Methanolic extracts of leaves independently agroinfiltrated with pK7WG2.*SlTDC1* (positive control), pK7WG2.*GFP* (negative control) and pK7WG2.*Solyc03g044120* were analysed by HPLC-ESI-MS. Tryptamine levels were assessed showing once again the production of this indolamine in *SlTDC1* plants and its complete absence in *Solyc03g044120* transiently expressing plants (Figure 2.13). Even in this case, the expression of Solyc03g044120 in *N. benthamiana* expressing plants was evaluated by RT-PCR analysis on the total cDNA of leaves collected after three, four and five days after infiltration, confirming the expression of *Solyc03g044120* (Figure 2.14). Curiously, the RT-PCR analysis revealed the amplification of a band with a length of about 1500 bp also in the negative control plants, suggesting that *N. benthamiana* expressed a gene that shared common regions with *Solyc03g044120*. The direct sequencing of the gel-purified amplicon by using the SlTDC4-for primer, resulted in a partial sequence of 885 nt that was used as query in the next Blastn analysis against two distinct databases including *N. benthamiana* genetic resources: "Sol Genomics Network" and "*Nicotiana benthamiana* genome website". The former returned a sequence named Niben101Scf02857g02001.1, with a length of 1431 bp and including only the putative coding region, which should codify for a putative tyrosine decarboxylase. The second database returned a 1867 bp sequence, deposited as Nbv6.1trP5228, including also the 5' and 3' UTRs. The alignment between the two *in silico* translated amino acid sequences gave a 100% identity match, indicating that the two sequences codify for a unique protein (data not shown). The ClustalO alignment between this amino acid sequence and *Solyc03g044120* gave 75.6% identity (Figure 2.15), suggesting that an orthologous of *Solyc03g044120* is expressed *N. benthamiana* plants.

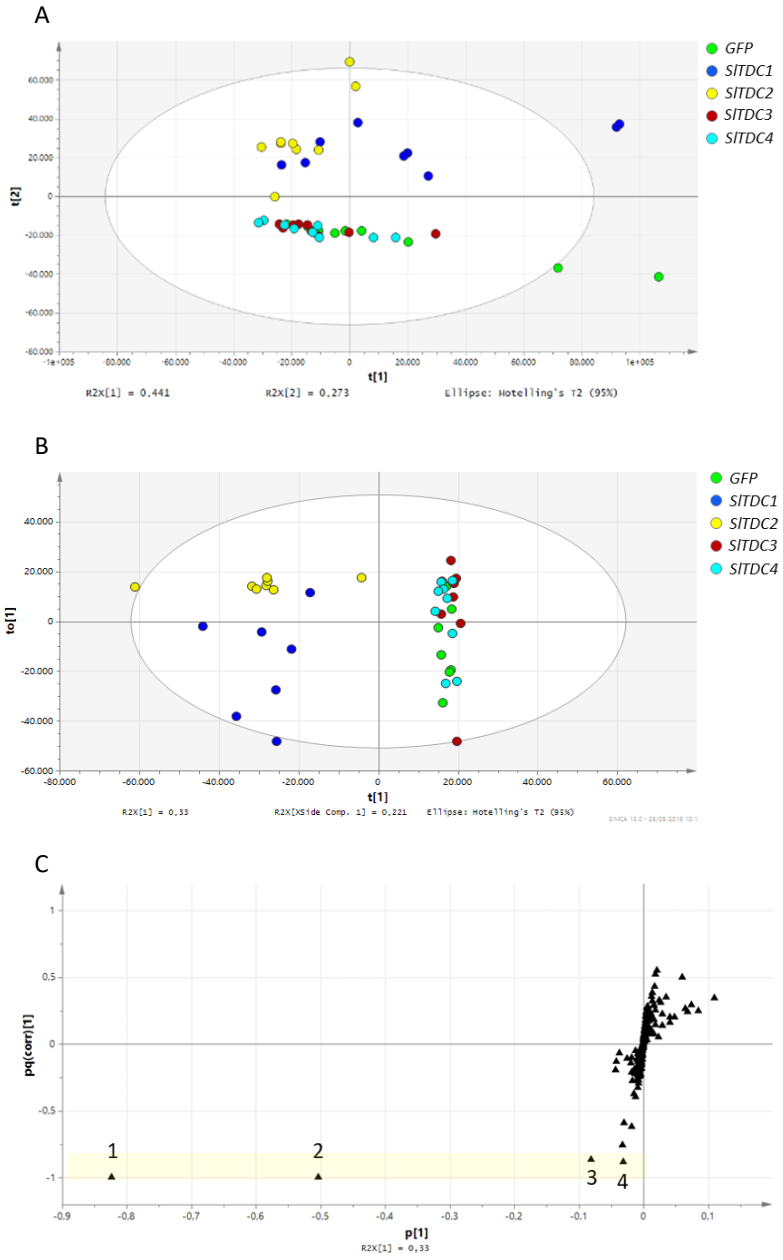

Figure 2.11 Multivariate statistical analysis of the untargeted metabolomics dataset (positive ionization) obtained from the HPLC-ESI-MS analysis of *Nicotiana benthamiana* plants transiently expressing *SlTDCs*. A) PCA score scatter plot; B) OPLS-DA score scatter plot. C) OPLS-DA S-loading plot. Each metabolite is represented by a black triangle. Yellow area include the characterizing metabolites of *SlTDC1/SlTDC2* cluster against the *GFP*/*SlTDC3*/*SlTDC4* cluster: 1 and 2, molecular and diagnostic ions of tryptamine (161 and 144 *m/z* respectively); 3, serotonin molecular ion (177 *m/z*, Rt 6.9 min); 4, unidentified metabolite (177*m/z*, Rt 11.5 min).

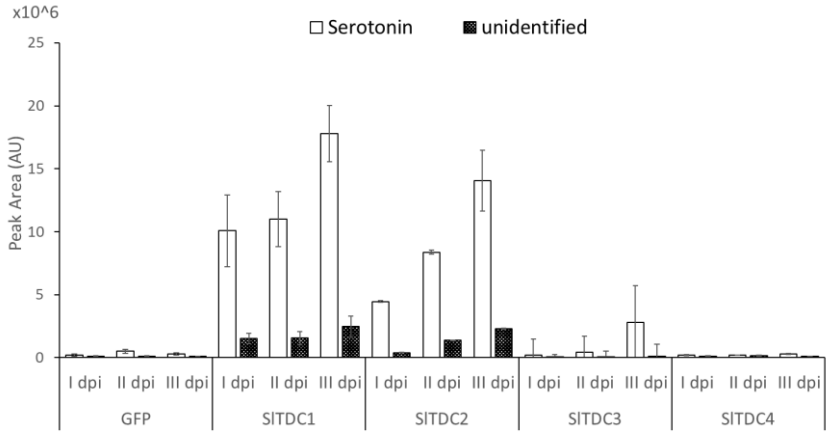

Figure 2.12 Accumulation levels of serotonin and of an unidentified metabolite (number 4 listed in Figure 2.11C) expressed as peak area, arbitrary units (AU). Bars indicate standard deviations (n=3).

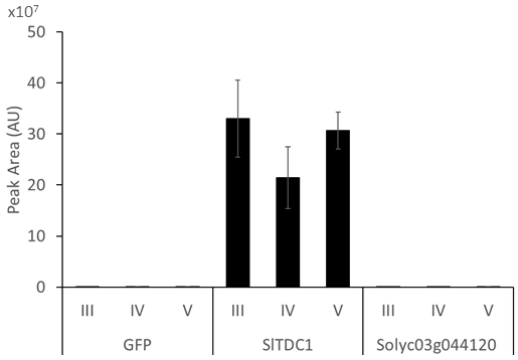

Figure 2.13 HPLC-ESI-MS analysis of leaf methanolic extracts of *N.benthamiana* plants used in *Soly03g044120* functional characterization assay. Relative tryptamine levels expressed as peak area, arbitrary units (AU) are shown. Bars indicate standard deviations (n=3).

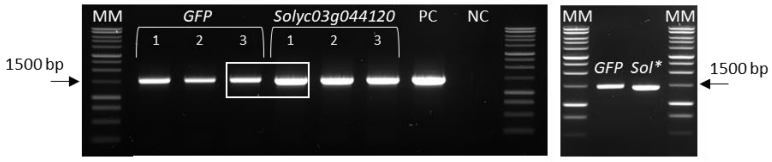

Figure 2.14 Gel electrophoresis of agroinfiltrated-*Nicotiana benthamiana* amplified cDNA. cDNA solutions of *Wild type N. benthamiana* plants and those transiently expressing *GFP* and *Solyc03g044120* were used as template. Legend: PC, positive control (i.e. the pK7WG2.*Solyc03g044120* construct used for the plant transformation); NC, negative control; MM, 1-Kb molecular marker. The primers used for the amplification were SlTDC4_for and SlTDC4_rev reported in Table 2.2. On the left box: gel-electrophoresis in which PCR solutions including *GFP*, *Solyc03g044120*, PC and NC samples are charged. 1, 2 and 3 mean the biological replicates of leaves collected at 5 days post infiltration. On the right: magnification of the white box. The asterisk stands for *Solyc03g044120*.

Figure 2.15 Sequence alignment by ClustalO of the amino acid sequences of Solyc03g044120 (SlTDC4 of Heinz1706 tomato cultivar) and its putative *N. benthamiana* orthologous (Niben101Scf02857g02001.1)

Identification and functional characterization of the tomato *T5H* gene involved in serotonin biosynthesis

Identification and cloning of putative Micro-Tom SlT5H

The high levels of serotonin in *S. lycopersicum* reported in literature suggest the existence of a tryptamine-5-hydroxylase (SlT5H) enzyme capable to convert tryptamine to serotonin. As did for *SlTDCs*, candidate genes coding for this protein were sought by querying the amino acid sequence of the previously characterized OsT5H (Fujiwara et al., 2010) in the SGN-Blastp tool. It was thus identified and selected as putative SlT5H a sequence with 55.3% identity that was annotated as "cytochrome P450" (Figure 2.16) and predicted to be targeted to the ER by Predotar. For the same reasons mentioned above, a Blastn research in KafTom database was performed by using the *SlT5H* CDS. A sequence with high similarity (99.93% identity) was found (LEFL1021DE05, DDBJ Acc. Number AK321232) and the comparison among the *in silico* translated amino acid sequences revealed that only one residue was different between the two deposited sequences (data not shown). The *SlT5H* CDS deposited in the SGN database was cloned from the cDNA obtained from the mature-green Micro-Tom fruit (Table 2.7). Once confirmed that the cloned Micro-Tom sequence was equal to the SGN-deposited one, its CDS was cloned into the pK7WG2 (Figure 2.9, Figure 2.17) and its function characterized through heterologous expression in *N. benthamiana* plants.

SubjectId	id%	Aln	evalue	Score	Description
Solyc09g014900.2	55.34	254/459	0.0	535	Cytochrome P450 Length = 495
Solyc06g076160.2	39.54	191/483	e-134	401	Cytochrome P450 Length = 504
Solyc04g083140.1	39.88	195/489	e-128	387	cytochrome P450 Length = 501
Solyc09g092590.1	37.34	180/482	e-125	380	Cytochrome P450 Length = 497
Solyc11g006590.1	37.82	191/505	e-125	380	Cytochrome P450 Length = 497

Figure 2.16 Blastp homology research output showing the list of matched *Solanum lycopersicum* proteins from the SGN database towards the *Oryza sativa* functionally characterized T5H (OsT5H).

Gene	Source	Organ	Putative CDS length (bp)	identity (%)[1]	Putative protein length (aa)
SlT5H	Total cDNA	Mature-green fruit	1588	100	495

Table 2.7 Structural features of the Micro-Tom cloned *SlT5H* (see also Figure 2.17). [1] Identity is referred towards the *Solyc09g014900* SGN-deposited sequence.

SlT5H|CACCATGGAAGCATCAATTCTACAGCTACTTCTTCTACTATCACTTACATCCTGCACAATTCTCTTTTACAAAATCAGAGGCCGATGGCGTCGTCGGCCTCCGT
CTCCACCATCTCTCCCTATAATCGGTCACCTCCATCTCCTCAACCAAATGCCTCATCACACCTTCTTCAATCTATCTCAAAAACTCGGAAAAATTATCTATCTTCAACTCG
GCCAAATTCCGACTCTAATCATCTCATCTCCTCGTCTAGCTGAACTCATCCTCAAAACGAACGATCATATCTTCTGTAGCCGTCCACAAATCATTGCAGCTCAGTACCTC
TCCTTCGGTTGCTCCGATATCACTTTTTCACCGTACGGTCCTTACTGGCGTCAAGCTAGAAAAATCTGCGTAACGGAATTACTCAGTTCCAAACGAGTTCACTCGTTTG
AATTCATACGAGATGAGGAAATTAACCGTATGATAGAATTGATTTCGTCTCGTTCTCAATCTGAAGTAGATCTGAGTCAGGTTTTCTTCGGTCTAGCGAATGATATTTT
GTGTAGAGTAGCGTTTGGGACGAGATTTATTGATGATAAATTGAAAGATAAGGATTTAGTGAGTGTACTGACGGAGACACAGGCGTTGTTAGCTGGGTTTTGTTTTG
GGGATTTTTTTCCAGATTTTGAATGGGTGAATTGGTTGAGTGGGATGAAGAAGAGATTGATGAATAATTTGAAAGATTTGAGAGAAGTTTGTGATGAGATTATAAAA
GAGCATTTGATGAAAACCAGAGAGGATGGTTCAGAAGATTTTGTTCATGTATTGTTGAAGGTTCAGAAAAGAGATGATCTACAAGTGCCTATTACTGATGACAACCT
CAAAGCTCTTATCCTGGATATGTTTGTGGCTGGAACAGATACATCAGCAGCTACACTAGAATGGACAATGACTGAGTTGGCTAGGCATCCAAGTGTTATGAAAAAGG
CACAAAATGAAGTAAGAAAGATTGTAGCTAATAGAGGAAAGGTAGAAGAATTTGATCTTCAACATCTTCACTATATGAAAGCAGTAATAAAGGAGACTATGCGATTG
CATCCCCCTGTCCCTCTTCTCGTACCTCGTGAATCCATCGAAAAATGTAGTATCGATGGCTATGAAGTACCTGCGAAAACTAGAGTGTTGATCAACACTTATGCAATCG
GAAGAGATCCTGAGTATTGGAACAACCCTCTTGACTACAACCCCGAAAGGTTTATGGAGAAGGATATCGATTTGAGGGGACAAGATTTTAGGTTTTTACCGTTTGGA
GGAGGGAGAAGAGGTTGTCCAGGTTATGCTCTTGGATTAGCTACAATTGAGTTATCGTTGGCTCGTTTGTTGTATCGCTTTGATTGGAAATTGCCTAGTGGAGTTGAA
GCTCAGGATATGGACTTGTCTGAGATATTTGGATTGGCTACTAGAAAAAAAGTGGCTCTAAAGCTTGTTCCAACCATCAACAAGTTGTAA

Figure 2.17 5'-3' nucleotide sequences of the Micro-Tom cloned *SlT5H* Start and stop codons are highlighted in green and red respectively. Attachment sites for SlT5H-for and SlT5H-rev primers (Table 2.2) are underlined.

Functional characterization of Micro-Tom SlT5H in Nicotiana benthamiana

Serotonin is produced through the hydroxylation of tryptamine, which is in turn synthesized by TDC. Since *N. benthamiana* plants do not show detectable levels of tryptamine nor serotonin, this species is a suitable model to investigate the identity of putative SlT5H as well. Plants were agroinfiltrated at the same time with pK7WG2.*SlTDC1* and pK7WG2.*SlT5H* and the experiment was set-up by using the proper control groups: *N. benthamiana* agroinfiltrated independently with either pK7WG2.*SlTDC1* or pK7WG2.*SlT5H* were both considered as negative controls, whereas plants transiently expressing *SlTDC1* and *OsT5H* (the already characterized *bona fide T5H* of rice) together were the positive controls. The experimental procedure of *N. benthamiana* leaf sampling was the same as described in *SlTDCs* functional assay (Figure 2.2). The methanolic extracts were analysed by following an untargeted metabolomics approach and the detection of tryptamine and serotonin was performed as previously

described. Plants expressing *SlT5H* alone did not accumulate neither tryptamine nor serotonin, whereas when *SlT5H* was expressed together with *SlTDC1*, leaves were able to accumulate serotonin at the same levels observed for the positive control (Figure 2.18). In these plants, tryptamine was detected in traces. Plants transiently expressing *SlTDC1* alone accumulated mainly tryptamine, even though low serotonin levels were noticed, as previously observed in *SlTDCs* functional assay (Figure 2.12). In this case as well, in order to complete the information about other eventual modifications in *N. benthamiana* metabolome following transient expression of *SlTDC1* and *SlT5H*, the untargeted metabolomics datasets were explored by multivariate statistical analysis. PCA of positive data matrix showed three distinct groups: 1) plants expressing *SlTDC1*; 2) plants expressing *SlT5H* and 3) plant expressing together *SlTDC1* and *OsT5H*, *SlTDC1* and *SlT5H* (Figure 2.19A). The O2PLS-DA score scatter plot remarked the clustering observed in PCA (Figure 2.19B) and allowed to identify the molecules that correlated with one specific class (Figure 2.19C). Beyond serotonin, an unidentified *m/z* feature (222 *m/z*) that increased only in *SlTDC1+OsT5H* and *SlTDC1+SlT5H* plants but with levels lower than 10 folds (data not shown). These evidences indicated that SlT5H enzyme mainly converted tryptamine to serotonin, and thus can be considered a *bona fide* T5H.

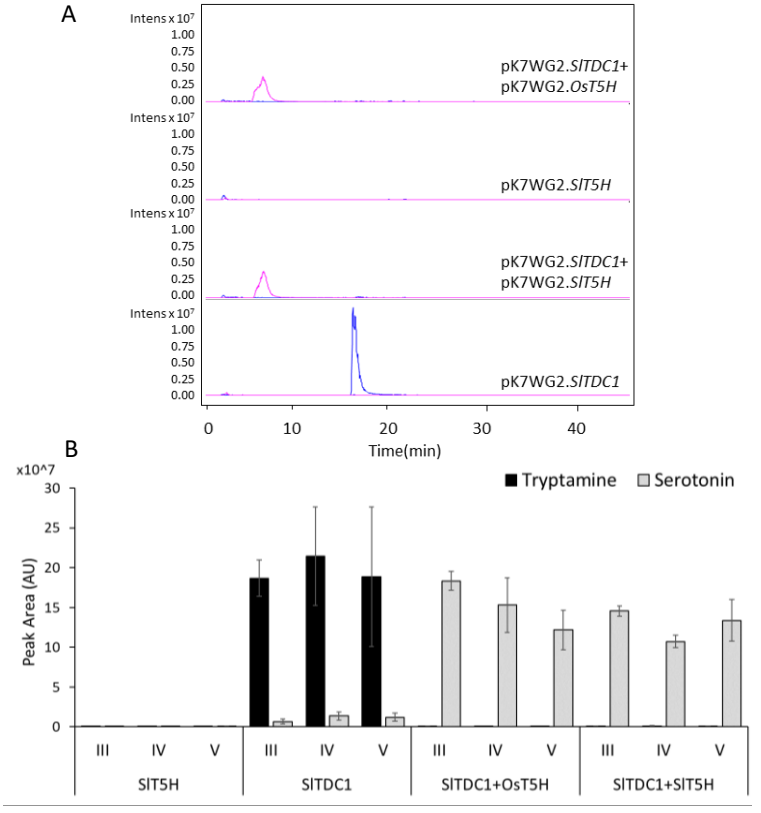

Figure 2.18 HPLC-ESI-MS analysis of leaf methanolic extracts of *N.benthamiana plants* used in *SlT5H* functional characterization assay. A) Extracted Ion Chromatograms (EICs) of tryptamine (144 *m/z*, Rt 19.2 min, blue) and serotonin (160 *m/z*, Rt 6.9 min, fucsia) diagnostic ions detected in positive ionization mode. All chromatograms are scaled to the highest signal intensity. B) Relative tryptamine and serotonin levels expressed as peak area, arbitrary units (AU). Bars indicate standard deviations (n=3).

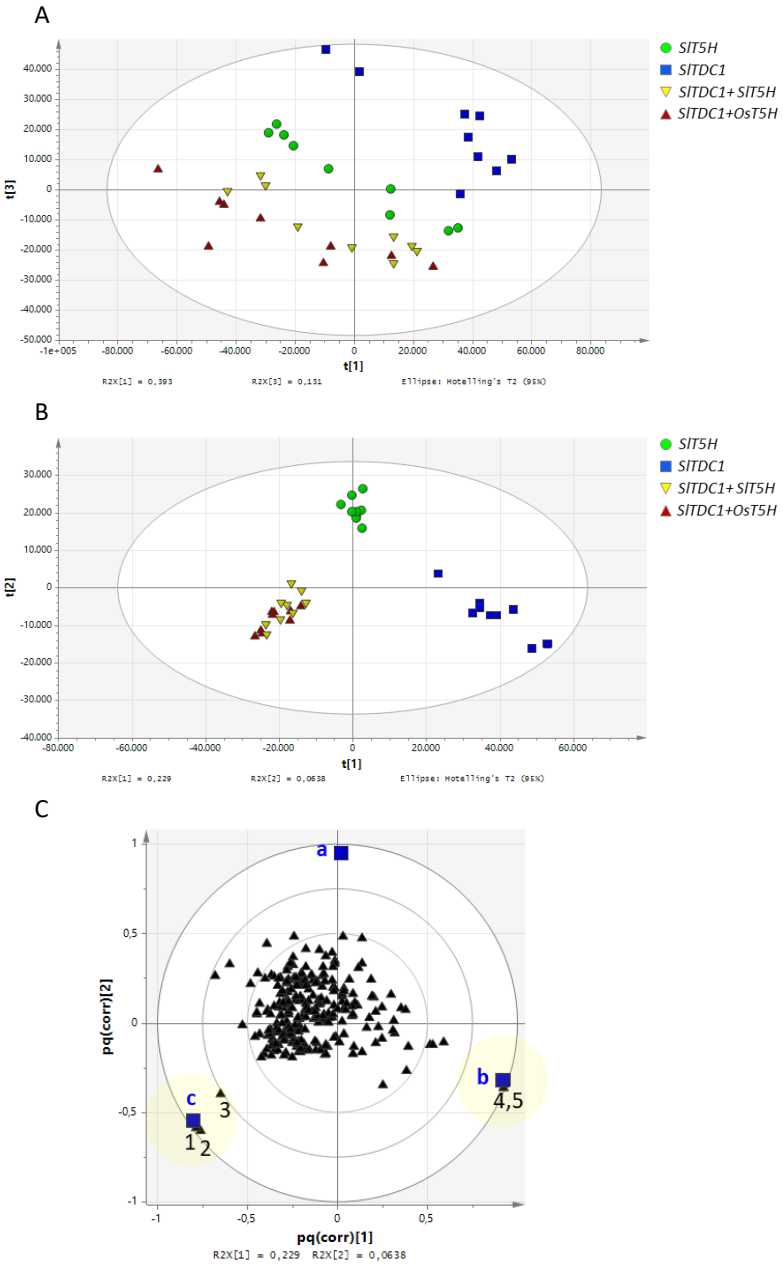

Figure 2.19 Multivariate statistical analysis of the untargeted metabolomics dataset (positive ionization) obtained from the HPLC-ESI-MS analysis of *Nicotiana benthamiana* plants transiently expressing *SlTDC1* and *T5H* genes. A) PCA score scatter plot; B) O2PLS-DA score scatter plot. C) O2PLS-DA correlation loading plot. Metabolites are represented by black triangles and classes by blue squares (a, *SlT5H*; b, *SlTDC1*; c, *SlTDC1+OsT5H* and *SlTDC1+SlT5H)*. Yellow areas include the most characterizing metabolites of each class: 1 and 2, serotonin molecular and diagnostic ions (177 and 160 *m/z* respectively); 3, unidentified metabolite (222 *m/z*); 4 and 5, tryptamine molecular and diagnostic ions (161 and 144 *m/z* respectively).

Discussion

Computational analysis of putative SlTDC candidates highlighted the need for a functional characterization of protein activity

The findings that various medicinal plants produce powerful antitumoral alkaloids by relying on tryptamine for the construction of their indole backbone, stimulated many authors to study the biosynthesis of this indolamine by focusing on the decarboxylation mechanism of tryptophan. Since the functional characterization of the first plant tryptophan decarboxylase (TDC), achieved in 1989 by De Luca et al., several other plant TDCs were in turn functionally characterized, thus providing a useful source of information for the identification of TDC orthologs in other species (Kumar, 2016).

In the first part of this chapter, four potential *Solanum lycopersicum* TDC candidates were identified following *in silico*-revealed homology towards the functionally characterized TDCs from *Catharanthus roseus, Oryza sativa* and *Capsicum annuum*. Similarly, two recent *in silico* investigations suggested the existence from two up to five different TDCs in this species (Hano et al., 2017; Pang et al., 2018).

The alignment of the four SlTDCs candidates with the major part of plant characterized TDCs so far revealed that SlTDC1, SlTDC2 and SlTDC3 shared many conserved residues typical of tryptophan decarboxylase enzymes (Torrens-Spence et al., 2018). This observation was in line with the information revealed by the aromatic L-amino acid decarboxylases (AADcs) phylogenetic tree, in which SlTDC1 and SlTDC2 clustered into a Solanaceae characteristic clade. This was in turn part of the exclusive TDC clade comprising both putative and characterized TDCs from twenty more species from different families including Rubiaceae, Apocynaceae and Poaceae. On the other hand, albeit Blastp homology analysis returned SlTDC4 among the TDCs candidate, this protein was observed to be phylogenetically closer to functionally characterized tyrosine decarboxylases (TyDCs) from *Petroselinum crispum*, *Papaver sominferum* and *Citrus reshni,* and also the identity levels towards the functionally characterized TDCs were the lowest among those displayed by the other TDC candidates. Moreover*,* SlDTC4 showed only the first putative catalytic amino acid typical of TDCs, whereas the other residues were noticed to be different. The absence of the PLP-binding residue, which is necessary for the decarboxylation process, and the second putative catalytic residue suggested that SlTDC4 might not be active.

Nevertheless, these automatic classifications are poorly reliable because of the high similarity between TDCs and TyDCs (Abu-Zaitoon, 2014). In fact, SlTDC3, which did not fall into the Solanaceae TDC clade, clustered together with the well characterized TDCs from C. annuum and O. sativa (Park et al., 2009; Kang et al., 2007_b), all showing more phylogenetic proximity to TyDCs than to other plant TDCs. Therefore, the results obtained from the computational investigation of the structural features and the phylogenetic relationships of the four identified SlTDCs candidates clearly pointed out the

need for a functional characterization assay in order to prove that these enzymes were effectively designated to the decarboxylation of tryptophan.

A 3-member TDC family is responsible for tryptamine production in tomato

Functional characterization of plant TDCs always started from the evaluation of the *in vitro* enzymatical properties following their expression in the bacterial heterologous system *Escherichia coli* and subsequent purification (De Luca et al., 1989, Lopez-Meyer and Nessler, 1997; Kang et al., 2007$_b$; Park et al., 2009; Liu et al., 2012; Charoonratana et al., 2013; Jadaun et aò., 2017). This approach allows to get very useful information to understand the enzyme kinetics such as the measure of Km, specificity towards different substrates or sensitivity to inhibitors and, furthermore, it offers the possibility to obtain protein crystals for deep structural characterization studies. Nonetheless, polypeptide trans-domain expression suffers of some drawbacks including the need of adapting the sequence to be expressed by a different codon usage and the risk of recombinant protein aggregation into inclusion bodies as well as the lack of typical plant post-translational modifications that may affect protein fate under different aspects (Yin et al., 2007). Since the interest of this PhD project was to focus on the biological roles of tryptamine and serotonin in plant biology, it was chosen to develop a functional *in planta* assay system to investigate tomato TDCs and T5H activities in a real plant physiological context. The functional *in vivo* characterization of the *Solanum lycopersicum* cv. Micro-Tom TDC candidates was, therefore, carried out through transient expression in a heterologous suitable host, i.e. *Nicotiana benthamiana*, which, beyond being another Solanaceae species, does not accumulate detectable levels of tryptamine (nor serotonin) in the leaves. The presence of the substrate for the decarboxylation reaction, i.e. tryptophan, together with the absence of the reaction product, i.e. tryptamine, was the essential advantage of the assay. With this approach it was demonstrated that SlTDC1, SlTDC2 and SlTDC3 were *bona fide* tryptophan decarboxylases since plants transiently expressing the coding sequences of these genes were able to accumulate tryptamine after III, IV and V days after infiltration (dpi). Moreover, plants transiently expressing the CDS of the *Actinidia chinensis* TDC gene (Commisso et al., 2019), i.e. the positive control plants, accumulated much lower levels of tryptamine than *SlTDC1* and *SlTDC2* infiltrated leaves, suggesting greater enzymatic performances by the two *Solanum lycopersicum* TDCs. *SlTDC3* expressing plants accumulated lower levels of tryptamine, yet keep increasing during the three days of sampling, respect to *SlTDC1* and *SlTDC2*, and this lower performance suggested the putative lower affinity towards tryptophan/lower activity. The real advantage of having developed this *in vivo* functional assay through an untargeted metabolomics approach relies on the fact that the high sensitivity of the LC-MS analysis allows to reveal even fine modifications in metabolite composition when complex metabolomes such as those of plants might be putatively perturbed by the transient expression of a heterologous biosynthetic gene. Even in the case that substrates other than tryptophan might be preferred by SlTDC3, no exclusive metabolites

accumulating only in *SlTDC3* expressing plants were revealed by multivariate statistical analysis of the untargeted metabolomics dataset.

Experimental evidences confirmed the non-TDC nature of putative SlTDC4 candidate

The failure in the amplification of *SlTDC4* cDNA from several Micro-Tom specimens was in line with what reported from various sources. In a recent work, for instance, the *in silico* analysis based on RNA-seq data of tomato cv. Heinz 1706 and quantitative Real Time-PCR experiments on tomato var. zhefen702 showed that *Solyc03g044120* was not expressed in different tissues and organs of this species (Pang et al., 2018). Therefore, it was decided to clone *SlTDC4* by using genomic DNA of Micro-Tom and it was observed that *N. benthamiana* plants transiently expressing *SlTDC4* did not show detectable levels of tryptamine, although the presence of the corresponding transcript in the agroinfiltrated leaves was demonstrated. This result suggested that the *SlTDC4* gene from Micro-Tom does not codify for a tryptophan decarboxylase. As suggested by the *in silico* translation of the transcript-derived cDNA clone, it was hypothesized that the lack of the C-terminal region in the Micro-Tom *SlTDC4* might compromise the decarboxylation process. Therefore, the *SlTDC4* CDS deposited in SGN database (i.e. the *Solyc03g044120*), which included the C-terminal region but lacked the PLP-binding site as well, was cloned. The corresponding mRNA was observed in *N. benthamiana* plants and tryptamine was not detected, suggesting that even *Solyc03g044120* does not codify for a tryptophan decarboxylase. The presence of a different substrate specificity residue (serine instead of a glycine; Torrens-Spence et al., 2014) in the C-terminal region of Solyc03g044120, as well as the putative functional annotation of the *Niben101Scf02857g02001.1* ortholog detected while looking for its transcript in *N.benthamiana*, suggested that this gene could be involved in tyrosine decarboxylation. This final assessment was furtherly supported by the clustering of Solyc03g044120 closer to other TyDCs in the phylogenetic tree.

Altogether, the experimental evidences shown in this chapter strongly suggest that SlTDC4 is not a tryptophan decarboxylase and, although further analysis and genetic investigation are needed, it could be hypothesized that *SlTDC4* might be a pseudogene in *Solanum lycopersicum*. This last statement derives from the following observations: a) both Micro-Tom *SlTDC4* and Heinz1706 *Solyc03g044120* seem not to be expressed in tomato; b) the amino acid sequences lack specific key residues putatively responsible for cofactor binding ; c) the fact that the 52-bp intronic region of the Micro-Tom *SlTDC4* gene was not spliced out once transcribed in *N. benthamiana* could derive from the fact that the sequence might have lost throughout evolution the recognition sites necessary to splicing proceeding, which is a typical feature of some classes of pseudogenes (Zhu & Niu, 2013).

One *SlT5H* gene mediate the conversion of tryptamine to serotonin in tomato

Metabolomics analysis of *Solanum lycopersicum* (Chapter 3) and several literature reports demonstrated the ability of this species to accumulate serotonin with different organ and developmental stage-specific patterns (Islam et al., 2016; Hano et al., 2017). The occurrence of serotonin strongly suggests the presence of a gene involved in the conversion of tryptamine to serotonin. Simultaneously to this PhD thesis work, Hano and colleagues suggested that tomato might possess an orthologous of the *Oryza sativa* tryptamine 5-hydroxylase gene (*OsT5H*, Fujiwara et al., 2010). By performing *in silico* analysis only, they revealed a strong similarity between the two amino acid sequences and that both belonged to the CYP71 group of the cytochrome P450. Moreover, although further analyses are required to clarify this aspect, it was hypothesized that SlT5H, as it was suggested for OsT5H, could be targeted to the ER (Fujiwara et al., 2010).

The functional characterized of SlT5H activity was performed by relying on the same *in vivo* plant assay adopted for SlTDCs characterization. The untargeted metabolomics analysis revealed that *N. benthamiana* plants agroinfiltrated with both *SlTDC1* and *SlT5H* were able to accumulate serotonin, thus confirming the identity of SlT5H as Tryptamine 5-Hydroxylase. Moreover, the evidence that tryptamine was detected only in trace amounts as residual substrate in these plants suggested a high rate of conversion and, thus, a great enzymatic performance by both SlT5H and OsT5H. Finally, plants transiently expressing *SlTDC1* accumulated low but still significant levels of serotonin and, therefore, the presence of a non-specific hydroxylase able to recognize tryptamine as substrate in *N. benthamiana* plants was hypothesized.

Conclusions

The work presented in this first experimental part of the thesis provides essential evidences to the identification of tomato genes that were recently speculated to be involved in tryptamine and serotonin production (Hano et al., 2017) and, moreover, it stresses the fact that homology-based research is a useful yet insufficient tool to assign gene function if not coupled to accurate functional analysis (Pang et al., 2018).

The proposed *in vivo* functional assay based on the transient heterologous expression of putative tomato tryptophan decarboxylase and tryptamine 5-hydroxylase proteins from *Solanum lycopersicum* in the indolamine non accumulator-host *Nicotiana benthamiana* was demonstrated to be a very reliable technique that finally confirmed the presence of a small family of three *bona fide TDCs* genes and of one *bona fide T5H* gene in *Solanum lycopersicum*. The conversion of tryptophan to tryptamine mediated by the three TDCs resulted in remarkably different tryptamine levels in *N. benthamiana* plants which might indeed reflect distinct enzymatic properties, representing an issue that deserves further investigations through in *in vitro* biochemical assays.

Chapter 3

Development of a gene expression and metabolite accumulation atlas for the preliminary investigation of the biological roles of the tomato serotonin pathway

Abstract

Plant tryptamine and serotonin have long been considered as mere metabolic intermediates in the biosynthetic pathway of other secondary metabolites such as indole-alkaloids and melatonin. Nonetheless, by exploiting high-resolution techniques for the analysis of plant metabolomes (Kueger et al., 2012), it was observed that melatonin is generally accumulated at very low levels in plant tissues while serotonin and tryptamine can be accumulated in some plant species at considerable higher amounts. This difference is particularly marked in the reproductive organs such as the fruit, in which melatonin ranges at the ng/g scale (Nawaz et al., 2016) against the thousand times more concentrated tryptamine and serotonin (up to hundreds of µg/g of fresh weight; Islam et al. 2016; Erland et al., 2016). Such an investment of resources must result in a concrete advantage for the tryptamine/serotonin accumulating plants. However, still little is known about the biological roles of these molecules and their biosynthetic genes. Plant *TDCs* have been shown to be active in different organs and tissues, sometimes being induced by different types of stresses when multiple *TDC* genes were found within the same species. In the previous chapter the existence of three tomato *TDC* genes and of one *T5H* gene was demonstrated. In order to investigate if such gene redundancy reflects into different biological functions in the plant, gene expression analysis coupled to targeted metabolomics analysis of tryptamine and serotonin in various Micro-Tom organs collected at different stages was performed. Briefly, *SlTDC1* was found to be mainly active during fruit development, *SlTDC2* was expressed only in the vegetative aerial organs and in the very early reproductive phase, whereas *SlTDC3* was ubiquitously expressed at different levels. Serotonin amounts in plant organs largely exceeded those of tryptamine except in the fruit. On the other hand, complex non-correlating accumulation and expression gradients were observed along the longitudinal axis of Micro-Tom plants making the function of these genes in leaves and stems a very intricate yet attracting issue.

Introduction

Tryptamine and serotonin biosynthesis are mediated in plants by the activity of *TDC* and *T5H* genes. The attention of plant biologists has been focused for years on the former gene, mainly from a biotechnological rather than a botanical perspective, with the aim to improve the channelling of the amino acid tryptophan into the production of attractive indole-alkaloid compounds. Much information about TDC enzymatic properties and gene regulation was therefore collected from both exogenous administration of tryptamine, or its precursor, and elicitation of *TDC* in plant cell cultures and from metabolic engineering approaches through heterologous expression of characterized plant TDCs, yet without putting much attention into the biological function of this gene or of its related product, tryptamine, in the real plant physiological context (Merillon et al., 1986; Songstad et al., 1990; Islas et al., 1994; Canel et al., 1998; Geerlings et al., 1999; Withmer et al., 2002). Later, more and more attention was put in understanding the mechanisms that drive melatonin production in plants leading to the identification of tryptamine and serotonin as metabolic intermediates of this high-valuable indolamine (Murch et al., 2000; Kang et al., 2007$_a$; Back et al., 2016). Since then serotonin, yet not tryptamine, started to be investigated in deep and several types of approaches, most of whom relying on exogenous serotonin administration, resulted in a plethora of observations supporting this compound to be active at multiple levels within the plant, from the regulation of plant morphogenesis and architecture likely though hormone cross-communication to environmental adaptation, regulation of circadian rhythms, improvement of the antioxidant status and response to different types of stress. All these putative activities of serotonin have been extensively reviewed by Erland and co-workers in the past five years, which were often reported together with functional information related to melatonin and other downstream serotonin phenolic derivatives, e.g. feruloyl-serotonin and coumaroyl-serotonin (Erland et al., 2015-2019). Various authors strongly emphasized the suggested involvement of tryptamine and serotonin in stress response. *TDC* genes from *Camptotheca acuminata* and *Capsicum annuum* that are usually not expressed in plant tissues are, in fact, strongly induced upon treatment with pathogen elicitors (López-Meyer & Nessler, 1997; Park et al., 2009). Moreover, recent findings supporting the role of serotonin as mediator in the stress response were provided by experimental evidences in *Oryza sativa*. Serotonin over-production in vegetative tissues has been reported to occur under particular conditions in rice. Normally, rice leaves contain about 0.5 µg/g fw of serotonin but when infected by a fungal pathogen or during the senescence process this amount can rise up, respectively, to about 40 µg/g fw in leaf necrotic areas (Ishihara et al., 2008) and 350 µg/g fw in the senescent leaf tip, consistently with an increase in *TDC* expression (Kang et al., 2009$_a$). Moreover, in rice *sl* (i.e. Sekiguchi lesion) mutants that are unable to convert tryptamine to serotonin, leaves inoculated with the fungus *Magnaporthe grisea* (Ueno et al., 2003; Fujiwara et al.,

2010) or *Bipolaris oryzae* (Ishihara et al., 2008) showed an increased susceptibility towards the pathogens and formed lesions without a typical brown material deposition. The exogenous administration of serotonin restored the resistance against pathogens and the typical colour of the necrotic lesions in *sl* plants, strongly suggesting a role of serotonin in the activation of the immune responses (Fujiwara et al., 2010). Tryptamine, on the other hand, although it seems to be not effective in plant protection from fungal pathogens in rice, was demonstrated to have anti-feeding and anti-ovipositor activity against the larvae of some herbivore insects (Thomas et al.; 1995,1998). However, the existing dynamics between the activity of *TDC/T5H* genes and the production of tryptamine and serotonin as well as their functions *in vivo* are still far from being clearly understood.

Serotonin production in plants, contrarily to tryptamine, has been extensively reviewed in the last years witnessing a wide range of concentrations that vary according to plant species or cultivars, plant organs and tissues as well as the fruit maturity stage (Erland et al., 2019; Ramakrishna et al., 2011). Nonetheless, although there are more and more evidences of the high amounts of this indolamine in the fruit of several and commonly consumed plant species, the investigation of the biological roles of serotonin in this organ have never been taken in account by researchers. The accumulation pattern of serotonin, together with the expression of two tomato *TDCs* and *T5H*, has been recently investigated, yet only in developing and ripening fruits of tomato and not in the whole plant, whereas current literature data on tryptamine content refer only to the ripe fruit (Hano et al., 2017: Islam et al., 2016). Studying the accumulation pattern of secondary metabolites in both spatial and temporal terms, i.e. organs/tissues and developmental phases, might tell much of their putative involvement in plant physiological functions and represents often a starting point in the investigation of their biological role. In this chapter a detailed picture of the expression of all the biosynthetic genes involved in tryptamine and serotonin production in relation to their accumulation within the Micro-Tom plant is presented.

Materials and methods

Plant material and sampling procedure

Seeds of *S.lycopersicum* (cv. Micro-Tom) were sown in a 4:1 mixture of peat and sand and grown in a growth chamber at 25°C with a 15h/9h light/dark photoperiod. One month after germination, plants at the flowering stage were used for sampling roots, hypocotyl, epicotyl, cotyledons, first leaves following cotyledons, true leaves from six different nodes, the stem (by keeping separate the internodes identified by the various nodes), flower buds and flowers. Roots were further separated into primary root, primary-proximal secondary root and primary-distal secondary root. Following fruit set, fruits were collected at various developmental and ripening phases based on the observation of the phenological stage: immature green (i.e. the green berry still growing in size), mature green (i.e. the green fruit at his maximum size as still unripe), early breaker (i.e. the green-white/yellow fruit), late breaker (marked by comparison of red-orange turning), ripe and over-ripe. Immature green together with mature green fruits and ripe together with over-ripe fruits were furtherly collected and dissected to sample also peels, flesh and seeds.

All samples consisted of three biological replicates, each one represented by a pool of material collected from five distinct plants. The samples were immediately frozen in liquid nitrogen and grinded to fine powder by using an A11 basic analytical mill (IKA-Werke, Staufen, Germany). The powders were stored at –80°C till metabolite or RNA extraction.

Metabolomics

Metabolite extraction and sample preparation for targeted metabolomics analysis

For each sample, 100 mg of frozen powder was extracted in 1 mL of a 2:1 (v/v) chloroform-methanol solution (LC-MS grade, Honeywell) adding 150 µL of ultrapure water (LC-MS grade, Honeywell) to allow phase separation. The samples were mixed vigorously for 30 sec, sonicated at 40 KHz in an ultrasonic bath (Sonica® Ultrasonic Cleaner, SOLTEC) at 4°C for 15 min and centrifuged (16000 rcf, 15 min, 4°C). The upper methanolic phase was recovered and the volume for each sample was annotated. In order to give a proper signal to be detected in the UPLC-ESI-MS analysis, the samples were differentially diluted (according to the type of original matrix) in methanol and a further 1:2 dilution with an aqueous solution containing known amounts of deuterated (d4) tryptamine and serotonin (Sigma-Aldrich) was performed prior to the injection. The spiking of the deuterated molecules was done in order to evaluate the levels of the two metabolites overcoming the possible matrix effect, by comparing the signals of endogenous tryptamine and serotonin to those of the related deuterated compounds. The

final hydro-alcoholic mixtures were passed through Minisart RC4 filters (0.2 µm pores) and 1 µL was injected into the UPLC device.

Detection and quantification of tryptamine and serotonin by UPLC-ESI-MS

An Acquity I Class UPLC system (Waters, Milford, MA, USA) was connected to a Xevo G2-XS Q-ToF mass spectrometer (Waters) featuring an electrospray ionization (ESI) source operating in either positive or negative ionization mode and was controlled by MassLynx v4.1. All extracts were injected into a Waters Acquity UPLC BEH C18 column (2.1 mm × 100 mm, 1.7 µm) kept at 30 °C and the mobile phases consisted of 0.1% formic acid in water (A) and acetonitrile (B). The initial conditions were 99% A and 1% B, and the following elution profile was applied: 0–1 min, 1% B; 1–10 min, 1–40% B; 10–13.50 min, 40–70% B; 13.50–14.00 min, 70–99% B; 14.00–16.00 min, 99% B; 16.00–16.10 min, 99–1% B (initial conditions). Subsequently, the system was equilibrated in 99% A and the elution was complete after 20 min. The flow rate was set to 0.350 mL/min. Samples were kept at 8 °C and randomized. A quality control (QC) sample was prepared by mixing equal parts of each sample in order to check the UPLC-Q-ToF performance along the whole experiment. QC was injected after nine samples had been analysed. The ion source parameters were: capillary voltage 0.8 kV, sampling cone voltage 40 V, source offset voltage 80 V, source temperature 120 °C, desolvation temperature 500 °C, cone gas flow rate 50 L/h and desolvation gas flow rate 1000 L/h. Nitrogen gas was used for the nebulizer and in desolvation whereas argon was used to induce collision-induced dissociation. An MS method was created to acquire data in continuum mode using a fixed collision energy in two scan functions. In function 1, the low energy was disabled, whereas in function 2 the high energy was set to 35 V. In both functions, the Xevo G2-XS was set to perform the analysis within the range 50–2000 *m/z* and with a scan time of 0.3 s. The lock mass solution used as "calibrator" to verify the accuracy of the mass spectrometer consisted of a 100 pg/µL leucine-enkephalin solution (Waters) injected with a flow rate of 10 µL/min, generating a signal of 556.2771 in positive mode and 554.2615 in negative mode.

MassLynx v4.1 (Waters) was used to manually extrapolate the peak areas relative to the tryptamine and serotonin signals and the corresponding deuterated commercially authentic standards. Peak extrapolation was based on the following *m/z* values, previously chosen after analysis of the commercial standards: 160.0777 for serotonin and 164.1009 for d4-serotonin; 144.0863 for tryptamine and 148.1061 for d4-tryptamine. These *m/z* values corresponded to the highest in-source generated fragments detected in positive ionization mode.

To calculate the amounts of tryptamine and serotonin in the samples, two 8-point calibration curves (r2=0.99) were built by analysing at the UPLC-ESI-MS different solutions with increasing amounts (within 1-1000 pg) of d4-tryptamine and d4-serotonin.

Molecular biology

RNA extraction and cDNA synthesis

Total RNA was extracted from 50-150 mg of plant material according to the type of organ or tissue by using the Spectrum™ Plant Total RNA Kit (Sigma-Aldrich). RNA quality was checked by considering Abs_{260}/Abs_{280} (1.8-2.2) and Abs_{260}/Abs_{230} (1.7-2.2) and samples not matching these requirements were treated with 1/3 volume of 7.5 M LiCl precipitation solution (ThermoFisher) and resolubilized according to manufacturer's instructions. RNA integrity was checked by gel electrophoresis on 2% agarose. Following treatment with the Ambion® TURBO DNA-free™ DNase Treatment and Removal Reagents (Life Technologies, Carlsbad, USA), SuperScriptIII Reverse Transcriptase (Thermo Fisher) was used to synthesize cDNA from 2 µg total RNA from each sample by oligo(dT) transcription initiation. The newly formed cDNA was checked through PCR by amplifying a 100-bp region with primers designed on the constitutive *SlCAC* gene (*Solyc08g006960.2.1*; González-Aguilera et al., 2016).

Expression analysis of SlTDCs and SlT5H genes by q Real-time PCR

A 1:10 dilution of cDNA served as a template in quantitative Real-time PCR (q Real-time PCR) analysis to assess the expression levels of the *SlTDC1*, *SlTDC2*, *SlTDC3* and *SlT5H* genes by referring to the constitutive *SlCAC* calibrator gene. The primers used to generate amplicons of about 100 bp from the coding region of the genes were designed using PRIMER3 software and are listed in Table 3.1. The 25 µL reaction was performed in triplicate for each sample on 96-well plates using the GoTaq®qPCR Master Mix (Promega, Madison-WI, USA) according to manufacturer's instructions. In each plate five samples were analysed, each to be tested for the expression of *SlTDCs*, *SlT5H* and *SlCAC*. A cDNA pool with the contribute of the cDNA from all samples was also tested in order to normalize expression data among the different analysis. The cycling conditions were set as follows: initial denaturation step of 95°C for 2 min followed by 40 cycles of denaturation at 95°C for 15 s, annealing at 60°C for 30 s and extension at 60°C for 30 s. The amplification process was followed by a melting curve analysis, ranging from 55°C to 95°C, with temperature increasing steps of 0.3°C every 15 s. The q Real-time PCR analysis was carried out with the StepOne Plus instrument (Applied Biosystems, Foster City - CA, USA). Raw data were processed with the LinRegPCR software to determine baseline and threshold cycles (Ct). Transcript levels were expressed as MNE (mean normalized expression) by relative Ct comparison with the *SlCAC* calibrator gene as described by Muller et al. (2002).

Integration of metabolomics and expression data was performed by evaluation of Pearson correlation coefficient calculated with Excel software (Microsoft).

GoI	Primer name	5'-3' sequence	Tm (°C)	Amplicon (bp)
SlTDC1	RT-SlTDC1 for	CCACTTCCACTACAGCCGTCG	62.99	104
	RT-SlTDC1 rev	ACATGCGCTCCCTCCATAAGC	62.85	
SlTDC2	RT-SlTDC2 for	TCCGATCCCATGTTTGATGTCGT	62.25	100
	RT-SlTDC2 rev	ACTTGGCCCGATGTAGCTCAAAA	62.43	
SlTDC3	RT-SlTDC3 for	CCGGGGCTATATGAATGGTGTCG	63.03	103
	RT-SlTDC3 rev	AGGCGAGAGACCCAGTTCCTG	63.56	
SlT5H	RT-SlT5H for	CGGCCAAATTCCGACTCTAA	62.47	105
	RT-SlT5H rev	TGAGCTGCAATGATTTGTGGA	62.70	
SlCAC	RT-SlCAC for	GGGTTGTTACATCACCAAAGC	62.48	121
	RT-SlCAC rev	GTGCTGGTGTGATTGCATCC	62.85	

Table 3.1 List of primers used in q Real-time PCR analysis for the evaluation of gene expression.

Results

Experimental design

Micro-Tom plants were grown for about one month till flowering and used to collect samples for both metabolomics and gene expression analysis. Each of the three biological replicates consisted in a pool of the same organ collected from 5 different plants. The organs were chosen by considering their physiological function together with the developmental stage. Roots were distinguished among primary embryonal root (PR) and secondary roots, whose portion proximal to the primary root (PSR) was furtherly distinguished from the distal part (DSR) that includes also the root apical meristem and the absorption zone. Cotyledons (Co) were collected separately, as well as the first true leaves (FL) that in tomato have a distinct morphology from the following true leaves. Leaves from six different nodes (L1 to L6) were collected by considering them as separate samples, as well as the six internodes (In1 to In4; In5 and In6 were joined together) identified by the former, the hypocotyl (Hy) and the first internode of the epicotyl (Ep). Flower buds (FB) and fully open flowers (at the stage of anthesis, FA) were also collected. Then, to investigate in deep the presence of tryptamine and serotonin and their accumulation trends throughout fruit formation, development and ripening, another group of plants was grown and let to set fruits that were collected till the end of the life cycle, i.e. from one month and half to four months from germination. Basing on phenological signs, fruits were collected at crucial phases including the immature-green developing berry (IG), the mature-green berry at the end of fruit development (MG), the breaker (B) and colour turning (T) berry at the physiological switch in between development and ripening, the ripe berry (R) and the over-ripe berry representing the fruit senescence phase (OR). Moreover, given the interest in unravelling the functions of the two indolamines in the fruit, unripe (IG together with MG) and ripe (R together with OR) fruits, representative of the developmental and ripening phases respectively, were furtherly collected and dissected to sample peels (exocarp, Ec), flesh (mesocarp, Mc) and seeds (S). A schematic representation of the sampling is depicted in Figure 3.1.

Targeted metabolomics revealed distinct distributions of tryptamine and serotonin in different organs and developmental stages of tomato plant

Tryptamine and serotonin were extracted from Micro-Tom samples by relying on a standard method suitable for the extraction of high and medium-polar metabolites and detected, following separation in UPLC, with a high-resolution mass spectrometer (Q/ToF). The absolute quantification of these indolamines in the samples was performed prior the construction of a calibration curve with deuterated standards of tryptamine and serotonin (d4-tryptamine/d4-serotonin). Matrix effect,

evaluated by spiking known amounts of d4-tryptamine/d4-serotonin in the measure of 20% respect to the estimated abundance of the endogenous molecules, was negligible (data not shown).

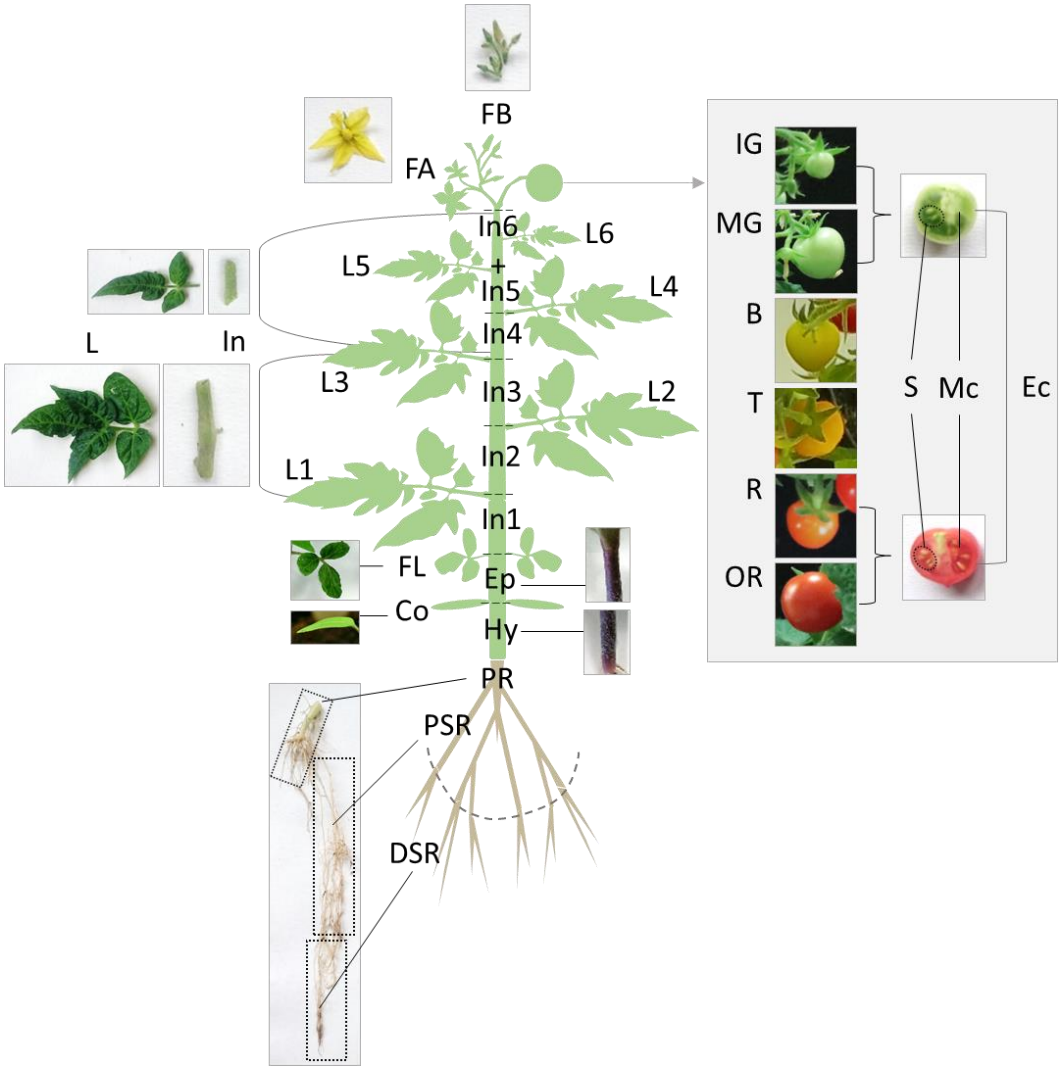

Figure 3.1 Schematic representation of the sample design for metabolomics and expression analysis. Vegetative organs: roots (PR, primary root; PSR, proximal secondary root; DSR, distal secondary root), stem (Hy, hypocotyl; Ep, Epicotyl; In, internode), cotyledons (Co), leaves (FL, first leaves; L, true leaves). Reproductive organs: flowers (FB, flower buds; FA, flowers at the anthesis), fruit (IG, immature-green; MG, mature-green; B, breaker; T, late breaker/turning; R, ripe; OR, over-ripe), dissected fruit (Ec, exocarp; Mc, mesocarp; S, seeds).

Tryptamine and serotonin accumulation in the vegetative organs and flowers

Major differences in the levels of the two indolamines in Micro-Tom were found in the vegetative organs revealing distinct accumulation patterns (Figure 3.2). By looking at the values reported to the fresh weight of plant material in Table 3.2, serotonin was accumulated in some organs up to 150 times

more than tryptamine which ranged, respectively in between 27.19-9322.02 and 1.60-337.60 ng/g of fresh weight. For both molecules, roots were the organs reporting the lowest amounts in which the accumulation trends were opposite while moving from the primary embryonal root to the distal part of secondary roots with tryptamine being most abundant in the latter. On the other hand, the highest levels of both indolamines were found in the leaves, featured by different accumulation trends between older leaves at the base of the plant and younger leaves close to shoot apex. In fact, while tryptamine showed a clear increasing accumulation gradient (Figure 3.2A), while moving along the longitudinal axis of the plant from the first leaves to the leaves of the last upper node, serotonin increased till the leaves of the fourth node and then sharply dropped in the leaves of fifth and sixth node. Moreover, for serotonin, another gradient opposite to the one found in the leaves was observed in the stem with the levels of this metabolite gradually decreasing moving from the epicotyl up to the last internodes (Figure 3.2B). In flowers, serotonin was about 6 times more abundant than tryptamine but no differences in the accumulation of both molecules were observed between the stage of flower buds and fully-open flower.

			Tryptamine (ng/g fw)			**Serotonin (ng/g fw)**		
		Id	Mean		SD	Mean		SD
Roots	Primary root	**PR**	1.60	±	0.63	183.15	±	88.25
	Proximal secondary root	**PSR**	3.35	±	0.83	146.57	±	28.54
	Distal secondary root	**DSR**	8.34	±	1.44	27.19	±	4.44
Stem	Hypocotyl	**Hy**	23.92	±	4.89	2808.37	±	88.61
	Epicotyl	**Ep**	76.33	±	7.10	6365.03	±	501.34
	Internode 1	**In1**	83.90	±	6.78	3695.51	±	146.27
	Internode 2	**In2**	76.55	±	5.41	2848.10	±	439.97
	Internode 3	**In3**	54.49	±	16.26	2184.30	±	359.12
	Internode 4	**In4**	55.64	±	12.65	2177.71	±	185.88
	Internode 5+6	**In5+In6**	63.79	±	9.44	1280.63	±	606.75
	Cotyledons	**Co**	11.37	±	6.69	1746.21	±	295.30
Leaves	First leaves	**FL**	73.45	±	2.59	4258.30	±	515.44
	Leaves 1	**L1**	68.66	±	12.42	5809.25	±	680.17
	Leaves 2	**L2**	82.37	±	15.49	7169.12	±	487.78
	Leaves 3	**L3**	127.30	±	25.57	8592.63	±	370.54
	Leaves 4	**L4**	217.38	±	38.39	9322.02	±	1377.22
	Leaves 5	**L5**	221.97	±	27.31	4428.07	±	1102.46
	Leaves 6	**L6**	337.60	±	21.12	1218.88	±	242.74
Flower	Flower buds	**FB**	95.43	±	18.38	737.16	±	171.25
	Flower (anthesis)	**FA**	123.07	±	39.03	758.54	±	538.48

Table 3.2 Tryptamine and serotonin amounts detected in Micro-Tom vegetative organs and flowers expressed as ng/g of fresh weight (fw). SD stands for standard deviation (n=3).

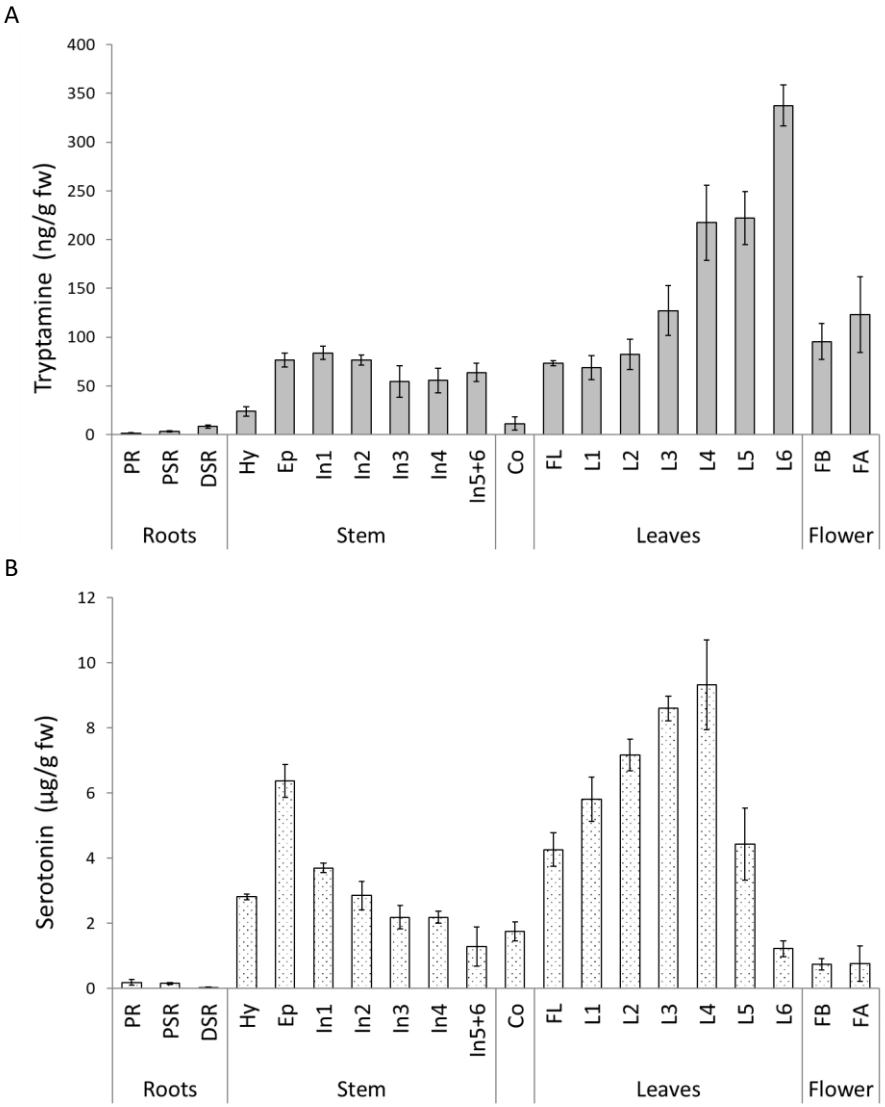

Figure 3.2 Quantities of tryptamine (A) and serotonin (B) detected in Micro-Tom organs by UPLC-ESI-MS analysis expressed as ng/g fw (fresh weight) or µg/g fw respectively. Bars represent standard deviations (n=3). Acronyms refer to the name of the samples presented in Table 2.2.

Tryptamine and serotonin accumulation during fruit development and ripening

Fruit was the sole Micro-Tom organ in which tryptamine levels were similar to those of serotonin. (Table 3.3, Figure 3.3 A). It is clearly visible that tryptamine was already present at the immature green stage, being even more abundant than serotonin, and increased at the mature green stage simultaneously to a rapid growth in fruit size. Then, its amount levelled off during ripening with a slight reduction in the over-ripe fruit. Serotonin was ten-times less accumulated in the immature green fruit with respect to tryptamine and then its levels burst toward the end of development, reaching the maximum at the onset of ripening, i.e. at the breaker stage, and remaining quite constant till fruit senescence.

		Tryptamine (µg/g fw)			Serotonin (µg/g fw)		
	Id	Mean		SD	Mean		SD
Fruit							
Immature green	**IG**	1.11	±	0.16	0.18	±	0.09
Mature green	**MG**	2.00	±	0.50	2.24	±	0.16
Breaker	**B**	1.53	±	0.11	5.58	±	0.89
Turning	**T**	2.12	±	0.39	5.17	±	0.47
Ripe	**R**	1.27	±	0.35	3.37	±	0.76
Over-ripe	**OR**	0.40	±	0.14	5.30	±	0.40

Table 3.3 Tryptamine and serotonin amounts detected in Micro-Tom fruits at various developmental and ripening stages expressed as µg/g of fresh weight (fw). SD stands for standard deviation (n=3).

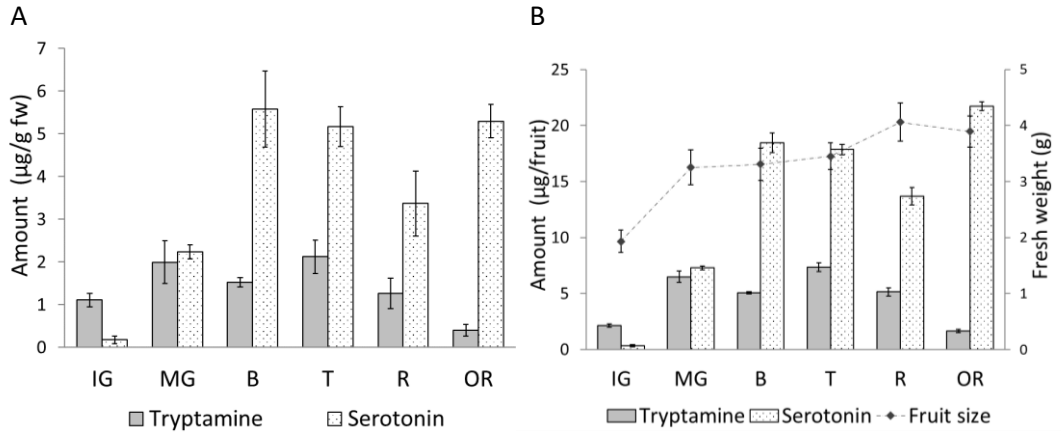

Figure 3.3 Quantities of tryptamine and serotonin detected by UPLC-ESI-MS in Micro-Tom fruits at different developing and ripening stages expressed as µg/g fw (fresh weight, A) or per whole berry (B). Bars represent standard deviations (n=3). Acronyms refer to the name of the samples presented in Table 3.3.

By normalizing the amounts of tryptamine and serotonin to the average fresh weight of the fruits at each stage, it was possible to express the content of these indolamines per whole fruit (Table 3.4, Figure 3.3 B). The fully-ripe berry fruit contained ~ 5 µg of tryptamine and ~ 14 µg of serotonin.

A further investigation (Table 3.5, Figure 3.4) was performed to unravel the distribution of these metabolites in the exocarp, the mesocarp and the seeds of Micro-Tom fruits in unripe (immature green and mature green stages) and fully-ripe berries (ripe and over-ripe stages). Seeds contained the highest levels of tryptamine and serotonin and only a slight increase of the latter was observed as the fruit ripened. Tryptamine was much less abundant in the pericarp respect to the seeds, showing the lowest amount in the skin. Similarly, serotonin content was less represented in the exocarp but in this tissue it was four times and twice the amount of tryptamine at the unripe and ripe phases respectively. A slight reduction was observed for both tryptamine and serotonin in the mesocarp after the ripening process.

		Id	berry weight (g)	Tryptamine (µg/fruit) Mean	SD	Serotonin (µg/fruit) Mean	SD
Fruit	Immature green	**IG**	1.93	2.14 ±	0.31	0.34 ±	0.18
	Mature green	**MG**	3.25	6.49 ±	1.63	7.29 ±	0.52
	Breaker	**B**	3.31	5.06 ±	0.36	18.46 ±	2.96
	Turning	**T**	3.45	7.33 ±	1.34	17.86 ±	1.60
	Ripe	**R**	4.06	5.14 ±	1.44	13.69 ±	3.10
	Over-ripe	**OR**	4.10	1.66 ±	0.57	21.72 ±	1.62

Table 3.4 Tryptamine and serotonin amounts detected in Micro-Tom fruits at various developmental and ripening stages expressed as content (µg) per whole fruit. SD stands for standard deviation (n=3).

		Id	Tryptamine (µg/g fw) Mean	SD	Serotonin (µg/g fw) Mean	SD
Unripe fruit (IG+MG)	Exocarp	**Ec**	1.06 ±	0.20	4.24 ±	0.44
	Mesocarp	**Mc**	4.17 ±	0.33	7.81 ±	1.44
	Seeds	**S**	7.57 ±	0.19	5.51 ±	1.09
Ripe fruit (R+OR)	Exocarp	**Ec**	1.37 ±	0.15	2.89 ±	0.08
	Mesocarp	**Mc**	2.65 ±	0.22	4.99 ±	0.58
	Seeds	**S**	8.33 ±	0.92	9.24 ±	1.54

Table 3.5 Tryptamine and serotonin amounts detected in different tissues of Micro-Tom fruits at the unripe (IG+MG) and ripe (R+OR) phases expressed as µg/g of fresh weight (fw). SD stands for standard deviation (n=3).

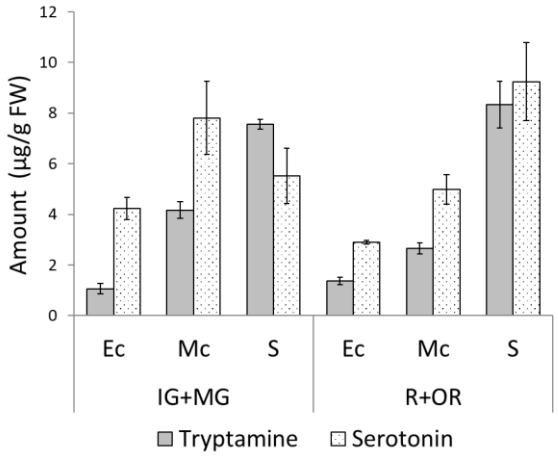

Figure 3.4 Quantities of tryptamine and serotonin detected by UPLC-ESI-MS in peels, flesh and seeds of unripe and ripe Micro-Tom fruits expressed as µg/g fw (fresh weight). Bars represent standard deviations (n=3). Acronyms refer to the name of the samples presented in Table 3.5.

Expression levels of SlTDCs and *SlT5H* revealed by q Real-time PCR

The same plant material analysed by UPLC-ESI-MS was used to investigate the expression patterns of *SlTDCs* and *SlT5H* genes. The RNA extracted from each sample served to produce the cDNA to be used as a template in quantitative Real-time PCR by using primers designed to obtain 100-bp amplicons. The relative transcript levels were reported for each gene as MNE (Mean Normalized Expression), which was calculated following comparison of Ct values measured for *SlTDCs* and *SlT5H* in the samples with those of the *SlCAC* housekeeping gene. The reliability of this gene as a reference for expression studies in tomato was recently demonstrated by Gonzalez and co-workers (2016).
The analysis reported marked differences in the expression of the tomato genes involved in tryptamine and serotonin biosynthesis highlighting both organ-specific ad developmental-specific patterns.

Expression patterns of SlTDC genes

SlTDC1, for instance, resulted expressed only during the reproductive phases. As reported in Figure 3.5 A, expression levels were low in the flowers and within the immature green berry but burst as the berry went through the end of the developmental phase at the mature green stage. This peak in expression was subsequently followed by a drop from the breaker stage till fully-ripe berry with a further increase in the over-ripe stage. Moreover, by looking at the pattern reported in different tissues of unripe and ripe berries, it was possible to notice that the highest levels of *SlTDC1* transcript were localized in the exocarp of the developing berry and, to a lesser extent, in the seeds. This pattern was maintained in the ripe berries and, also in this case, the transcript levels in the flesh were remarkably low.
In a way that was kind of complementary to the expression pattern of *SlTDC1*, *SlTDC2* (Figure 3.5 B) resulted expressed mainly in the aerial vegetative organs and the flowers of Micro-Tom plants, whereas extremely low levels were present within the primary root and the fruit. Interestingly, as it was previously observed for the accumulation of the relative indolamines, the expression of *SlTDC2* seemed to follow an increasing gradient in the stem, with very low transcript levels in the basal part of the plant that reached a maximum in the last internode. On the other hand, the expression of this gene was higher in the cotyledons and the oldest leaves of the plant, then it showed a sharp decrease immediately after the first node. In the flowers high levels of transcript were observed as well.

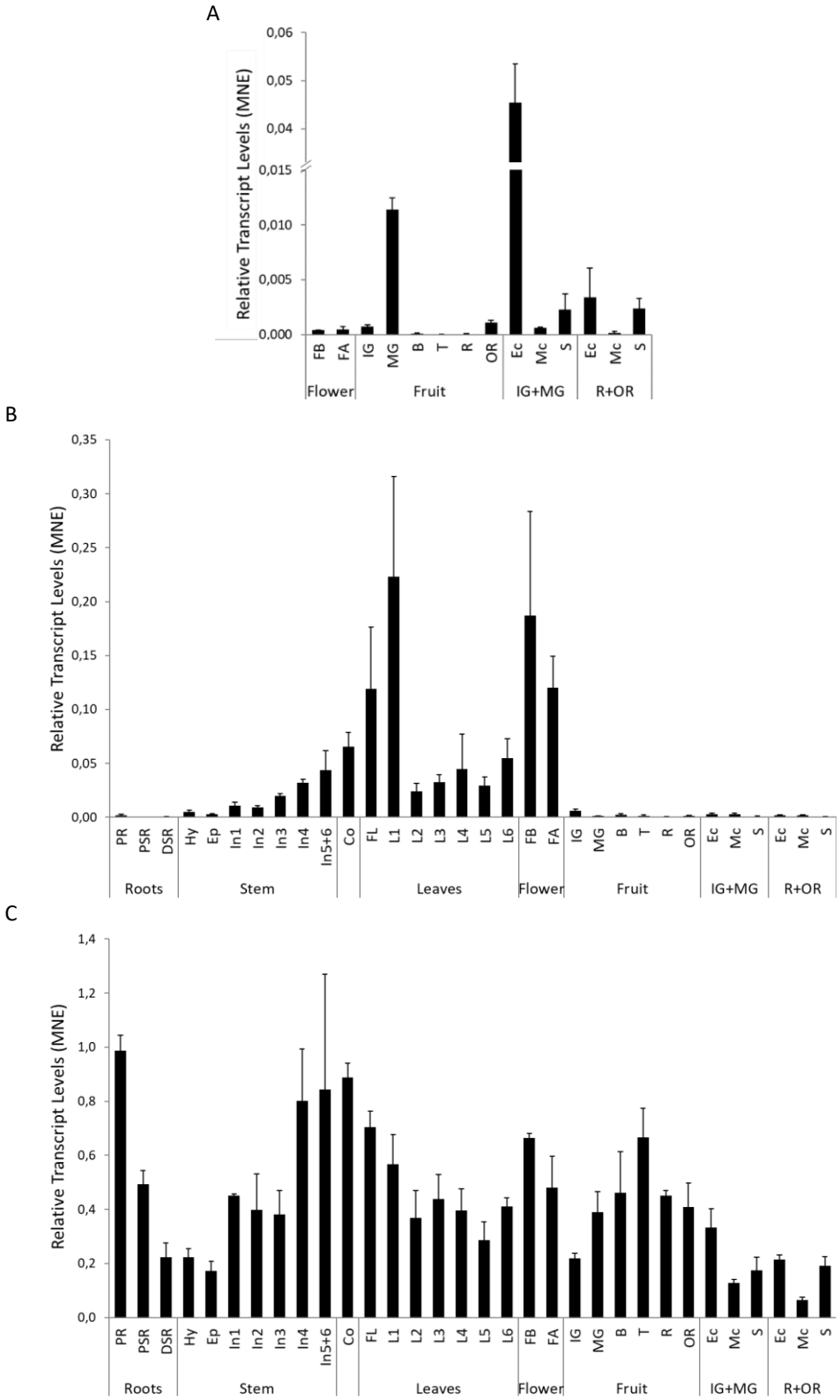

Figure 3.5 Expression levels of *SlTDC1* (A), *SlTDC2* (B) and *SlTDC3* (C) in Micro-Tom organs detected by q Real-time PCR analysis. Bars represent standard error (n=3). Acronyms refer to the name of the samples presented in Figure 3.1.

Distinctly from what observed for the previous *SlTDC* genes, *SlTDC3* was ubiquitously expressed in all plant organs analysed (Figure 3.5 C). Moreover, this gene was also expressed in the roots in a range similar to those observed in the other organs. Very interestingly, also for this gene the presence of expression gradients was noticed in both stems and leaves, acting once again in opposite directions: in the stem increasing transcript levels were observed from the hypocotyl to the upper internodes whereas for the leaves the expression was higher at the base of the plant and gradually decreased of about one half in the youngest leaves. *SlTDC3* was highly expressed in the primary root and lower but still significant transcript levels were observed in the secondary roots. Within the fruit, this gene showed increased expression following the end of berry development and peaked at the breaker and turning stages, phases in which, curiously, *SlTDC1* displayed extremely low expression. Also in this case, the flesh of both unripe and ripe berries showed less transcript levels respect to the peels and the seeds.

Expression pattern of SlT5H

As observed for *SlTDC3*, also *SlT5H* appeared to be ubiquitously expressed (Figure 3.6). For this gene, the highest transcript levels in the vegetative organs were observed in the primary root. A slight increase in the expression was observed in the stem from the hypocotyl to the third internode, followed by a decrease in the younger stem portion, thus mirroring the distribution of serotonin in the leaves. In all leaves and the cotyledons, the levels of the transcript were constant whereas in the flower buds it was slightly higher than in the flower at the anthesis. *SlT5H* was always expressed throughout fruit development and ripening peaking at the mature-green stage and then keeping constant till the over-ripe stage when a further significant increase in transcript levels occurred. Notably, as observed for *SlTDC1*, the exocarp of unripe berries had very high levels of *SlT5H* transcript.

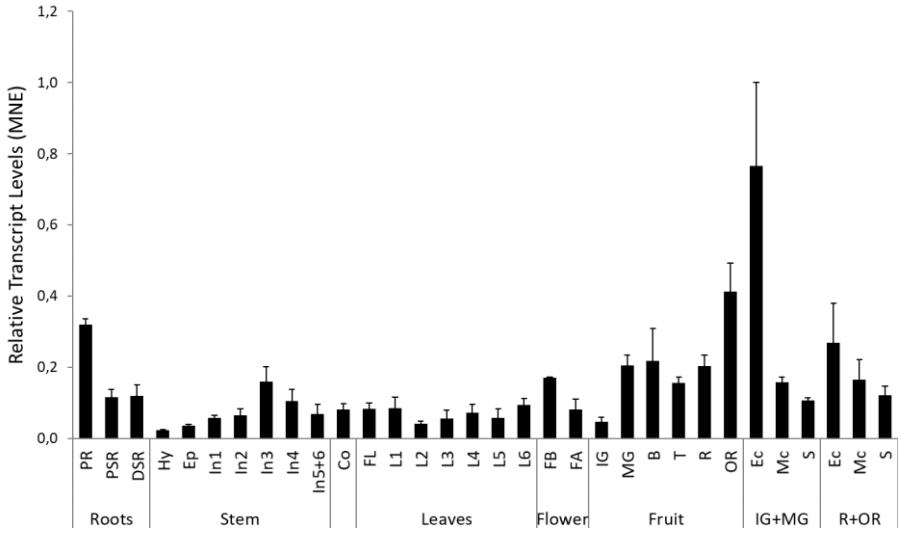

Figure 3.6 Expression levels of *SlT5H* in Micro-Tom organs detected by q Real-time PCR analysis. Bars represent standard error (n=3). Acronyms refer to the name of the samples presented in Figure 3.1.

Evaluation of the relationships among indolamines accumulation and the expression of their biosynthetic genes

To summarize and compare the results presented in the previous paragraphs, the relative accumulation and expression levels of tryptamine, serotonin, *SlTDCs* and *SlT5H* were represented by using a colour code in two heatmap atlas, one depicting the vegetative organs (Figure 3.7) and one relative to fruit development and ripening (Figure 3.8). Nonetheless, given the complex patterns observed for tryptamine and serotonin distribution and the expression of the relative biosynthetic genes in Micro-Tom organs, extrapolating information useful in determining the relationships among these actors might not be obvious. For this reason, metabolomics and expression datasets were further explored by looking for linear correlation among metabolite accumulation and gene expression through the calculation of Pearson correlation coefficient (PCC, Figure 3.9). By exploiting this approach, the expression of *SlTDC3* in roots which appeared consistent with that of *SlT5H* in the plant heatmap was demonstrated to highly correlate with the expression of the latter and also with the production of serotonin. Moreover, in the root apparatus, tryptamine had a very negative correlation with both *SlTDC3*, *SlT5H* and serotonin, indicating that as these genes are expressed and serotonin - although at very low levels - is produced, this indolamine is depleted, being canalized towards serotonin biosynthesis. In the basal leaves (from cotyledons to the leaves of the third node, L3) it was observed a positive correlation between tryptamine and serotonin and between *SlT5H* and *SlTDC2*. The levels of the two indolamines, indeed, increased in the basal leaves moving upwards along plant axis even if for tryptamine this increase was very slight compared to that of serotonin. In addition, these patterns were negatively correlated with the expression of *SlTDC3*. On the other hand, in the upper leaves (from fourth till sixth node) a strong negative correlation was observed between tryptamine and serotonin, due to the fact that the latter accumulated in the leaves up to the fourth node then rapidly dropped in leaves next to shoot apex. In these organs, also a positive correlation between *SlTDC3* and *SlT5H* was observed that was, anyway, not linked to indolamines accumulation. In the fruit no particular relationships were clear until PCCs were calculated by distinguishing the phases of fruit development and ripening. In unripe berries, for which PCCs were calculated on the dataset from IG, MG and B samples, the expression of *SlTDC1* showed high positive correlation with the accumulation of tryptamine whereas *SlTDC3* highly correlated with the expression of *SlT5H* and the accumulation of serotonin. Later, during the ripening phase, for which PCCs were calculated on the dataset from T, R and OR samples, tryptamine accumulation is strongly negatively correlated with *SlTDC1,* which is effectively not expressed if not in the over-ripe stage, but it rather slightly correlates with the expression of *SlTDC3*. Tryptamine also shows a strong negative correlation with *SlT5H* but, this in turn, does not positively correlates with serotonin.

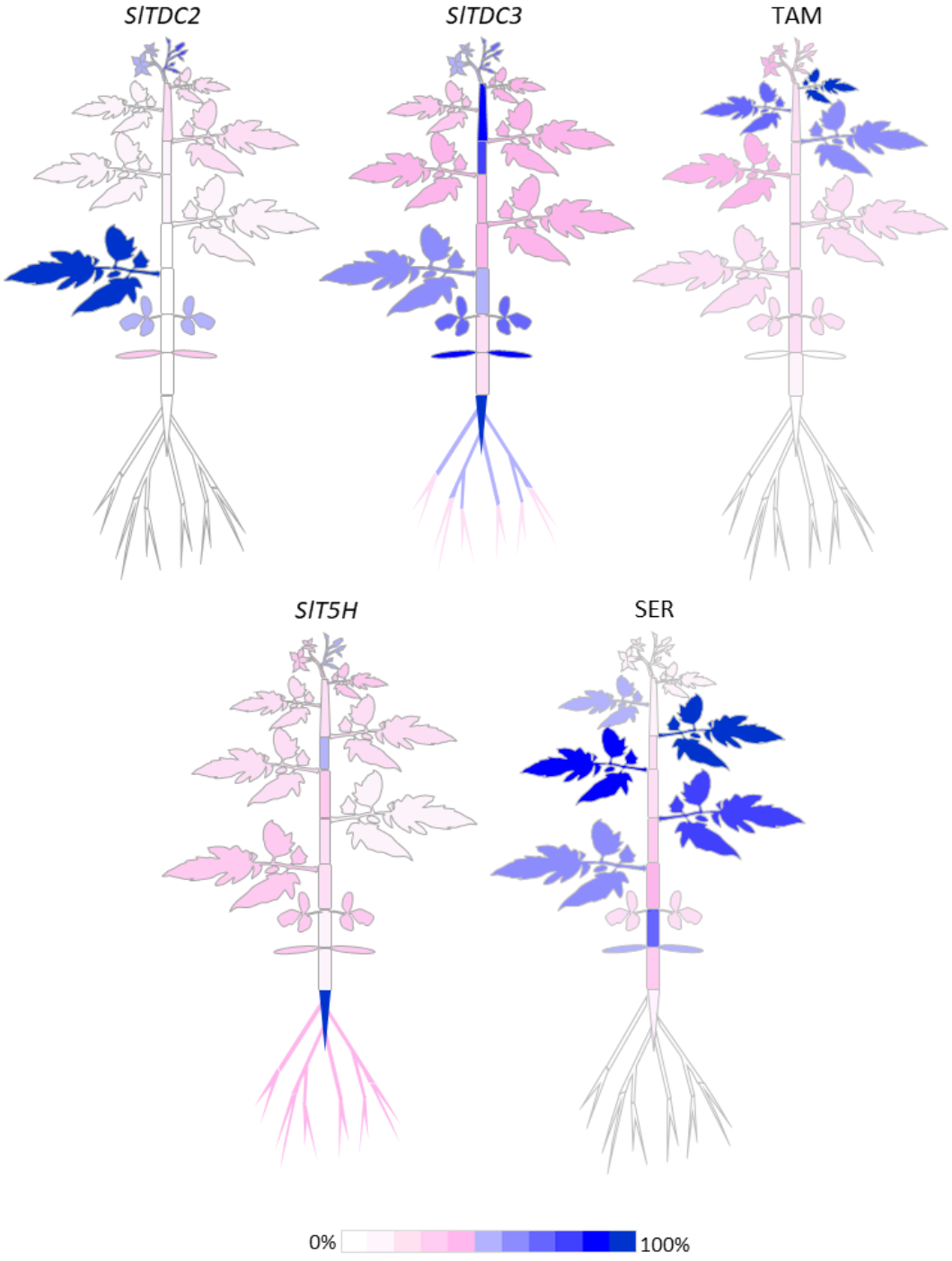

Figure 3.7 In-planta heatmap representing with a colour code the percentage of relative expression of *SlTDC/SlT5H* genes and the accumulation of tryptamine (TAM) and serotonin (SER). Each organ identified in this heatmap refers to the sampling design depicted in Figure 3.1.

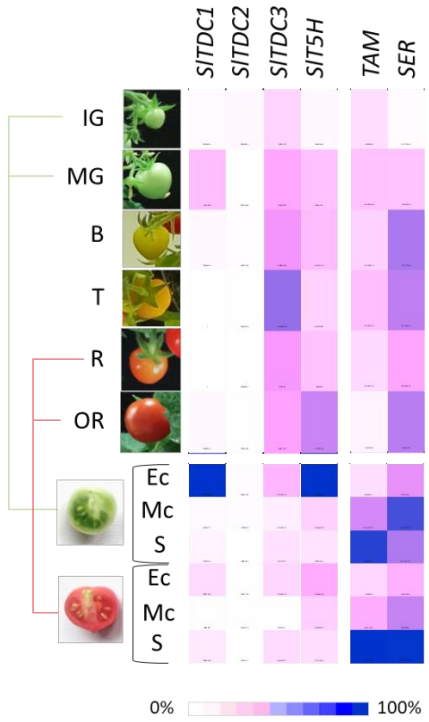

Figure 3.8 Heatmap representing with a colour code the percentage of relative expression of *SlTDC/SlT5H* genes and the accumulation of TAM/SER in Micro-Tom berries at different stages and within different tissues. Each stage/tissue identified in this heatmap refers to the sampling design depicted in Figure 3.1.

Roots	*SlTDC2*	*SlTDC3*	*SlT5H*	*TAM*
SlTDC3	0,52			
SlT5H	0,71	0,87		
TAM	-0,47	-0,82	-0,68	
SER	0,07	0,79	0,55	-0,78

Developing fruit	*SlTDC1*	*SlTDC2*	*SlTDC3*	*SlT5H*	*TAM*
SlTDC2	-0,46				
SlTDC3	0,30	-0,24			
SlT5H	0,35	-0,33	0,81		
TAM	0,78	-0,72	0,47	0,54	
SER	-0,08	-0,42	0,60	0,70	0,28

Basal leaves	*SlTDC2*	*SlTDC3*	*SlT5H*	TAM
SlTDC3	0,08			
SlT5H	0,71	0,22		
TAM	0,01	-0,63	-0,26	
SER	0,02	-0,78	-0,43	0,83

Ripening fruit	*SlTDC1*	*SlTDC2*	*SlTDC3*	*SlT5H*	*TAM*
SlTDC2	0,11				
SlTDC3	-0,27	0,37			
SlT5H	0,93	0,04	-0,21		
TAM	-0,79	0,18	0,67	-0,77	
SER	0,42	0,59	0,21	0,22	0,05

Upper leaves	*SlTDC2*	*SlTDC3*	*SlT5H*	TAM
SlTDC3	0,53			
SlT5H	0,49	0,81		
TAM	0,17	-0,04	0,44	
SER	0,00	0,21	-0,19	-0,77

PCC
-1.00 0 1.00

Figure 3.9 Heatmap representation of the Pearson correlation coefficients (PCC) calculated for genes and metabolites of the tomato serotonin pathway from the metabolomics and expression datasets.

Discussion

Tryptamine and serotonin show marked differences in quantity and distribution within tomato plant and fruit

In the first part of this chapter a detailed picture of the amounts of tryptamine and serotonin in *Solanum lycopersicum* cv. Micro-Tom was provided, focusing the attention not only in the fruit at various stages from early development to senescence but also in other vegetative and reproductive organs of the plant, i.e. roots, stem, leaves and flowers. The data collected contributed to improve the knowledge about the distribution of these indolamines in tomato plant, which has been investigated only within the fruit so far (Udenfriend et al., 1959; West, 1960; Feldman, & Lee, 1985; Hano et al., 2017) and provide, moreover, detailed information for tryptamine production in the whole plant which, to date, is still a missing piece in plant biology.

Tryptamine and serotonin are accumulated at very different levels in Micro-Tom organs

The targeted UPLC-ESI/MS analysis allowed to identify organ-specific and, in the fruit, tissue-specific trends in the accumulation of these compounds. Interestingly, it was observed that tryptamine reached considerable amounts only in the fruit (up to ~ 8.33 µg/g fw in the seeds) whereas in the rest of the plant its levels were much lower (up to ~ 0.34 µg/g fw in younger leaves). The fact that serotonin, instead, displayed amounts in some vegetative organs as high as in the ripening fruit (up to ~ 9.32 µg/g fw) is a hint that these two molecules could serve distinct functions in different parts of the plant. Other species including *Helianthus annuus*, *Mimosa pudica*, *Brassica oleracea, Cichorium intybus* and *Coffea canephora* accumulate similar or even higher amounts of serotonin in their leaves (~ 9-18 µg/g fw; Mukherjee et al., 2014; Giridhar & Ravishankar, 2009; Islam et al., 2016; Ly et al., 2008; Ramakrishna et al., 2012), whereas some others like *Lactuca sativa, Solanum tuberosum* and the medicinal plant *Hypericum perforatum* have a lower leaf content (~ 0.1-3 µg/g fw; Ly et al., 2008; Islam et al., 2016; Lavizzari et al., 2006; Engström et al., 1992; Murch et al., 1997).

The presence of indolamine accumulation gradients along the plant growth axis opens intriguing questions about their biological roles in the vegetative organs

Curiously, the different content in both tryptamine and serotonin observed in Micro-Tom leaves sampled at various nodes along the longitudinal axis of the plant strongly reflected the presence of an accumulation gradient for the two molecules. The fact that serotonin peaked at the fourth node and then sharply decreased in the leaves close to the terminal bud suggests that the detected gradient is not just a consequence of the mere dilution effect due to the major leaf expansion of older leaves. Conversely, tryptamine levels continuously increased in the two top leaves. Several reports suggest a

plausible protective effect of tryptamine against herbivores by interfering with insect reproduction as antioviposition and antifeedant agent or as inhibitor of larval development (Thomas et al., 1998; Thomas et al., 1999; Gill et al., 2003). The higher content of tryptamine observed in tomato young leaves, which are more attractive to insects for their feeding, could be hypothesized to serve as deterrent to protect these developing photosynthetic organs. Moreover, while tryptamine levels did not vary in different parts of the stem, an opposite gradient to that detected for the leaves was observed for serotonin in this organ, with the internodes next to the shoot apex having a lower content of this amine. The presence of metabolite concentration gradients in plant stem is a feature that has already been reported for phytohormones including auxin (Kojima et al., 2002), abscissic acid (Everat-Bourbouloux & Charnay, 1982) and cytokinins (Eklöf et al., 1996), yet at much lower levels (10-0.1 ng/g fw) than serotonin, but no observations so far are available for secondary metabolites.

Serotonin was clearly more distributed in plant aerial organs, but some reports witness considerable levels also in underground apparatus like the roots of *Oryza sativa* (Kang et al., 2007$_a$) and *Helianthus annuus* (Mukherjee et al., 2014) and the rhizome of *Zingiber officinale* (Badria, 2002). Nonetheless, it was found that both tryptamine and serotonin were very low in Micro-Tom roots. No significant changes were also observed in the reproductive organs during the transition from flower buds to flowers at the anthesis in which serotonin was about six times the amount of tryptamine. However, in *Datura metel*, another member of the family Solanaceae, the highest amount of serotonin was detected in the developing flower bud and then it gradually decreased while maturing to the open flower (Murch et al., 2009).

Accumulation dynamics in the fruit call the need for functional studies to unravel tryptamine and serotonin roles during fruit development and ripening

Many fruit berries accumulate tryptamine and serotonin at similar or even higher levels than tomato including bell pepper, pomegranate, papaya, kiwifruit, banana and cranberries as well as other fruit types like pineapple and plum (Erland et al., 2016; Islam et al., 2016). In previous works these indolamines have been found to vary within the ripe fruit of different tomato cultivars and the results presented in this chapter are in line with recent data published by Islam et al. (2016) and Hano et al. (2017) that report ~4-12 µg/g fw of serotonin and ~3 µg/g fw of tryptamine in cherry-tomato varieties. Beyond the differences in the levels of these compounds observed among the cultivars of the same species, a point that deserves major considerations is that there are no general trends observed for fruit indolamine accumulation among different plant species. In Micro-Tom, for instance, it was here demonstrated that serotonin and tryptamine increased in the developing fruit peaking just prior to the onset of ripening, i.e. at the mature green stage for tryptamine and at the early breaker stage for serotonin, and then their levels did not exhibit further variations till completion of the ripening process. Similarly, previous investigations in banana (*Musa spp*) revealed that serotonin increased in the pulp of the green fruit as it ripens (Udenfriend et al., 1959), whereas in green kiwifruit (*Actinidia*

deliciosa) it has been recently shown that serotonin and tryptamine were highest in the early stages of development, gradually decreasing as the berry approaches to ripening (Commisso et al., 2019). Another trend was observed, again, in pineapple (*Ananas comosus*) where the high abundance of serotonin at the immature phase is followed by a sharp decline in the mature and super mature fruit (Foy & Parrat, 1960). The accumulation of these indolamines appears, thus, to be under the control of a defined plant program during the reproductive phases, reflecting a plausible important function during fruit formation, growth and maturation. This issue was more deeply investigated by comparing the accumulation pattern of these molecules in different parts of the fruit in the unripe and ripe berry of Micro-Tom. Both unripe and ripe seeds represented a very good source of tryptamine and serotonin whereas medium to lower levels were observed in the mesocarp and the exocarp respectively. This only partially agrees with previous reports by Feldman & Lee (1985) and Hano and colleagues (2017) that observed a lower accumulation of serotonin in skin fruit respect to the pulp, which had, however, a higher content than the seeds. The presence of high levels of serotonin in the seeds is an issue that was already debated for *Juglans regia*, in which a possible role in embryo protection for this molecule was proposed by channelling free toxic ammonium into the serotonin biosynthetic pathway (Grobe, 1982). However, this is, to date, the only information concerning a putative biological role for serotonin in the fruit.

Organ and stage-specific expression of *SlTDC* and *SlT5H* genes controls tryptamine and serotonin production at different levels and strongly suggests their involvement in distinct biological functions

In the second part of the chapter, the expression patterns of *SlTDC* and *SlT5H* genes were investigated by quantitative Real-time PCR and considered in relation with the amounts of the corresponding metabolites detected in the same organs and developmental stages within the Micro-Tom plant.

Complementary but non-redundant expression of SlTDCs genes provide tryptamine for the ubiquitous activity of SlT5H in tomato

The molecular analysis revealed the existence of complementary expression trends among *SlTDC* genes that coordinate tryptamine biosynthesis with an organ-specific distribution. *SlTDC1* was found to be expressed only during the plant reproductive phase, especially in the unripe fruit and to a lesser extent also in the flowers and the senescent berry. Conversely, *SlTDC2* was highly expressed in aerial plant vegetative organs and within the flowers but not in the fruit. *SlTDC3* showed different expression levels in all plant organs collected, representing the only *SlTDC* gene active also in the roots. In order to reflect on the biological meaning of the observed expression patterns, the fact that SlTDC enzymes seem to perform differently *in vivo* must be considered. In fact, SlTDC1 and SlTDC2 were shown in the previous chapter to be much more efficient in the conversion of tryptophan to tryptamine respect to

SlTDC3 when expressed in a heterologous system. Therefore, the expression of SlTDC1 and SlTDC2 even at very low levels in specific organs such as the flowers, the shoots or in fruit tissues might have more relevance to tryptamine production in these sites than that merely deduced by gene expression levels. On the other hand, SlTDC3, yet found to be ubiquitously expressed, might have a different role in determining tryptamine levels within the plant given its lower enzymatic performance suggested by the *in vivo* expression assays. In this context, it appears that tryptamine levels in tomato are thus finely regulated by notably distinct mechanisms suggesting that this indolamine might cover more than one biological function in the plant, thus representing, in this case, more than a mere metabolic intermediate for the production of downstream products (i.e. serotonin, melatonin and their derivatives).

In other plant species having at least a two-member *TDC* gene family, e.g. *Camptotheca acuminata* and *Capsicum annuum,* it was observed that while one gene was active at a whole plant scale with different expression levels in the various organs, the other one appeared not to be expressed in plant tissues unless they were stressed or following induction with pathogen elicitors (López-Meyer & Nessler, 1997; Park et al., 2009). The stress-inductive effect on *TDC* was observed also in *Oryza sativa* in which the expression of these genes, normally negligible or present at very low levels, initiated upon nutrient depletion-induced senescence in the leaves (Kang et al., 2009_a). At present this is the first work that, adding remarkable details to the partial work of previous authors in tomato (Hano et al., 2017), demonstrates such a complex regulation for a plant *TDC* gene family in which different isoforms show specific expression patterns in different plant organs and developmental stages.

The expression analysis revealed that *SlT5H* was expressed in all Micro-Tom organs, as previously observed in tomato (Hano et al., 2017) and rice (Kang et al., 2007_a). In both the species, *T5H* activity is highest in the roots but in tomato, differently from rice, this did not reflect into huge serotonin accumulation in this organ. However, the fact that *T5H* is always expressed in these two species strongly suggest that serotonin, or its derivatives, might play important functions in the plant.

Evidences for linear correlation between biosynthesis and accumulation might reflect complex dynamics of the tomato serotonin pathway

By comparing the expression patterns of the serotonin-related biosynthetic genes and the levels of tryptamine and serotonin measured it was possible to hypothesize some dynamics that regulate the accumulation of these indolamines or their channelling into further downstream pathways: i) Pearson correlation analysis suggested that within the roots *SlTDC3,* which showed high positive correlation with *SlT5H* and serotonin but was negatively correlated to tryptamine accumulation, might serve to channel tryptamine into serotonin production. However, since serotonin did not reach considerable levels in this organ, it might be also speculated it could be further converted to melatonin or other downstream products, i.e. phenolic derivatives, or be translocated to other parts of the plant. ii) Within the fruit two *SlTDC* genes are active (*SlTDC1* and *SlTDC3*) and the correlation between their

expression with the accumulation of tryptamine and serotonin reflects the existence of different genetic and biochemical fates: while *SlTDC1* is expressed early during fruit development (mature green stage), *SlTDC3* mirrors *SlT5H* expression pattern and serotonin accumulation throughout fruit formation and ripening. In this sense *SlTDC3* together with *SlT5H* might regulate and keep constant serotonin levels within the fruit while *SlTDC1* might address tryptamine production for a specific function during a narrow but core phase of fruit production, which is berry development. Interestingly, despite the high expression levels of both *SlTDC1* and *SlT5H* in this tissue, the amounts of tryptamine and serotonin were lower respect to other plant tissues and organs in which the expression of these genes was not as high. Several options could be thus hypothesized including the translocation of these indolamines to the berry flesh or even the seeds which, on the other hand, showed a notable content of these metabolites but a rather low expression of their biosynthetic genes.

The simultaneous presence of expression and accumulation gradients raises the question of possible relationships between SlTDCs/SlT5H genes and related metabolites with the phytohormone auxin

Interpreting the relationships among the actors of the serotonin pathway in the rest of the plant is much more complex due to the observation of metabolite and expression gradients in the leaves and the internodes of the stem. *SlTDC2* apparently covers a fundamental role in determining indolamine production in the vegetative aerial organs of Micro-Tom, however its trend in the expression did not match or reflect tryptamine or serotonin distribution in these organs. Moreover, also the expression of *SlTDC3* and the interplay with *SlT5H* has to be taken in account. In general, the tryptamine/serotonin levels observed in the root and along the longitudinal axis of the plant, as well as the *SlTDCs* and *SlT5H* gene expression pattern, roughly resemble the auxin gradients, as visualized in the *Arabidopsis* roots by many authors (Ljung et al., 2005; Petersson et al., 2009) and as measured in tomato stem by Kojima and co-workers (2002). Recent progresses in the elucidation of the tryptophan-dependent pathways that lead to auxin biosynthesis suggest the involvement of tryptamine as a biochemical intermediate in one possible route, but, although it is reasonable not to exclude it, it is still a hypothesis under debate (Brumos et al., 2014). Moreover, mechanisms other than those hypothesizing the direct involvement of tryptamine in auxin biosynthesis should be considered such as the eventual participation in cascade signalling through interaction with auxin receptors which might be possible due to high structural similarities between the plant indolamines and IAA (Erland et al., 2015; Pelagio-Flores et al., 2018; Mukherjee, 2018).

Conclusions

The coupling of targeted metabolomics to assess the levels of tryptamine and serotonin and gene expression analysis to evaluate the expression pattern of the indolamines biosynthetic genes was carried out in Micro-Tom plants and allowed to speculate some dynamics of the serotonin biosynthetic pathway in tomato. The high amount of serotonin in all the plant tissues and the high amount of tryptamine in the flowers, fruit and seeds, lead to consider these metabolites not only intermediate but also end products, suggesting that the observed map of concentration, that in some organs do not correspond to gene expression, are not simply due to the canalization of these metabolites to produce some other final products. However, metabolic canalization of tryptamine and serotonin towards other metabolites, i.e. melatonin or feruloyl and coumaroyl derivatives, although not detected with the analytical method adopted, might represent an issue and deserves further future investigations.
Of course, it might not be excluded as well the existence of other eventualities such as protein translocation.
In any case, the complex pattern of expression of the three genes suggests that these, which share identical enzymatic functions, play distinct roles. On the other side, the high level and the complex pattern of metabolite accumulation, possibly obtained also by metabolite translocation or enzyme regulation, raise the question of the real function of these metabolites, not indispensable for plant life, since they are not ubiquitous in plant kingdom, but probably very useful for plant species able to accumulate them. To date, this is the first work that presents at a very sophisticated level (from experimental design to the use of HRMS) spatial and developmental-related information about the distribution of tryptamine and serotonin together with the expression pattern of all their characterized biosynthetic genes within the plant.

Chapter 4

Preliminary results in the metabolic engineering and promoter study of the tomato fruit-specific *SlTDC1* gene

Abstract

Many edible plant species including *Solanum lycopersicum* accumulate notable levels of tryptamine and serotonin in the pericarp and the seeds of their fruits (Ravishankar & Ramakrishna, 2016). Although many recent investigations encourage the idea of considering serotonin like a multi-active metabolite involved in several plant physiological mechanisms, the precise biological roles of this indolamine in the plant and in the reproductive organs still represent, respectively, an unclear or unknown issue. This holds true also for tryptamine, whose biological roles, apart that of being a metabolic intermediate in indole-alkaloids metabolism and tryptamines, have never been investigated. Moreover, the fact that many fruits, commonly consumed in our diet, are rich in these metabolites could represent a further reason to encourage the study of fruit indolamines, not only for botanical interests considering their importance in animal biology. However, their bioavailability in the human body following tryptamine/serotonin-rich fruit consumption have still to be demonstrated. In this chapter, a metabolic engineering approach was adopted as a first attempt to elucidate tryptamine function in tomato by inducing a further accumulation or a drastic reduction of this indolamine in the whole plant and in the fruit, respectively. This was done by overexpressing and knocking-out the fruit specific *SlTDC1* gene. Preliminary results obtained from transgenic T_1 plants analysis showed that overexpressing lines presented altered plant architecture but no tryptamine nor serotonin hyperaccumulation. On the other hand, knock-out lines did not display any obvious phenotype in the fruit. Moreover, in order to shed a light into *SlTDC1* function in the fruit, which seems to be the main effector of tryptamine accumulation in this organ, the activity of its promoter was investigated by its fusion with the *GFP* reporter gene.

The preliminary data that will be discussed in this chapter represent very early results on this topic; further biochemical and phenotypical characterizations of the transgenic lines here produced will be required.

Introduction

The alteration of endogenous levels of tryptamine and serotonin as well as their *de novo* production through heterologous expression by metabolic engineering approaches is not a novelty in plants (Kumar et al., 2016). The overexpression of aromatic acid decarboxylase genes has been widely practiced in many plant species given the central role of AADC enzymes in diverting primary metabolites into attractive secondary metabolic pathways (e.g. indole-alkaloids, biogenic amines). However, manipulating these metabolic fluxes by inducing the constitutive expression of high levels of the tryptophan-consuming enzyme TDC has the potential to be detrimental to plant growth since the canalization of this essential amino acid into secondary pathways might decrease the pool of tryptophan-derived indole metabolites, some of which exhibit central roles in plant physiology (e.g. auxin). Nonetheless, many reports witness successful attempts in increasing tryptamine levels by CaMV 35S promoter-driven expression of *TDC* genes and only in a few cases this resulted in plant growth defects (Thomas et al., 1995; Yao et al., 1995). The heterologous constitutive expression of *TDC* was also used to generate metabolic sinks, as demonstrated in transgenic canola in which tryptophan flux was addressed to high amounts of tryptamine rather than undesirable indole glucosinolates (Chavadej et al., 1994). Since the earlier experiments carried out in the 1990s, which aimed to trigger the production of indole-alkaloids through both *in vitro* plant cell cultures and *in planta* approaches, it was evident that tryptophan decarboxylation mediated by TDC represents the rate limiting step in addressing tryptophan to tryptamine downstream products (De Luca et al., 2000). Several authors were able to induce strong tryptamine accumulation in the tissues of model plants as tobacco (up to 1% of plant dry weight), petunia and poplar, which are not natural accumulators of this indolamine, without interfering with their growth and development (Songstad et al., 1990; Thomas et al., 1999; Gill et al., 2003, 2006). Other authors reported also that transgenic tryptamine-hyperaccumulating tobaccos did not show alterations in the expression of branch point enzymes of the shikimate pathway, demonstrating that the normal route of tryptophan biosynthesis in those plants was sufficient to supply a considerable amount of this essential amino acid for tryptamine hyperaccumulation (Poulsen et al., 1994). In the same way, in species showing endogenous indolamine production, such as the medicinal plants *Catharanthus roseus* and *Cinchona officinalis*, the overexpression of *TDC* genes in their tissue cultures lead to high production of both tryptamine and of its catabolised downstream products (Goddijn et al., 1995; Geerlings et al., 1999; Hughes et al., 2004). Nonetheless, the same approach applied to cell and root cultures of *Peganum harmala* did not result in higher tryptamine levels but significatively burst serotonin amounts (Berlin et al., 1993). Similarly, the same effect was observed more recently *in planta* by several authors which attempted to modify the levels of serotonin and melatonin in rice by enhancing TDC or T5H activity. Rice, as tomato, possess

a small family of *TDC* genes that, in this species, are expressed at very low or negligible levels, while *T5H* is constitutively expressed and their coordinated activity regulates the indolamine flux towards the biosynthesis of melatonin. In general, *TDC*-overexpressing transgenic rice plants presented higher tryptamine and serotonin levels respect to wild-type plants, even if this was associated to a series of different effects, from stunted growth and dark brown phenotypes to enhanced resistance to senescence (Kang et al., 2007$_b$; Kang et al., 2009$_b$; Kanjanaphachoat et al., 2012). However, to further complicate this scenario, Byeon and co-workers (2014$_b$) while overexpressing three *TDC* isogenes from rice, observed that melatonin levels were incresead from slight to high levels in the three transgenic lines, although various intermediates including tryptamine and serotonin were exclusively increased only in one line.

On the other hand, there is not such much information in the literature about the contrary effect, i.e. the depletion or reduction of indolamine levels by silencing or knocking-out their biosynthetic genes. Only two cases report the inhibition *in planta* of *TDC* and *T5H* by RNA interfering which in rice resulted, respectively, in lower serotonin levels (Kang et al., 2009$_b$) and in increased tryptamine and melatonin content (Park et al., 2013).

The aim of this last part of the research is to modify the amounts of tryptamine in tomato plant and fruit by targeting the fruit specific *SlTDC1* gene with a metabolic engineering approach in order to observe eventual effects. As just reported, constitutive *TDC* overexpression driven by the CaMV 35S promoter seems a reliable technique to get increased amounts of tryptamine in the plant, although several implications concerning the perturbation of other tryptophan-derived compounds and tryptamine downstream products, especially serotonin, should be taken in consideration. On the other hand, it is also interesting to obtain plants in which these indolamines are depleted or whose levels are decreased. As a starting point, this step was decided to be performed in the fruit by knocking-out *SlTDC1*, which appears to be the main responsible for tryptamine accumulation in this organ where indolamines functions have never been investigated so far. To get tryptamine depleted fruits, it was chosen to rely on the CRISPR/Cas9 (clustered regularly interspaced short palindromic repeat) technology, the most cutting-edge technique for plant genome editing and gene knock-out. Since 2014, the year of its first application in tomato, numerous publications witnessed the success of this approach in this species mainly focusing on the topics of resistance to abiotic and biotic stresses, improvement of tomato fruit quality and domestication (Wang et al., 2019$_b$).

The second part of this chapter deals with the study of *SlTDC1* expression and preliminary results on transgenic plants in which its promoter was fused to the GFP (green fluorescent protein) reporter gene are discussed.

Materials and methods

Molecular biology

Culture media, bacterial strains and bacterial transformation procedures were the same as previously described in "Materials and Methods" from Chapter 2.

GoldenBraid vectors for molecular cloning

The assembly of the plant expression vectors carrying the T-DNA inserts to obtain the overexpression and knock-out of *SlTDC1* and for the study of its promoter was carried out through the GoldenBraid platform (https://gbcloning.upv.es/), an evolution of the GoldenGate technology. This innovative cloning system is based on the modular assembly of *domesticated* genetic elements that can be exchanged among different types of entry and destination plasmids (pUPD2 and pDGB3 respectively) through the activity of type IIS restriction enzymes (*BsaI*/*BsmBI*). Basically, this system works in three steps: *domestication* of gene sequence, multipartite assembly of the transcriptional unit (TU) and binary assembly to join together multiple TUs. The *domestication* step consists in modifying the sequence of interest with flanking sites to be recognized by *BsaI* or *BsmBI* enzymes and to substitute, if present, inner nucleotides that might be recognized as well. The domesticated sequence is thus cloned into the pUPD2 entry plasmid (Figure 4.1) to produce a pUPD2-GBpart that needs to be combined with other pUPD2-GBparts harbouring genetic modules such as promoters and terminators, which might be included in the vector library provided by the developer or created *de novo*. This step proceeds through a multipartite reaction that results in the assembly of a complete TU (promoter, gene of interest, terminator) into a pDGB3 binary destination vector (Figure 4.1). This might be of α or Ω type whether it requires *BsaI* or *BsmBI* respectively to clone the insert, and each type is furtherly differentiated into version 1 and 2. Moreover, the transcriptional units, assembled in different pDGB3 vectors, might be joined to have multiple gene cassettes into a unique expression vector. This is possible by binary assembly between type 1 and 2 pDGB3 vectors of the same α or Ω type. All GoldenBraid vectors contain the cloning site within the *LacZ* gene in order to allow white/blue screening of positive clones on IPTG/X-Gal containing medium. The antibiotics of selection for replicating the plasmids in *Escherichia coli* are chloramphenicol, kanamycin and spectinomycin for pUPD2, pDGB3α and pDGB3Ω respectively. All GoldenBraid vectors used in this work were supplied by Dr. Diego Orzaez (University of Valencia). Type IIS restriction enzymes were purchased by New England BioLabs (Ipswich, USA).

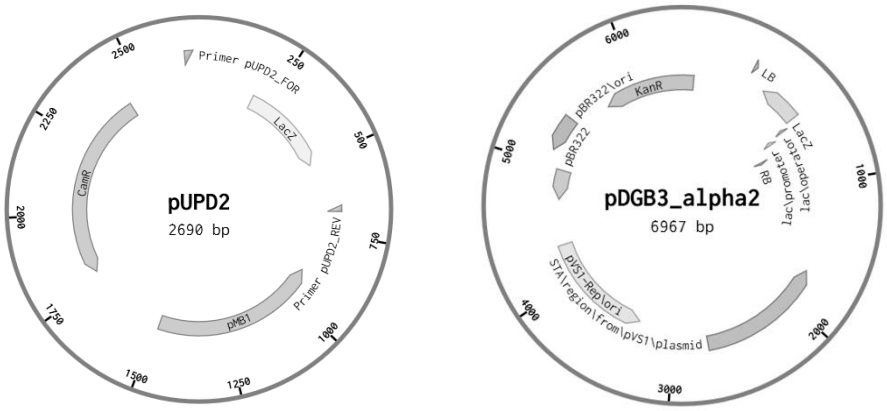

Figure 4.1 GoldenBraid pUPD2 (left) and pDGB3 (right, α-type example) vectors used in the preparation of the constructs for the overexpression, knock-out and promoter study of *SlTDC1* (LacZ: gene operon codifying for β-galactosidase; LB and RB: Left and right T-DNA borders; CamR: chloramphenicol resistance; KanR: kanamycin resistance).

Multipartite and binary assemblies of pUPD2 or pDGB3 vectors were performed according to developer's instructions by mixing the vectors, the proper restriction enzyme (*BsaI* or *BsmBI*), T4 DNA ligase and its buffer (Thermo Fisher) in a volume of 10 µL and performing 25 cycles of restriction /ligation reaction (37°C, 2 min / 16°C, 5 min). For each assembly, presented in the next paragraphs, the ligation product was transformed into One Shot TOP10® *E.coli* cells by heat-shock, which were then plated on LB medium with the proper concentration of antibiotic (25 mg/L for chloramphenicol or 50 mg/L for kanamycin or spectinomycin) and 0.5 mM IPTG and 40 mg/L XGal (all purchased by Promega) to allow blue/white screening of positive clones. For each transformation event, five white colonies were propagated in liquid culture and plasmid purification was carried out through the E.Z.N.A.® Plasmid Mini Kit I (Omega Bio-Tek). The purified plasmids were checked for proper assembly by restriction analysis according to the instructions of the supplier (New England BioLabs) and by PCR analysis by using specific primers' pairs (Table 4.1).

Target sequence	Primer name	5'-3' sequence	Aim
Common primers			
pUPD2 vector	pUPD2-for	GCTTTCGCTAAGGATGATTTCTGG	a,b
	pUPD2-rev	CAGGGTGGTGACACCTTGCC	a,b
pDGB3 vector	pDGB3-for	GGTGGCAGGATATATTGTGG	a
	pDGB3-rev	GTTTTCAGATGACGGCTGCACT	a
KanR cassette	Kan-for	CAGAGTCCCGCTCAGAAGAACTCGTCA	a
	Kan-rev	GGAAGGGACTGGCTGCTATTGGGCGAA	a
CaMV 35S promoter	35S-for	AAGATGCCTCTGCCGACAGT	a
	35S-rev	TGACGCACAATCCCACTATC	a
Primers for SlTDC1 overexpression			
SlTDC1 CDS	SlTDC1-revA	GTTCCGCAGCGTTCATTGG	a
	SlTDC1-revB	GTTTGCTGAGAAAAAGTGTGTTTTAA	a
Primers for SlTDC1 Knock-out			
SlTDC1 target1	target1-for	ATTGCAATTGTTTCAACTCCGTC	c
	target1-rev	AAACGACGGAGTTGAAACAATTG	c
SlTDC1 target2	target2-for	ATTGGTTCTAAGCCAAGTCGAAC	c
	target2-rev	AAACGTTCGACTTGGCTTAGAAC	a,c
Cas9 CDS	Cas9-for	CATCAGGGAGCAGGCAGAAA	a
	Cas9-rev	GGCTCAAAAGAACAGCACGG	a
Primers for the study of SlTDC1 promoter			
SlTDC1 5 kb upstream region	GBpromTDC1-rev	GCGCCGTCTCGCTCGGGAGCTCAATTATTTTAG AGATATTCTTTTAAG	c
	GBpromTDC1-rev	GCGCCGTCTCGCTCACATTGATTTGATTTTTGGA ACAATTTAAGG	c
	promTDC1-for1	CATCTTGAACAAAAGCTCCCTCCTT	b
	promTDC1-for2	GTGTTTCCAAAACTGATTACTCCTC	b
	promTDC1-for3	TGACCTGCGTTATGGTTTCA	b
	promTDC1-for4	AATAACATCCGTTCCACCATATTT	b
	promTDC1-for5	TGCACATTATCTCTTTCCTTCCT	b
	promTDC1-for6	TTTGTGAATAAAAATTGGGTTCTTC	a,b
	promTDC1-for7	AGCCCAACAAAATTGGCTGCT	a,b
	promTDC1-rev1	TCGTCCATGTAGGGTTAACTTGTCATC	a,b
	promTDC1-rev2	TTTTGCCATTAAGTTATCATTTCTCA	b
	promTDC1-rev3	GTGGTCCTTTAGTAGGATATACAAGCA	b
	promTDC1-rev4	GGGATTCCAAAAATCAATCAAA	b
	promTDC1-rev5	AAACATGTGTTACGTCAATGCAA	b
	promTDC1-rev6	AAAAGGTGACGGGGATTGA	b
GFP CDS	GFP-for	ATGGTGAGCAAGGGCGAGG	a
	GFPmid-rev	GTAGCGGCTGAAGCACTGCAC	a,b
	GFP-rev	GCATGGACGAGCTGTACAAG	a

Table 4.1 List of all primers used in the assembly of vectors to perform the metabolic engineering of the *SlTDC1* gene. Legend: a, check of vector assembly by PCR; b, sequencing; c, cloning into pUPD2. All primers were purchased by Thermo Fisher. Underlined nucleotides refer to GB adaptors for cloning into pUPD2.

Preparation of the constructs for SlTDC1 overexpression

Since *SlTDC1* CDS contains a *BsaI* recognition site this was synthesized *de novo* through the GeneArt service (Thermo Fisher) after mutating the original sequence to eliminate *BsaI* site, yet maintaining the original frameshift and including the 4-nt flanking adaptors for cloning into pUPD2. The domesticated *SlTDC1* CDS was cloned into pUPD2 after restriction with *BsmBI*. Following *E.coli* transformation and plasmid purification, the success of the insertion was verified through *BsaI* restriction and PCR. The pUPD2.*SlTDC1* was then assembled in a transcriptional unit by using pUPD2-GBparts containing the CaMV35S promoter and Nos terminator into a pDGB3Ω2 destination vector by *BsmBI*. Following propagation and extraction from positive transformed colonies, the assembled plasmid was checked for the presence of the overexpression transcriptional unit (OE) p35SCaMV::*SlTDC1*::TNos by restriction analysis using *BsaI* and PCR. The final step consisted in the binary assembly between the newly formed pDGB3Ω2.OE and the pDGB3Ω1.KanR, which harbours the cassette (pNos::nptII::TNos) conferring Kanamycin resistance in reverse orientation within the T-DNA region of the vector. The two transcriptional modules where thus assembled into a pDGB3α1 binary destination vector by *BsaI*. The obtained final plasmid pDGB3α1.OE/KanR was checked by restriction analysis with *BsmbI* and by PCR analysis to verify the presence of all the genetic elements inserted. A schematic representation of the cloning procedure is depicted in Figure 4.2.

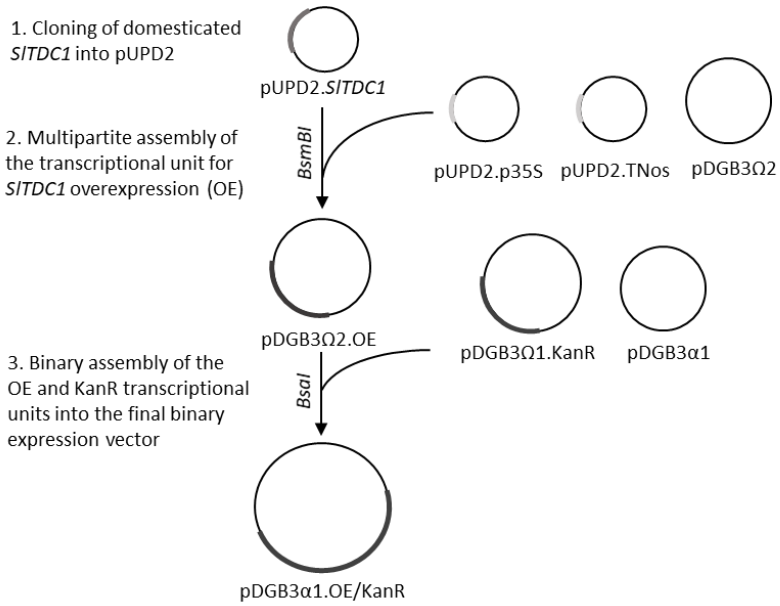

Figure 4.2 Cloning steps in the production of the construct for *SlTDC1* overexpression

Preparation of the construct for CRISPR/Cas9-mediated Knock-out of SlTDC1

As first step in the experimental design of *SlTDC1* knock-out, a preliminary *in-silico* investigation with the software CRISPR-P (http://crispr.hzau.edu.cn/CRISPR2/) was performed in order to identify proper Cas9 target sites in the *SlTDC1* sequence. Two 20-nt sequences in the upstream region of the CDS displaying the lowest number of possible Cas9 off-targets in the tomato genome were chosen. The construct assembly was then carried out using the "GB CRISPR domesticator" and "CRISPR assembler" tools (https://gbcloning.upv.es/tools/crisprs/) of the GoldenBraid platform. For both the identified targets, two primers (Table 4.1) were designed in order to obtain an annealed sequence to be cloned as GBpart into pUPD2 vectors according to developer's instructions. The resulting pUPD2.target1 and pUPD2.target2 were used in separate multipartite assembly with other pUPD2-GBparts containing the U6-*26 Arabidopsis thaliana* promoter (pAtU6) and the small guide RNA scaffold (sgRNA) in order to produce the genetic elements necessary to drive the Cas9 enzyme to the target sites in the tomato genome. These modules were assembled into pDGB3α1 and pDGB3α2 vectors by *BsaI*. The assembled plasmids (pDGB3α1.tgRNA1 and pDGB3α2.tgRNA2) were checked for the presence of the two target RNA-guide modules by restriction analysis with *BsmBI* and by PCR analysis. Then a binary assembly was performed in order to ligate these two modules into a pDGB3Ω2 vector by using *BsmBI*. The pDGB3Ω2.tgRNA1/tgRNA2 vector was checked by restriction analysis with *BsaI* and by PCR analysis. At the same time, the transcriptional units p35S::*Cas9*::TNos and pNos::*nptII*::TNos contained in pEGBα2 and pDGB3α1 vectors respectively supplied by the GB developer, were joined together in pDGB3Ω1 by binary assembly using *BsmbI*. Also in this case the resulting pDGB3Ω1.Cas9/kanR vector was checked by restriction analysis and by PCR analysis. The last step consisted in the final binary assembly of pDGB3Ω vectors to join the two targets small-guide RNAs with the Cas9 transcriptional unit and the kanamycin resistance cassette into the pDGB3α1 plant expression vector (pDGB3α1.KO). A schematic representation of this complex cloning procedure is depicted in Figure 4.3.

Preparation of the construct for SlTDC1 promoter study

A region of 5 kb upstream the *SlTDC1* ORF (pSlTDC1) was amplified by the mean of high-fidelity KAPA HiFi-DNA polymerase (Kapa Biosystems) using as template a genomic DNA extracted from the leaves of 2-months old Micro-Tom plants. Primers and PCR conditions used are listed in Tables 4.1 and 4.2. The amplicon was then cloned into pUPD2 following GB developer's instructions and the ligation product transformed into *E.coli* as previously described, with positive colonies being checked by PCR and used to amplify and purify the vector. Several aliquots of the plasmid were air-dried, each together with a primer pairing respectively to the pUPD2 cloning site flanking regions and to inner regions of pSlTDC1, the air-dried mixture was then sent to BMR Genomics laboratories (Padova, Italy) for sequencing analysis. Evaluation of sequencing data was performed by visualization in Chromas. Once confirmed the exactness of the insert, the pUPD2.p*SlTDC1* was used in a GB multipartite assembly with

other pUPD2-GBparts containing the coding sequence of the green fluorescent protein (*GFP*) and the Nos terminator. The pSlTDC1::*GFP*::TNos transcriptional unit was indeed assembled into a pDGB3α2 vector by *BsaI*. Following *E.coli* transformation and plasmid purification, this was checked by restriction analysis and PCR and used in the binary assembly with the pDGB3α1.KanR to give the final construct pDGB3 Ω1.pSlTDC1-GFP/KanR. A schematic representation of this cloning procedure is depicted in Figure 4.4.

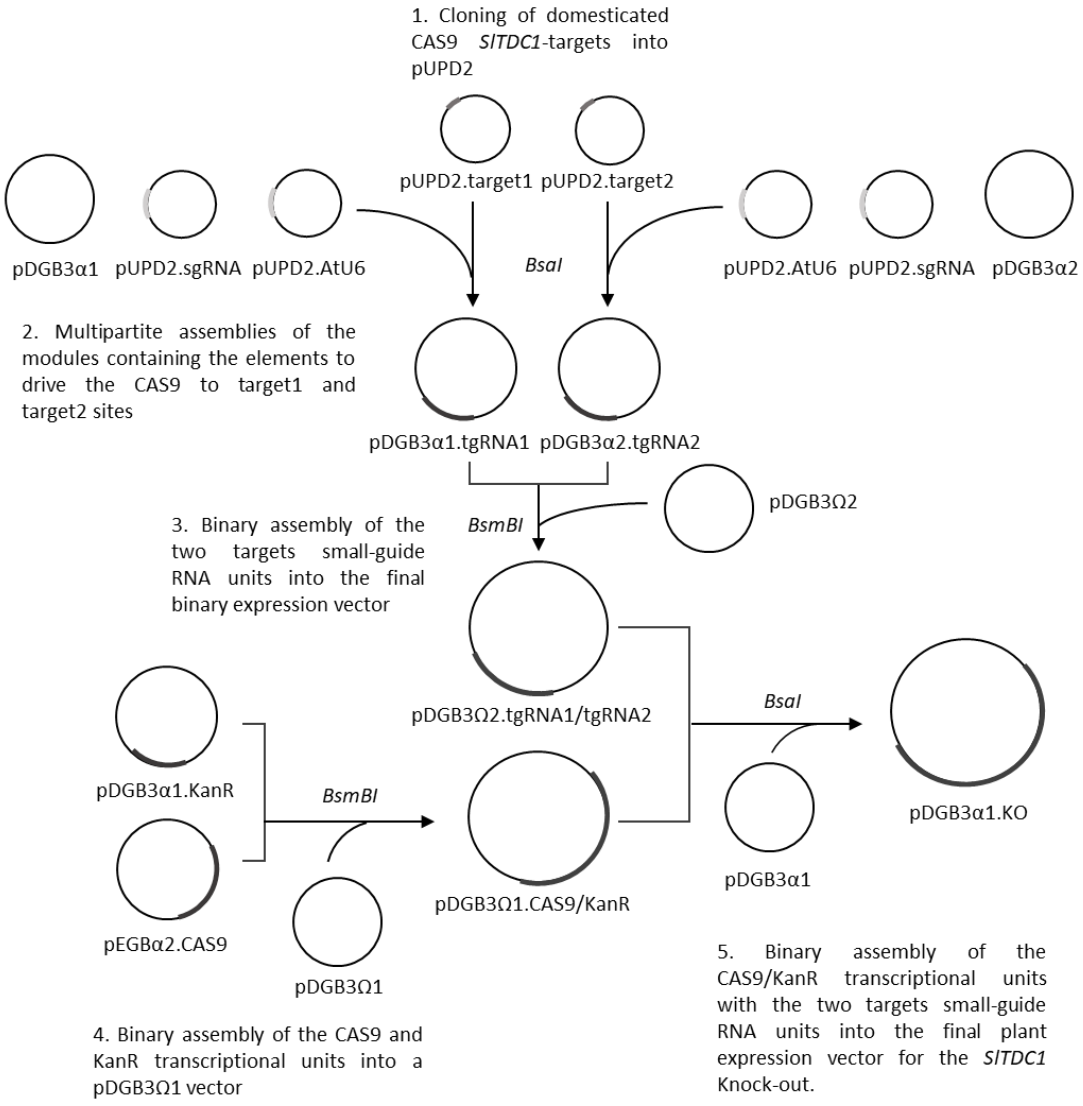

Figure 4.3 Cloning steps in the production of the construct for *SlTDC1* CRISPR/Cas9 mediated knock-out.

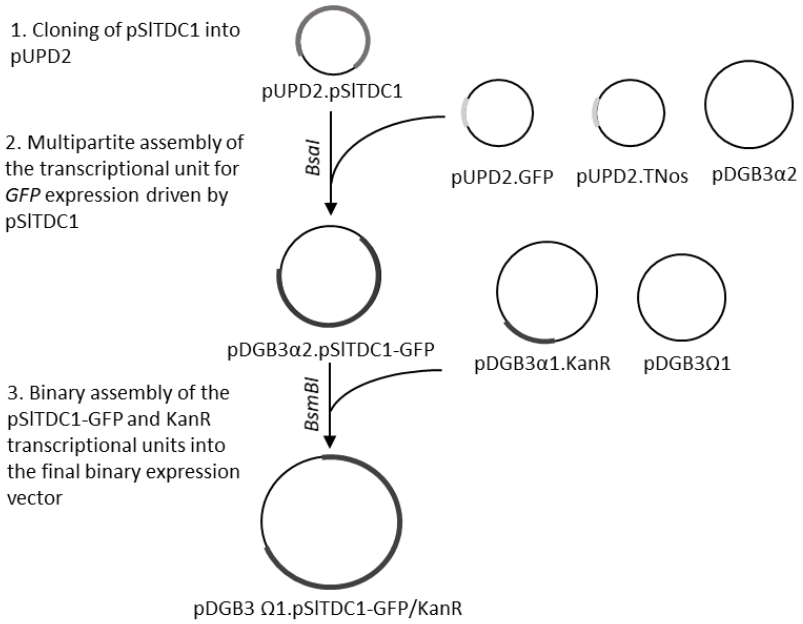

Figure 4.4 Cloning steps in the production of the construct for *SlTDC1* promoter analysis.

		***SlTDC1* promoter**
	Source	gDNA
	Lenght (bp)	5038
	Initial denaturation	95°C, 3 min
x 5	Denaturation	98°C, 20 sec
	Annealing	54°C, 60 sec
	Extension	72°C, 5 min
x 25	Denaturation	98°C, 20 sec
	Annealing	72°C, 60 sec
	Extension	72°C, 5 min
	Final extension	72°C, 5 min

Table 4.2 PCR conditions for the amplification of the 5 kb upstream region of *SlTDC1* by using GBpromTDC1-for/rev primers (Table 4.1) and KAPA HiFi-DNA polymerase.

Transformation of Agrobacterium tumefaciens

The three constructs prepared were used to transform *Agrobacterium tumefaciens* EHA105 electro-competent cells by electroporation method. These were then plated on solid LB medium containing the proper antibiotics for selection (50 mg/L rifampicin + 50 mg/L kanamycin or 50 mg/L spectinomycin for pDGB3α or pDGB3Ω vectors respectively) and colonies were checked by colony-PCR to assess the presence of all the putative inserted genetic elements.

Plant genetic transformation and *in-vitro* cultures

Stable genetic transformation of Micro-Tom mediated by Agrobacterium tumefaciens and in-vitro regeneration of transgenic plants

Ten days prior to plant transformation event, Micro-Tom seeds were sterilized as follows: they were put into 70% ethanol (Honeywell) solution and mixed for 1 min, then they were placed in a solution containing 10% commercial bleach and 0.1% Tween20 (Sigma-Aldrich) and mixed for 10 min. After removing the sterilizing solution, seeds were washed 4 times with sterile water, sown on germination medium (Table 4.3) and placed in growth chamber at 25°C. The day prior the transformation 0.5 cm cotyledons and hypocotyls explants were prepared from Micro-Tom plantlets and placed on KCMS medium (Table 4.3) in the dark of a growth chamber at 25°C for 24 h. The same day, 5-mL LB liquid suspensions of *A. tumefaciens* carrying the plasmids of interest were prepared and cultured at 28°C at 180 rpm for 24 h. After one day, bacterial suspensions were centrifuged for 15 min at 3000 rpm and the pellet was resuspended in liquid KCMS to an infection OD_{600} of 0.1. This suspension was added to the plate with Micro-Tom explants and, after 15 min at room temperature, it was removed while the plate was placed back to the growth chamber at 25°C in the dark for 2 days. Then the explants were transferred to regeneration medium A (Table 4.3). After 15 days, explants that formed calli were moved to regeneration medium B (Table 4.3) and refreshed to new medium each 2 weeks till shoot regeneration. Properly formed shoots were physically removed from the original calli and placed into magenta boxes with rooting medium (Table 4.3). When the T_0 regenerated plantlets reached about 5 cm in height and developed a proper root apparatus they were moved to pots with moisturized soil and kept in a humid microenvironment at 25°C for one week for acclimation.

Characterization of transgenic plants

T_0 acclimated plants were grown in a growth chamber at 25°C with a 15h/9h light/dark photoperiod and let to set fruits. T_1 seeds were collected, sterilized and sown on germination medium containing 75 mg/L kanamycin. Plantlets able to survive under these selective conditions were transferred to soil and, for each plant, a small portion of young leaf tissue was sampled for genomic DNA extraction in order to check the presence of transgenic T-DNAs by PCR (Table 4.1). Then, positive plants were used for further genetic and phenotypic characterization.

	Germination	Solid KCMS	Liquid KCMS	Regeneration A	Regeneration B	Rooting
MS powder mix	2.2 g/L	4.4 g/L	4.4 g/L	4.4 g/L	4.4 g/L	2.2 g/L
Sucrose	15 g/L	20 g/L	20 g/L	30 g/L	30 g/L	10 g/L
Biotin	-	-	-	0.05 mg/L	0.05 mg/L	0.05 mg/L
Folic acid	-	-	-	0.5 mg/L	0.5 mg/L	0.5 mg/L
Glycine	-	-	-	2.00 mg/L	2.00 mg/L	2.00 mg/L
Myo-inositol	-	-	-	100 mg/L	100 mg/L	100 mg/L
Nicotinic acid	0.25 mg/L	-	-	5 mg/L	5 mg/L	5 mg/L
Pyridoxine	0.25 mg/L	-	-	0.5 mg/L	0.5 mg/L	0.5 mg/L
Thiamine	0.5 mg/L	0.9 mg/L	0.9 mg/L	0.5 mg/L	0.5 mg/L	0.5 mg/L
KH2PO4	-	200 mg/L	200 mg/L	-	-	-
Acetosyringone	-	40 mg/L	0.2 mg/L	-	-	-
Kinetin	-	0.1 mg/L	-	-	-	-
Zeatin riboside	-	-	-	2 mg/L	2 mg/L	-
Naftaleneacetic acid	-	-	-	0.01 mg/L	0.01 mg/L	-
Augmentin*	-	-	-	9 ml/L	5 ml/L	2.5 ml/L
Kanamycin	-	-	-	100 mg/L	100 mg/L	75 mg/L
Plant agar	7.5 g/L	7.5 g/L	-	8 g/L	8 g/L	4 g/L
Phytagel	-	-	-	-	-	3 g/L

Table 4.3 Composition of the plant culture media used for genetic transformation of Micro-Tom and for *in-vitro* plant regeneration. * Augmentin (Glaxo Smith Kline, Brentford, UK) was prepared by dissolving the antibiotic powder (1g Amoxicillin/200mg Clavulanic acid) in 10 mL sterile water. All materials for *in-vitro* plant cultures were purchased by Duchefa (Haarlem, The Netherlands). All culture media were prepared at a pH of 5.8.

Genetic characterization of SlTDC1 knock-out plants

Genomic DNAs extracted from putative *SlTDC1*-knock-out T_1 plants were used as a template in a PCR reaction in which a region of about 1800 bp including the *SlTDC1* locus was amplified by using promTDC1-for7 and SlTDC1-revb primers (Table 4.1). Amplicons were checked by agarose electrophoresis and purified from gel by the mean of Wizard® SV Gel and PCR Clean-Up System (Promega). The amplicons were then sent together with the proper primers to BMR Genomics laboratories (Padova, Italy) for sequencing analysis in order to check and eventually characterize the type of mutation produced by the activity of Cas9 in the *SlTDC1* locus.

Sampling of plant material for gene expression and metabolomics analysis

Pools of leaves from basal, medium and upper nodes (three leaves in total) were independently collected from each *SlTDC1* overexpressing plant and from three wild type plants (control) and used for gene expression and untargeted metabolomics analyses.

Transgenic plants expressing the *GFP* CDS under the control of *SlTDC1* promoter were used to collect flowers and fruits at various stages of development and ripening (post fertilization, immature green, mature green, breaker and ripe berries). These samples were used in gene expression analysis.

Moreover, fruits at various developing and ripening stages were collected and used to produce sections for confocal microscope imaging.

Gene expression analysis

RNA extraction, cDNA synthesis and quantitative Real-time PCR analysis was performed as previously described in the "Materials and Methods" section of Chapter 3. The primers used in q Real-time PCR to target the *GFP*, *SlTDC1* and *SlCAC* (calibrator) genes are listed in Table 4.4.

GoI	Primer name	5'-3' sequence	Tm (°C)	Amplicon (bp)
GFP	RT-GFP for	GAAGTTCGAGGGCGACAC	59.88	66
	RT-GFP rev	CCGTCCTCCTTGAAGTCG	59.24	
SlTDC1	RT-SlTDC1 for	CCACTTCCACTACAGCCGTCG	62.99	104
	RT-SlTDC1 rev	ACATGCGCTCCCTCCATAAGC	62.85	
SlCAC	RT-SlCAC for	GGGTTGTTACATCACCAAAGC	62.48	121
	RT-SlCAC rev	GTGCTGGTGTGATTGCATCC	62.85	

Table 4.4 List of primers used in q Real-time PCR analysis for the evaluation of gene expression.

UPLC-ESI-MS metabolomics analysis

Extraction and quantification of tryptamine and serotonin in the samples were carried out as previously described in "Materials and Methods" from Chapter 3.

Results

Generation of transgenic Micro-Tom plants for the overexpression and knock-out of the fruit-specific *SlTDC1* gene

In the first part of this chapter is presented a metabolic engineering approach that aims to tune the levels of fruit indolamines tryptamine and serotonin through overexpression or knock-out of the fruit specific *SlTDC1* gene.

Plant expression vectors harbouring the genetic elements necessary to obtain the overexpression and knock-out of *SlTDC1* were assembled by relying on the GoldenBraid technology (Sarrion-Perdigones et al., 2011,2013) as described in the section "Materials and methods" of this chapter. The experimental design for obtaining the knock-out of *SlTDC1* deserves a brief description. The CRISPR/Cas9 approach was chosen to fulfil this aim given the increasing amount of literature witnessing the efficacy of this molecular technique to get gene loss of function in plant systems and, particularly, in the model species of tomato (Belhaj et al., 2015; Bortesi et al., 2015; Pan et al., 2016b). Moreover, GoldenBraid developers provide useful online tools and published protocols to design and obtain efficient CRISPR/Cas9-mediated gene knock-out with this technology (Vazquez-Vilar et al., 2016).

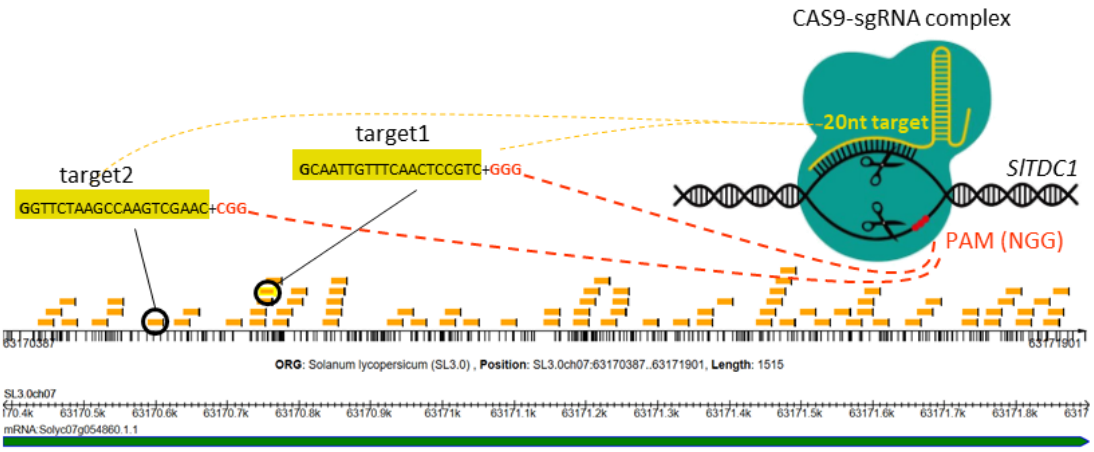

Figure 4.5 Schematic representation of all the 20-nt sequences that match on the *SlTDC1* CDS as Cas9 target candidates identified by CRISPR-P. The two targets chosen are highlighted by black circles. PAM, which stands for "Protospacer Adjacent Motif", is a 3-bp NGG-type sequence in target locus that is required for binding/cleavage of Cas9.

Following investigation on the CRISPR-P 2.0 website, two 20-nt sequences in the upstream region of the *SlTDC1* CDS were chosen (Figure 4.5) as best Cas9 target sites to rise the chances of successful gene knock-out with the minimal number of off-targets, i.e. other sites in the tomato genome that could be aspecifically recognized by the Cas9 enzymatic complex. However, two off-targets matching

on the CDS of putatively annotated "Ubiquitin-Ligase E3 fragment" (Solyc10g084760.1) and "Sulfotransferase family protein" (Solyc03g093620.1) genes were identified.

The two 20-nt target sequences were independently assembled in two CRISPR modules, each consisting in the *Arabidopsis thaliana* U6-26 promoter and a sequence that once transcribed produces a scaffold RNA (small-guide RNA) able to assemble to the Cas9 enzyme to form the genome-editor complex. The two target sequences, once transcribed jointly to the sgRNAs, lead the RNA-Cas9 complex to the two sites identified in the *SlTDC1* CDS by the small-guide RNAs to allow the editing. The two target modules were assembled into a plant expression vector together with the cassettes for the constitutive expression of the human *Cas9* CDS and of the *nptII* gene conferring the resistance to kanamycin as selective marker to transgenic plants.

In order to produce the construct for *SlTDC1* overexpression, the CDS of the gene was cloned under the control of the constitutive CaMV 35S promoter and joined with the cassette conferring kanamycin resistance into a GoldenBraid plant expression vector.

Schematic representations of the assembled T-DNA regions introduced in the Micro-Tom genome by *Agrobacterium tumefaciens*-mediated genetic transformation are depicted in Figure 4.6.

Micro-Tom explants infected with suspensions of *A. tumefaciens* carrying these genetic constructs were *in-vitro* regenerated via callus formation to produce T_0 plants and a regeneration efficiency of about 90% was achieved. Nonetheless, at the end of the regeneration on kanamycin selective media, only 12 and 19 T_0 plants putatively transformed for *SlTDC1* overexpression and knock-out, respectively, were able to develop proper shoots and roots. These were acclimated in soil and let to set fruits that produced T_1 seeds. These were then tested for their ability to germinate on kanamycin selective medium in order to furtherly discriminate transgenic plants from false positive ones. Just 4 out of 12 putative overexpressing lines (113, 125, 139, 166) and 15 out of 19 putative knock-out lines (22, 23, 71, 74, 84, 100, 115, 129, 156, 159, 165, 168, 171, 173 ,174) could produce vital plantlets that were then acclimated to soil. Given the low number of putative overexpressing lines obtained, several sibling plants germinated from the seeds of same T_0 lines were moved to soil for acclimation. A small portion of leaf tissue was then collected for each plant and the genomic DNA was extracted and tested by PCR (Figure 4.6). All the siblings from the four *SlTDC1* overexpressing lines were positive for the presence of the kanamycin-resistance cassette, the 35S promoter and the *SlTDC1* CDS. On the other hand, among the putative knock-out lines, four of them (22, 156, 165, 174) did not present the kanamycin-resistance cassette and 5 out of the 11 remaining lines (115, 129, 159, 168, 171) gave negative results when testing the presence of the T-DNA portion next to the right border, which included the modules for small-guide RNA transcription. Thus, six putative knock-out lines (23, 71, 74, 84, 100, 173) were carried on for further analyses.

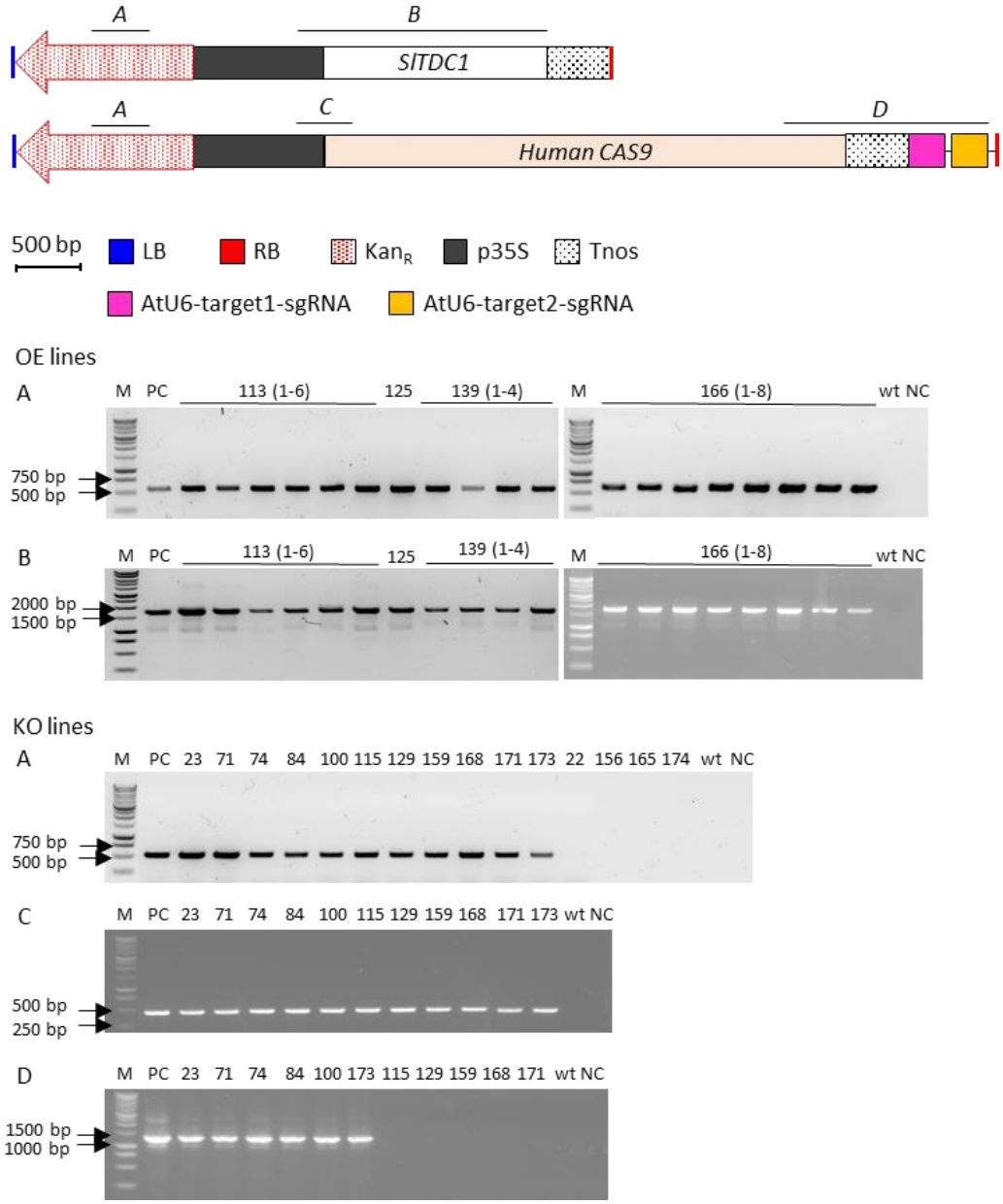

Figure 4.6 Schematic scale representation of the T-DNA regions assembled in GoldenBraid pDGB3 binary vectors to perform the overexpression (OE, top) and knock-out (KO, low) of the *SlTDC1* gene. Letters A-D represent the regions amplified by PCR reactions with specific primers (Table 4.1) to check the presence of T-DNA elements in the genomic DNA of T_1 transgenic lines. (A: kan-for/kan-rev, 545 bp; B: 35S-for/SlTDC1-revb, 1746 bp; C: 35S-for/Cas9-rev, 438 bp; D: Cas9-for/target2-rev, 1329 bp). Vector legend: LB and RB, left and right T-DNA borders; p35S, CaMV 35S promoter; TNos, Nopaline synthase gene terminator, AtU6, *Arabidopsis thaliana* U6 promoter; sgRNA, small-guide RNA; Kan_R, neomycin phosphotransferase (*nptII*) gene conferring kanamycin resistance in plants. PCR legend: M, molecular marker; PC, positive control; NC, negative control; wt, wild-type.

Characterization of T_1 transgenic plants overexpressing the *SlTDC1* gene

T_1 SlTDC1 overexpressing plants show altered plant architecture

T_1 plants successfully transformed with the T-DNA allowing *SlTDC1* overexpression were let grow in a growth chamber in controlled conditions and, as they reached the flowering phase, they started to exhibit an altered phenotype respect to control plants. As shown in Figure 4.7, sibling plants from the overexpressing line 166 showed altered plant architecture presenting a tangled aspect of the upper nodes and severe alterations of leaf morphology. Leaflets of the tomato compound leaf were asymmetrically arranged along leaf rachis and showed a crumpled-like leaf blade. For the moment, although these are just preliminary observations, no other obvious phenotypes were observed in Micro-Tom overexpressing lines, nor in the aerial organs of the plant nor in the fruit, under standard growing conditions.

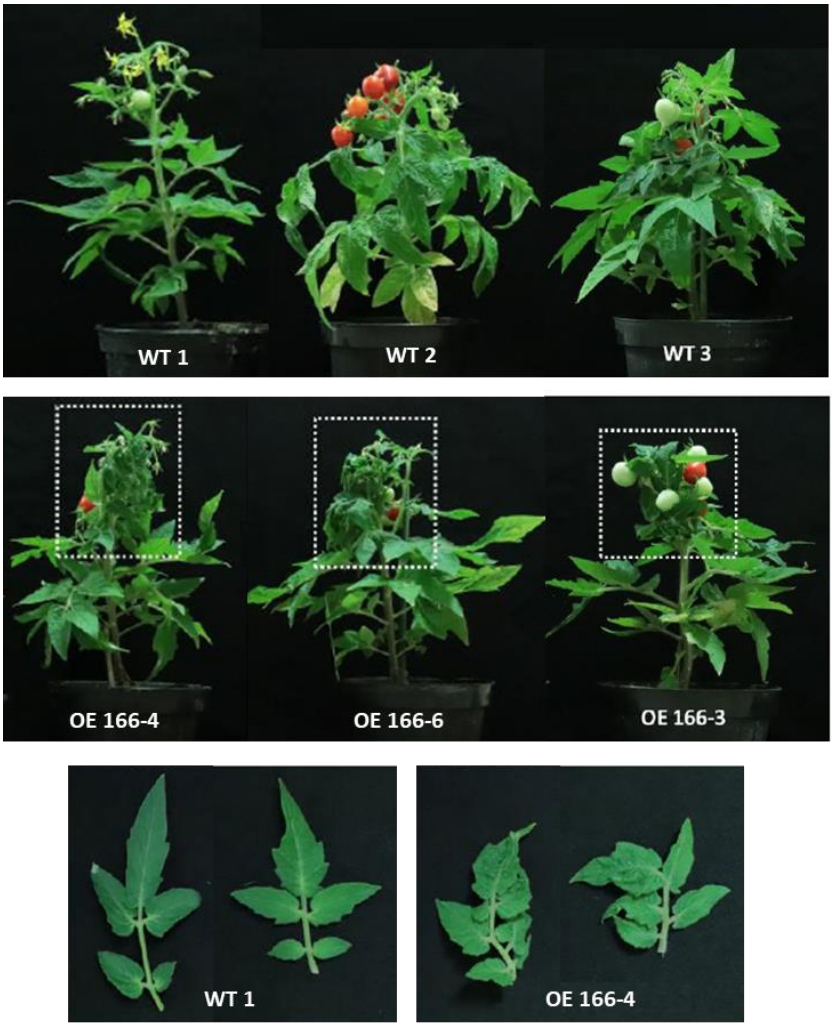

Figure 4.7 Plant phenotypes of Micro-Tom control plants (wild-type) and of three sibling plants from the overexpressing line 166. Leaves collected from the youngest nodes of control and transgenic plants are shown in the lower figures.

In order to start a preliminary characterization of the produced transgenic lines from both a genetic and biochemical perspective, a pool of leaves collected from basal, medium and upper nodes was formed for each single plant and used to extract RNA and metabolites to perform the expression analysis of the *SlTDC1* gene and various metabolomics analyses. RNA served to produce cDNA that was used as template in q Real-time PCR analysis in order to assess the transcript levels of *SlTDC1* and *SlCAC*, the tomato housekeeping gene used as calibrator to measure Mean Normalized Expression (MNE, "Material and methods" from Chapter 3). Q Real-time PCR revealed that *SlTDC1* transcript levels were higher, yet showing wide variety, in siblings from overexpressing line 166 whereas lower amounts were observed in plants from lines 113 and 125 (Figure 4.8). On the other hand, siblings from line 139 had extremely low expression levels of *SlTDC1* or showed no expression at all, as well as observed in control plants.

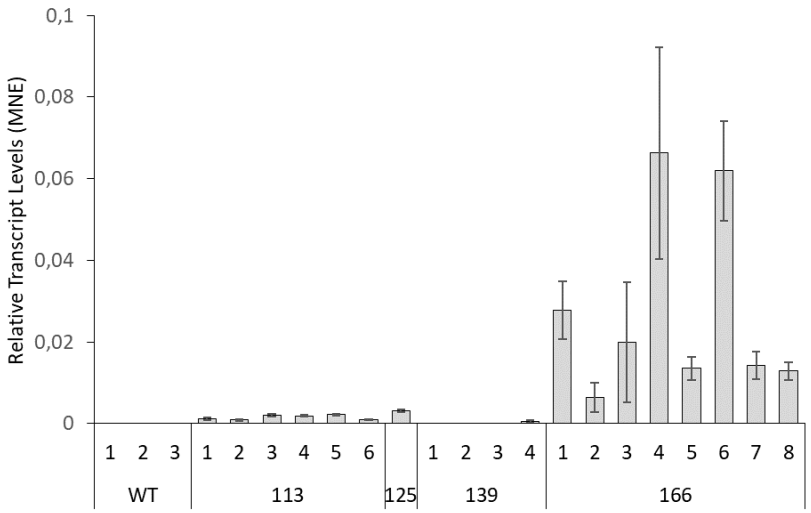

Figure 4.8 Expression levels of *SlTDC1* in Micro-Tom transgenic overexpressing plants detected by q Real-time PCR analysis. Bars represent standard error (n=3; technical replicates).

T_1 SlTDC1 overexpressing plants show deep metabolome modifications

To understand whether the overexpression of *SlTDC1* resulted in altered levels of the related product, i.e. tryptamine, but also serotonin, within the plant, the same leaf samples were used to extract polar and medium polar metabolites for untargeted UPLC-ESI-MS analysis. Tryptamine and serotonin detection and quantification in the samples were performed as previously described ("Material and methods", Chapter 3) but no significative variations in the levels of these indolamines were observed among transgenic and control plants (data not shown). In order to investigate whether tryptamine or serotonin might be addressed to other downstream products or if *SlTDC1* overexpression might have altered the upstream metabolic pathways interconnected to their biosynthesis, multivariate statistics analysis was used to explore the feature matrix produced by untargeted metabolomics in both positive and negative ionization mode. As shown in Figure 4.9A the PCA score plot revealed a clear separation

of the samples representing the overexpressing plants from the control group. This distribution was deeper investigated through O2PLS-DA by establishing three classes: control plants and two groups of overexpressing plants (OE/A and OE/B) that seemed to be discriminated by the second principal component of PCA. The corresponding O2PLS-DA loading plot revealed deep metabolome modifications occurring in transgenic plants given the high number of metabolites strongly correlated with both OE classes yet at the same time negatively correlated with control plants (Figure 4.9 B, fucsia circle). Moreover, control plants showed a bouquet of strongly characterizing metabolites (blue circle). This was in line with what observed from the comparison of base peak chromatograms of the methanolic extracts from control and transgenic plants, in which several peaks were noticed to diminish or augment and, in some cases, to appear *de novo* or being depleted. The identification of the differentially accumulated metabolites is currently in progress.

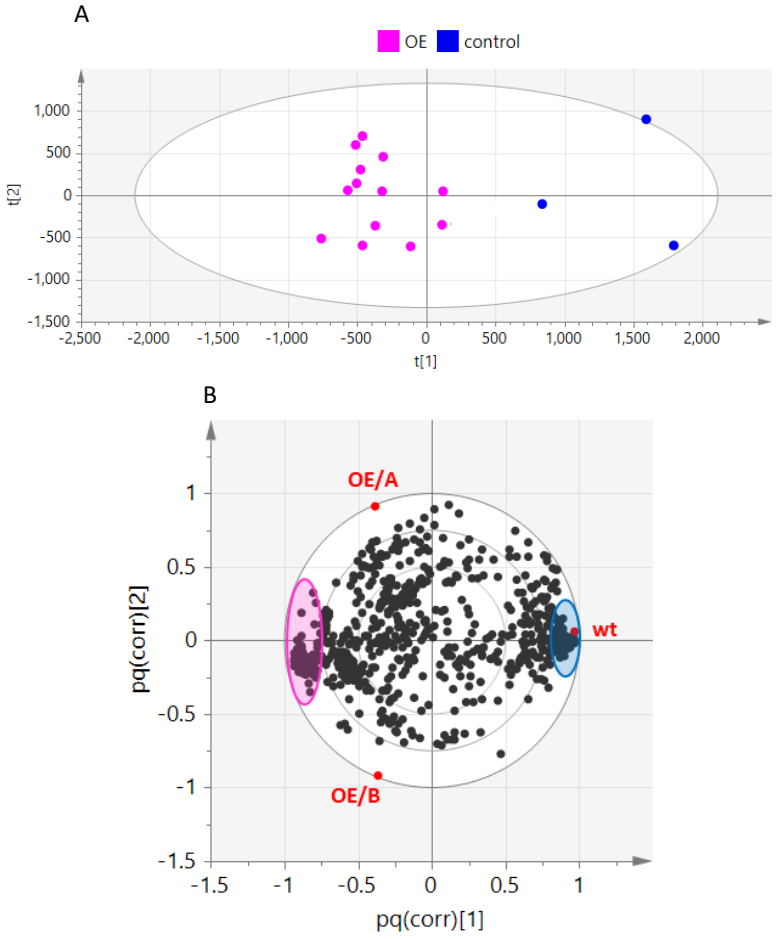

Figure 4.9 Multivariate statistical analysis of the untargeted metabolomics dataset (positive ionization) obtained from the UPLC-ESI-MS analysis of *Solanum lycopersicum* plants overexpressing *SlTDC1* and wild type control plants. A) PCA score scatter plot; B) O2PLS-DA correlation loading plot. Metabolites are represented by black dots and classes by red dots (OE/A: overexpressing plants, group A; OE/B: overexpressing plants, group B; wt, wild type control plants). Fucsia and light-blue areas include, respectively, the most characterizing metabolites of both OE groups and control group.

Characterization of *SlTDC1* Cas9-induced mutations in T_1 Micro-Tom knock-out lines

The six transgenic lines which presented the intact T-DNA for obtaining *SlTDC1* knock-out were furtherly studied to characterize the type of mutations introduced in the *SlTDC1* locus by the endonuclease activity of Cas9. Thus, the genomic DNA of these lines was used as template in a PCR analysis in which a region comprising the open-reading frame of *SlTDC1* was amplified (Figure 4.10). No large deletions were hypothesized to occur given the presence in all samples of a unique band of the same size of that observed in non-transgenic Micro-Tom plants. Therefore, in order to look for smaller lesions not detectable through DNA electrophoresis the amplicons were purified from the agarose gel and sequenced.

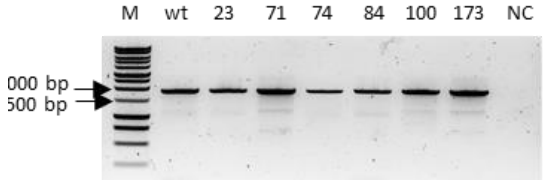

Figure 4.10 PCR analysis of *SlTDC1* locus in transgenic Micro-Tom plants. Primers matching on the terminal part of the promoter and of *SlTDC1* were used (Table 4.1, promTDC1-for7/SlTDC1-revb, 1819 bp).

The results of the sequencing analysis are summarized in Figure 4.11, which reports the alignment of wild-type and mutated *SlTDC1* sequences in the two nucleotide target regions. Higher knock-out efficiency was observed in the upstream target (target2) leading to the generation of three chimeric (mutation°/mutation*) lines (71, 74, 173), one homozygous (mutation/mutation) line (23) and one heterozygous (wt/mutation) line (100). By looking more in detail at target2 mutations, line 23 was homozygous for a 2bp-deletion, lines 71 and 74 were chimeres presenting different types of 1-bp insertions in the two alleles and line 173 was heterozygous presenting a 4bp-deletion in one allele and a 10 bp-deletion plus an AAvsGT substitution in the second allele. Only in 2 out of 6 knock-out lines (23 and 71) were observed mutations in target1 region: the 1-bp insertion (C) and the substitution of 4+1 bp downstream the target sequence. Although the presence in the genomic DNA of the Cas9 cassette, no mutations were observed in the *SlTDC1* locus in line 84. To verify if the mutations observed in *SlTDC1* locus of knock-out lines resulted in a compromised protein product, the nucleotide sequences were translated *in silico* and aligned against the amino acid sequence of SlTDC1 protein (Figure 4.12). All types of mutations observed in knock-out lines determined a shift in the reading frame of *SlTDC1*, thus generating premature stop codons that lead to the production of truncated proteins. Since line 100 was heterozygous, the complete knock-out of *SlTDC1* function was obtained in four transgenic lines, in which, however, no visible phenotypes were observed in their vegetative nor reproductive organs so far.

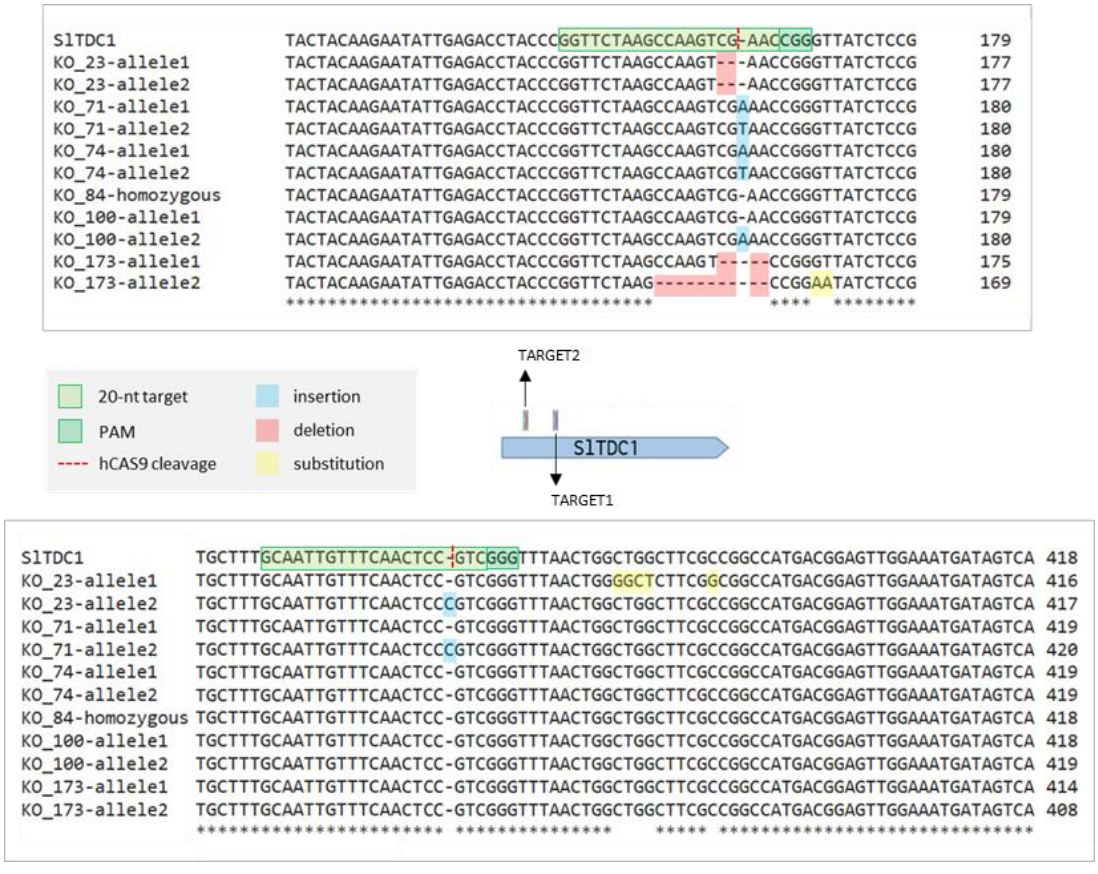

Figure 4.11 Alignments of the two nucleotide regions from the *SlTDC1* locus targeted by Cas9 showing the genotype of mutated knock-out lines versus the wild type gene.

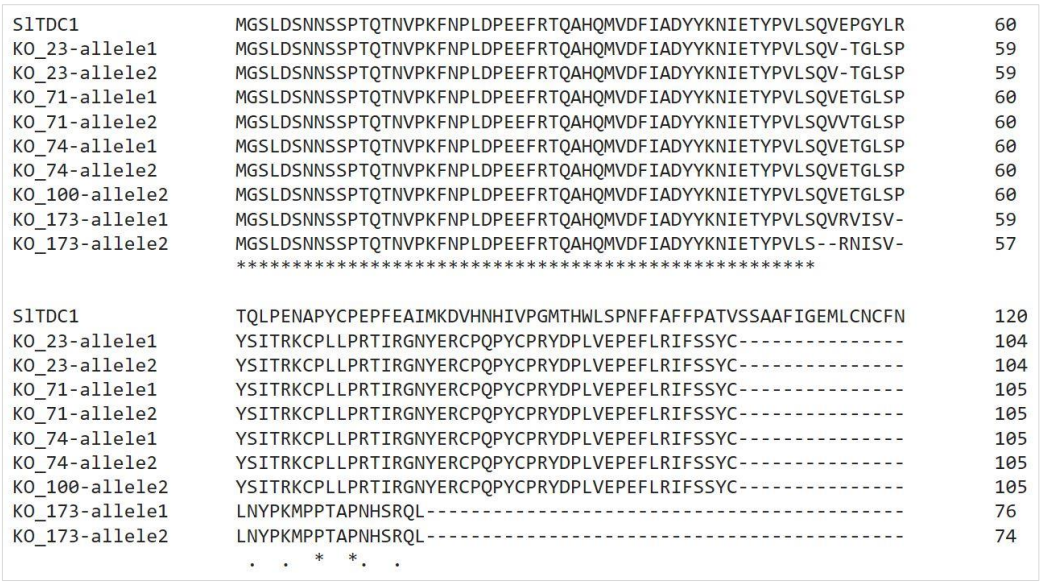

Figure 4.12 Alignment of the amino acid sequences of SlTDC1 protein with the truncated products derived from the *in-silico* translation of Cas9-mutated *SlTDC1*.

Preliminary investigation of *SlTDC1* promoter activity

In order to study the regulation of *SlTD1* expression in the fruit and to get information about its tissue and cellular localization, the 5-kb region (containing the *SlTD1* promoter) upstream the ATG was cloned to drive the expression of the GFP reporter gene. The promoter region was cloned using the genomic DNA extracted from Micro-Tom leaves and then it was assembled by GoldenBraid technology into a plant expression vector upstream the GFP CDS and together with the kanamycin-resistance cassette. Micro-Tom explants were transformed exploiting *Agrobacterium tumefaciens* for the delivery and integration of the assembled T-DNA into the tomato genome (Figure 4.13). At the end of the regeneration process, ten T_0 transgenic lines were obtained. These were let to set fruits and T1 seeds were sown on kanamycin selective medium. All the lines were able to produce vital plantlets and, thus, five of them (90, 118, 120, 130, 151) were chosen to be acclimated in soil and checked by PCR to assess the presence of T-DNA elements in their genomic DNA (Figure 4.13).

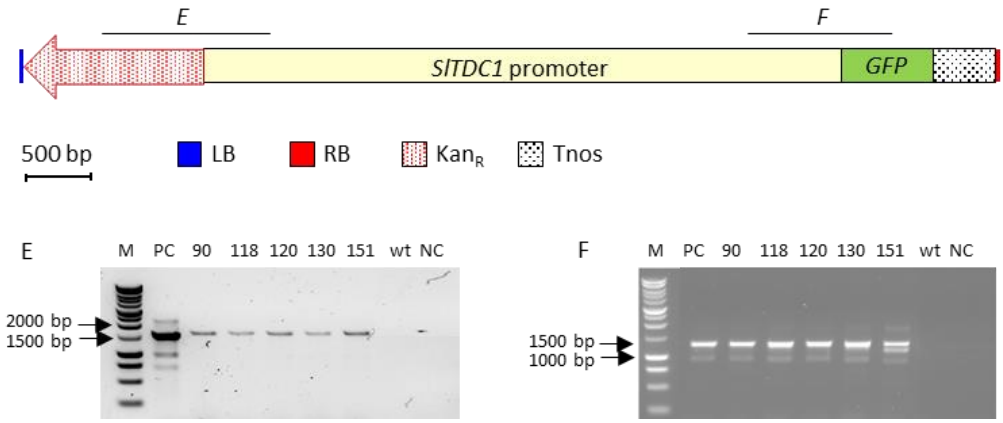

Figure 4.13 Schematic scale representation of the T-DNA region assembled in GoldenBraid pDGB3 binary vector harbouring the *SlTDC1*promoter::GFP::TNos cassette. Letters E-F represent the regions amplified by PCR reaction with specific primers (Table 4.1) to check the presence of T-DNA elements in the genomic DNA of T_1 transgenic lines. (E: kan-for/promTDC1-rev1, 1603 bp; F: promTDC1-for6/GFPmid-rev, 1370 bp). Vector legend: LB and RB, left and right T-DNA borders; TNos, Nopaline synthase gene terminator; Kan_R, neomycin phosphotransferase (*nptII*) gene conferring kanamycin resistance in plants. PCR legend: M, molecular marker; PC, positive control; NC, negative control; wt, wild-type.

T_1 transgenic plants were grown in a growth chamber under controlled conditions and as they entered the reproductive phase, flowers and berries at various developmental stages were collected to assess the expression of the reporter gene (*GFP*). Each sample consisted of a pool of flowers or berries at the same phenological phase collected from the same plant. All developmental stages were not represented in a single plant at the time of the sampling and, thus, samples were collected according to the availability of flowers and berries on the plant. These samples were used to extract the RNA and to synthesize the cDNA that served as template in q Real-time PCR analysis to monitor the transcript

levels of the reporter gene *GFP*. As shown in Figure 4.14, the highest transcript levels of *GFP* were observed in two transgenic lines (130 and 151) during early berry development, in particular in the 2-mm size berry (BPF, berry post fertilization; about 5 days after anthesis) and at the immature green stage (IG; about 15 days after anthesis). Interestingly, the availability of all phenological stages of berry development and ripening in line 151, allowed to observe a decreasing trend in the expression of *GFP* as the berry approaches to real ripening phase, as it was observed also in non-transgenic Micro-Tom fruits (Chapter 3). However, different trends were observed among transgenic lines: for instance, *GFP* transcripts were undetectable in the ripe berry of line 90 and were remarkably low in that one of line 118; the expression levels in the flowers were also differently modulated among the various lines whereas the mature green stage showed less variation. Despite the presence of *GFP* transcript in the fruit, preliminary observations of unripe and ripe berry sections at the confocal microscope did not reveal significative GFP fluorescence signals in the transgenic lines when compared to control fruits (data not shown).

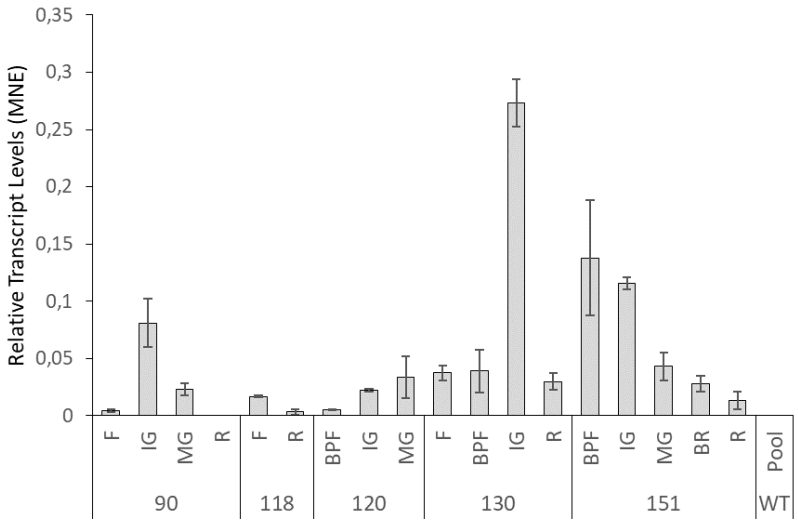

Figure 4.14 Expression levels of *GFP* in Micro-Tom transgenic plants detected by q Real-time PCR analysis. Bars represent standard error (n=3; technical replicates). Legend: F, flowers; BFP, berry post fertilization; IG, immature green berry; MG, mature green berry; BR, breaker berry; R, riper berry.

Discussion

In order to move a first step in the study of the biological roles of tryptamine and serotonin and of their biosynthetic genes in the whole tomato plant, a metabolic engineering approach was adopted by targeting the first step of the serotonin pathway, i.e. tryptamine production. *SlTDC1* was shown in the previous chapters to codify for a high performant tryptophan decarboxylase enzyme and to be fruit-specific, correlating with tryptamine accumulation in the developing berry. For these reasons it was chosen, among the other *SlTDC* genes, as the best target for tuning the levels of tryptamine, and hypothetically of serotonin as well, in the plant.

For our functional studies, the strategies here used were: 1) to increase the accumulation of tryptamine in the whole plant and 2) to drastically reduce the levels of this indolamine in the fruit.

The first strategy was pursued by performing the CaMV35S promoter-driven *SlTDC1* overexpression and the second by CRISPR/Cas9-mediated knock-out of the same gene.

The choice of evaluating the effects of tryptamine depletion in the fruit is due to the fact that one of the points of this PhD thesis is to investigate the biological role of this indolamine in this organ, which - despite it is well known that fruits contain high indolamine amounts - still represents an unexplored issue. The choice was conscious of the fact that within the tomato berry there is also another *TDC* gene expressed, i.e. *SlTDC3*, whose functions seems, however, to be related to tryptamine production in the finale ripening phase.

The ectopic overexpression of *SlTDC1* putatively results in altered plant architecture in one transgenic line

Micro-Tom explants transformed with a T-DNA harbouring the *SlTDC1* gene under the control of constitutive 35S promoter by the mean of *Agrobacterium tumefaciens* infection were regenerated *in vitro* to form T_0 plants. Although these did not present any evident phenotype, when 4 transgenic lines were brought to the next generation (T_1), curiously, a line that showed higher *SlTDC1* transcript levels exhibited altered architecture of the nodes next to shoot apex with younger leaves displaying impaired leaf morphology. Such altered architecture observed in *SlTDC1* overexpressing plants and the fact that, as discussed in Chapter 3, both expression and accumulation patterns of *SlTDC* genes, tryptamine and serotonin resembles in some way the distribution of auxin in some plant organs, lead to hypothesize that the overexpression of *SlTDC1* might have in a way caused an interference or disruption of the auxin gradients in the plant. In tomato developing leaves, in fact, auxin plays crucial roles in the formation of the dissected leaf since the asymmetric distribution of this hormone, driven by active transport, delineates the initiation of lobes and leaflets and specifies differential laminar outgrowth

(Koenig et al., 2009; Ben-Gera & Ori, 2012). Moreover, there are many current hypotheses on the roles of serotonin as plant growth promoter or as signalling molecule acting together with melatonin in a similar on antagonistic way to other plant hormones such as auxins and cytokinins (Erland et al. 2015; Mukherjee, 2018). Some studies suggest that endogenous auxin analogues, such as serotonin and tryptamine, may act as natural attenuators of the auxin signalling pathway given the high structural similarity and the possible competitivity for the same receptors in plants (Ma & Robert, 2014). For instance, serotonin has been shown to be a natural auxin antagonist on root development by competitively inhibiting auxin-induced gene expression (Pelagio-Flores et al., 2011). Another major point of debating the role of tryptophan-derived indolamines in a hormonal context is the fact that tryptamine has long been hypothesized to be an intermediate in one of the minor alternative tryptophan-dependent pathways that lead to indole-3-acetic acid synthesis (Kasahara, 2016; Di et al., 2016) but its putative involvement has still to be clearly demonstrated. However, since the altered phenotype was marked just in one overexpressing line, it might not to be excluded that the random integration of T-DNA in tomato genome might have caused knock-out of genes related to plant development.

As revealed by metabolomics analysis, both tryptamine and serotonin levels in *SlTDC1* overexpressing plants did not change respect to the control group but, however, deep metabolome modifications were observed by exploring the untargeted metabolomics data through multivariate statistical analysis. A substantial number of metabolites was observed to strongly correlate with the overexpressing plant and not with the control groups, and vice versa. This suggest that in transgenic plants some metabolites might pe produced *de novo* or increased by channelling of the tryptophan pool into downstream tryptamine pathways, whereas others might be depleted or reduced such as tryptophan-derived metabolites not related to tryptamine. However, deeper investigations to identify the metabolites responsible for such differences are required. It can also be hypothesized that, given the normal amounts of tryptamine and serotonin detected in the transgenic plants, their production and accumulation is, at least in the leaves, under strict regulative control in order to keep balanced levels of these indolamines in the vegetative tissues.

CRISPR/Cas9 mediated knock-out of *SlTDC1* results in no obvious phenotype

The application of CRISPR/Cas9 technique successfully resulted in the generation of Micro-Tom knock-out transgenic lines for the *SlTDC1* gene. The analysis of lesions induced by Cas9 activity in the locus of this gene demonstrated, at least *in silico*, to result in truncated protein products which did not present the catalytic sites required for TDC conversion of tryptophan to tryptamine. Both T_0 and T_1 lines did not present defects in growth nor in the formation and ripening of the mutant fruits. However, the biochemical characterization of these lines, which could provide significative details about the putative effect of *SlTDC1* knock-out on fruit metabolome, has not been carried out yet. It

appears, thus, that under normal growth conditions the lack of *SlTDC1* activity does not result in compromised physiological functions. Nonetheless, it might not be excluded that under conditions such as the presence of abiotic or biotic stress the fruits might exhibit some interesting phenotype. It has been shown in fact that *TDC* genes that are expressed only in particular organs or tissues are induced or triggered by several type of external factors, mainly by the presence of pathogens but also abiotic stress such as UV light and thermal stress (Ouwerkerk et al., 1999; López-Meyer & Nessler, 1997; Ishihara et al., 2008; Park et al., 2009; Ahammed et al., 2019).

Considerations on transgenic fruits expressing *GFP* under the control of *SlTDC1* promoter

Micro-tom transgenic lines able to express the *GFP* reporter gene under the control of *SlTDC1* promoter produced fruits that, although presenting its transcript, resulted in no clear GFP signals when pericarp sections of the unripe and ripe berries were examined at the confocal microscope. Although further investigation are need, there are several biological reasons which could justify the absence of a distinct GFP signal against control samples. *SlTDC1* seems to be, in fact, expressed in the fruit exocarp and in the seeds at very low levels (Chapter 3). If eventual GFP production would occur in these sites, it might thus be in very low amounts. Moreover, in these organs, the presence of structures (e.g. cuticle) or endogenous compounds able to emit fluorescence light in the same spectral region of GFP, which was observed in control plants (data not shown), could mask the real GFP signal.

Conclusions

The work presented in this chapter, although being just a preliminary investigation of the topic, started to put a focus on the functions of tryptamine and serotonin in the plant and the fruit of tomato. The metabolic engineering approaches adopted led to the production of transgenic Micro-Tom plants in which the fruit-specific gene *SlTDC1* was overexpressed or knocked-out. One overexpressing line exhibited altered plant architecture in the shoots and this, also in the light of what discussed in the previous chapter, raised reasonable questions about the putative interaction of tryptamine/serotonin and of their biosynthetic genes with the hormone auxin, which is a key regulator of plant development and for which several authors proposed a cross-talk with the tryptophan-derived indolamines. Moreover, deep metabolome modifications were observed in transgenic plants through multivariate statistical analysis of the untargeted metabolomic data, thus indicating that ectopic overexpression of *SlTDC1* results in the perturbation of the metabolic networks interconnected with the serotonin biosynthetic pathway or with its regulation.

Moreover, homozygous knock-out lines for the fruit specific *SlTDC1* gene were produced. Given the absence of obvious phenotypes in the transgenic fruits under normal growing conditions, as well as the fact that all transgenic lines gave rise to vital progeny, this gene seems not be involved in essential processes regulating formation and development of fruits or seeds. Nevertheless, given the induction of many plant *TDC* genes upon pathogen elicitation, it is not excluded that mutated fruits might exhibit specific phenotypes once subjected to several types of stress, an issue that will be investigated in the next generation of transgenic plants.

The preliminary data presented in this chapter are, therefore, not sufficient tools to speculate on the involvement of tryptamine and serotonin in precise functions in the plant or within the fruit but encouraged the need to shed light on this interesting topic.

Chapter 5

Concluding remarks

The work presented in this PhD thesis aimed to the investigation of the biological roles of tryptamine and serotonin within the plant and the fruit of *Solanum lycopersicum* (cv. Micro-Tom) in order to shed a light on the not fully-understood and puzzling physiological functions of plant indolamines. The results achieved are here summarized and discussed in relation to the future objectives that this research might address for a deeper investigation of the topic.

A three-member *TDC* gene family and one *T5H* gene of tomato were functionally characterized as *bona-fide* TDCs and T5H through homology-based identification with previously characterized plant genes and heterologous expression in *Nicotiana bethamiana* followed by metabolomics-based detection of their related products, i.e. tryptamine and serotonin. These genes constitute the tomato serotonin pathway.

The distribution of tryptamine and serotonin and the expression patterns of their characterized biosynthetic genes were then elucidated in Micro-Tom plants revealing the existence of a complementary, yet not redundant activity of the three *SlTDC* isogenes in the various plant organs and fruit developmental/ripening stages analysed. Briefly, *SlTDC1* was active during fruit development, putatively determining the accumulation of tryptamine in this organ, whereas the other two genes, which were expressed in the vegetative aerial organs and flowers (*SlTDC2*) or at an ubiquitous level (*SlTDC3*) were found to orchestrate complex expression/metabolite accumulation gradients of tryptamine and serotonin along the main axis of the plant. Moreover, the high amounts of serotonin and tryptamine observed in general in all parts of the plants leads to consider these metabolites not only intermediates but also end products.

Interestingly, the *SlTDC1* overexpression observed in transgenic Micro-Tom lines produced in this thesis resulted in no alterations of the fruit phenotype but caused the development of leaves with clear defects in leaf blade expansion in the higher part of the transgenic plants. Moreover, by exploiting the reverse approach, i.e. CRISPR-mediated knock-out, no obvious phenotypes resulted in *SlTDC1* knock-out fruits suggesting that this gene might not be essential in the fruit under normal growing conditions.

Future perspectives

Given the very interesting, yet still preliminary, evidences produced in this work suggesting important physiological functions for tryptamine and serotonin in tomato, it is reasonable to investigate in the future the following specific points.

1.How are the tryptamine/serotonin gradients generated in the vegetative organs?

To increase the knowledge on this issue, labelled precursors, the deuterated commercial tryptamine (dTAM) and serotonin (dSER), will be furnished to tomato young plants cultured *in vitro*, and the comparison of downstream deuterated products will be followed by high-resolution LC-MS (fluxomic experiments). The same precursors will also be administered to tomato leaves in planta by infiltration, applying a gentle pressure with a syringe without the needle. The untargeted metabolomics of young plants and leaves will allow to check both the possible known downstream products (melatonin and auxins) and the unknown ones.

The possible translocation of the metabolites can be tested feeding plant organs (stem cuts) with the dTAM and dSER at one side or the other, and then tracking the labelled metabolites downstream and upstream in stems and leaves, by high-resolution LC-MS.

The possible negative regulation of *SlTDC2* and *SlTDC3* by their products (tryptamine and/or serotonin) will be tested in two ways:

i) supplementing *in vitro* cultivated young plants and/or calli with different amount of dTAM/dSER and, after a suitable time, measuring the levels of newly produced not-labelled serotonin and tryptamine in comparison with negative controls (plants and calli that underwent the same manipulation but without dTAM/dSER supplementation);
ii) the already established *Nicotiana benthamiana* leaf transient expression assay will be used, infiltrating *SlTDC2*, *SlTDC3* or *SlTDC2+SlTDC3* genes together with the possible inhibitors (dTAM and dSER). In this way, the *SlTDC2* and *SlTDC3* enzyme activity can be measured in presence and absence of the possible inhibitor by monitoring the tryptamine level.

Of course, it is not excluded protein translocation which, to be investigated, requires antibodies to test in a specific way the protein levels in the various part of the plant.

2.How is the SlTDCs spatial expression pattern regulated?

The regulation of gene expression by endogenous/exogenous factors is an important tile for understanding the biological function of a gene. The regulation of *SlTDC* genes *SlT5H* will be investigated through in silico approach to study the possible responsive motifs in the promoters of the various genes and to study the co-expression of these genes with others having similar motifs.

Expression atlas available for the tomato cv. Micro-Tom and Heinz will be used for the co-expression studies. The expression levels of *SlTDCs* and *SlT5H*,as well as the tryptamine and serotonin amounts, will also be monitored by real time PCR in an already available callus of tomato; if the pathway will result to be active, the change in the levels of these genes and these metabolites will be measured after treatment with various hormones (especially with auxins), hormone combination, abiotic stress (cold, high temperature, low light, high light, high salinity, drought induced by high mannitol), and elicitors connected with biotic attacks (i.e. jasmonic acid, salicylic acid). If the pathway will result not active in the callus, in vitro cultured young plants will be used. Also *in situ* RNA-hybridization and methods that do not rely on GFP fusion for the localization of gene expression in plant tissues and cells, which for *SlTDC1* promoter study resulted challenging, might be adopted.

3.Which are, if any, the relations between TDCs, tryptamine and auxin?

Beyond what already described about this issue, proving or excluding the possibility of auxin production by tryptamine is necessary in this project: if the pathway of production of auxin from tryptamine would be active, the phenotypes observed after tryptamine levels alteration could be due to unintended alteration of auxin levels rather than be correlated to tryptamine itself.

The possible role of auxin on *SlTDC*/*SlT5H* gene regulation will be investigated as already described in point 2, whereas the possible production of auxin from tryptamine will emerge from the fluxomic experiments of point 1.

4.What happens if the amounts/gradients of tryptamine/serotonin are artificially perturbed at different levels in the fruit and the vegetative organs?

The perturbation of tryptamine/serotonin levels and gradients could be obtained in various ways, and the resulting phenotypes are crucial for this project since they are expected to give important clues on the biological roles of these metabolites and of the genes responsible for their biosynthesis.

i) *Accumulation – SlTDC1* overexpressing tomato plant lines, in which the *SlTDC1* has been ectopically expressed will be further characterized in order to measure indolamines levels in the fruit. Moreover, a new assay will be set up to administer chemicals to young leaves of tomato, as usually done with *Nicotiana*, through infiltration by pressure, exerted with a syringe without needle. The leaves will be treated with high doses of tryptamine and serotonin, alone and in combination, and the development of an eventual phenotypes will be followed. This approach can be done also in the fruit through the berry pedicel or the exocarp in order to evaluate the effect of indolamines supplementation in this organ.
ii) *Depletion – SlTDC1* knocked out tomato plant lines, obtained by CRISPR/Cas9 mediated genome editing, are available; *SlT5H*, *SlTDC2* and *SlTDC3* knocked-out plant lines will be generated. Double knock-out mutants (*SlTDC1*/*SlTDC2*, *SlTDC2*/*SlTDC3*, *SlTDC1*/*SlTDC3*) and the triple knock-out mutant *SlTDC1*/*SlTDC2*/*SlTDC3* will be generated by crossing the

single mutants between them. The effects of each mutation and combination of mutations on levels and gradients of tryptamine and serotonin will be directly determined by targeted metabolomics. What is expected is that *SlTDC2*/*SlTDC3* or *SlTDC1*/*SlTDC2*/*SlTDC3* knock-out mutants completely abolished the tryptamine and serotonin biosynthesis in shoots, while *SlT5H* knock-out mutant should abolish serotonin accumulation, maybe increasing tryptamine levels. In the fruit its expected, instead, that knocking-out both *SlTDC1*/*SlTDC3* would result in complete tryptamine and serotonin depletion, in the absence of metabolite translocation from the photosynthetic organs. The mutant fruits of this line as well as fruits of this line supplemented with exogenous serotonin will be tested under the stressing conditions described in point 2 to evaluate the involvement of tryptamine and serotonin in stress response, being able to discriminate among the putative protective effects of one molecule respect to the other one.

Bibliography

Abu-Zaitoon, Y. M. (2014). Phylogenetic analysis of putative genes involved in the tryptophan-dependent pathway of auxin biosynthesis in rice. *Applied biochemistry and biotechnology*, 172(5), 2480-2495.

Aerts, R. J., Alarco, A. M., & De Luca, V. (1992). Auxins induce tryptophan decarboxylase activity in radicles of *Catharanthus* seedlings. *Plant physiology*, 100(2), 1014-1019.

Ahammed, G. J., Xu, W., Liu, A., & Chen, S. (2019). Endogenous melatonin deficiency aggravates high temperature-induced oxidative stress in *Solanum lycopersicum* L. *Environmental and Experimental Botany*, 161, 303-311.

Al-Soqeer, A. A., Alsubaie, Q. D., Motawei, M. I., Mousa, H. M., & Abdel-Salam, A. M. (2017). Isolation and identification of allergens and biogenic amines of *Prosopis juliflora* genotypes. *Electronic Journal of Biotechnology*, 30, 24-32.

Anarat-Cappillino, G., & Sattely, E. S. (2014). The chemical logic of plant natural product biosynthesis. *Current opinion in plant biology*, 19, 51-58.

Araújo, A. M., Carvalho, F., de Lourdes Bastos, M., De Pinho, P. G., & Carvalho, M. (2015). The hallucinogenic world of tryptamines: an updated review. *Archives of Toxicology*, 89(8), 1151-1173.

Arnao, M. B., & Hernández-Ruiz, J. (2014). Melatonin: plant growth regulator and/or biostimulator during stress?. *Trends in plant science*, 19(12), 789-797.

Arnao, M. B., & Hernández-Ruiz, J. (2018). Phytomelatonin, natural melatonin from plants as a novel dietary supplement: Sources, activities and world market. *Journal of Functional Foods*, 48, 37-42.

Arnao, M. B., & Hernández-Ruiz, J. (2019). Melatonin: a new plant hormone and/or a plant master regulator?. *Trends in plant science*, 24(1), 38-48.

Azmitia, E. C. (2001). Modern views on an ancient chemical: serotonin effects on cell proliferation, maturation, and apoptosis. *Brain research bulletin*, 56(5), 413-424.

Azmitia, E. C. (2010). Evolution of serotonin: sunlight to suicide. In Handbook of behavioral neuroscience (Vol. 21, pp. 3-22). Elsevier.

Back, K., Tan, D. X., & Reiter, R. J. (2016). Melatonin biosynthesis in plants: multiple pathways catalyze tryptophan to melatonin in the cytoplasm or chloroplasts. *Journal of pineal research*, 61(4), 426-437.

Badria, F. A. (2002). Melatonin, serotonin, and tryptamine in some Egyptian food and medicinal plants. *Journal of medicinal food*, 5(3), 153-157.

Baixauli, E. (2017). Happiness: Role of Dopamine and Serotonin on mood and negative emotions. *Emergency Medicine*, 7, 350.

Bartley, G. E., Breksa III, A. P., & Ishida, B. K. (2010). PCR amplification and cloning of tyrosine decarboxylase involved in synephrine biosynthesis in *Citrus*. *New biotechnology*, 27(4), 308-316.

Bajwa, V. S., Shukla, M. R., Sherif, S. M., Murch, S. J., & Saxena, P. K. (2015). Identification and characterization of serotonin as an anti-browning compound of apple and pear. *Postharvest Biology and Technology*, 110, 183-189.

Belhaj, K., Chaparro-Garcia, A., Kamoun, S., Patron, N. J., & Nekrasov, V. (2015). Editing plant genomes with CRISPR/Cas9. *Current opinion in biotechnology*, 32, 76-84.

Ben-Gera, H., & Ori, N. (2012). Auxin and LANCEOLATE affect leaf shape in tomato via different developmental processes. *Plant signaling & behavior*, 7(10), 1255-1257.

Berlin, J., Rügenhagen, C., Dietze, P., Fecker, L. F., Goddijn, O. J., & Hoge, J. H. C. (1993). Increased production of serotonin by suspension and root cultures of *Peganum harmala* transformed with a tryptophan decarboxylase cDNA clone from *Catharanthus roseus*. *Transgenic Research*, 2(6), 336-344.

Bertani, G. (1951). Studies on lysogenesis: The mode of phage liberation by lysogenic *Escherichia Coli*. *Journal of bacteriology*, 62(3), 293.

Bhattarai, Y., Williams, B. B., Battaglioli, E. J., Whitaker, W. R., Till, L., Grover, M., ... & Kaunitz, J. D. (2018). Gut microbiota-produced tryptamine activates an epithelial G-protein-coupled receptor to increase colonic secretion. *Cell host & microbe*, 23(6), 775-785.

Bortesi, L., & Fischer, R. (2015). The CRISPR/Cas9 system for plant genome editing and beyond. *Biotechnology advances*, 33(1), 41-52.

Böttger, A., Vothknecht, U., Bolle, C., & Wolf, A. (2018). Secondary Metabolites in Plants: General Introduction. In Lessons on Caffeine, Cannabis & Co (pp. 143-152). Springer, Cham.

Bowden, K., BROWN, B. G., & BATTY, J. E. (1954). 5-Hydroxytryptamine: its occurrence in cowhage. *Nature*, 174(4437), 925-926.

Breitling, R., Ceniceros, A., Jankevics, A., & Takano, E. (2013). Metabolomics for secondary metabolite research. *Metabolites*, 3(4), 1076-1083.

Brumos, J., Alonso, J. M., & Stepanova, A. N. (2014). Genetic aspects of auxin biosynthesis and its regulation. *Physiologia plantarum*, 151(1), 3-12.

Brzezinski, A. (1997). Melatonin in humans. *New England journal of medicine*, 336(3), 186-195.

Byeon, Y., Lee, H. Y., Lee, K., Park, S., & Back, K. (2014_a). Cellular localization and kinetics of the rice melatonin biosynthetic enzymes SNAT and ASMT. *Journal of Pineal Research*, 56(1), 107-114.

Byeon, Y., Park, S., Lee, H. Y., Kim, Y. S., & Back, K. (2014_b). Elevated production of melatonin in transgenic rice seeds expressing rice tryptophan decarboxylase. *Journal of Pineal Research*, 56(3), 275-282.

Canel, C., Lopes-Cardoso, M. I., Whitmer, S., van der Fits, L., Pasquali, G., van der Heijden, R., ... & Verpoorte, R. (1998). Effects of over-expression of strictosidine synthase and tryptophan decarboxylase on alkaloid production by cell cultures of *Catharanthus roseus*. *Planta*, 205(3), 414-419.

Chae, L., Kim, T., Nilo-Poyanco, R., & Rhee, S. Y. (2014). Genomic signatures of specialized metabolism in plants. *Science*, 344(6183), 510-513.

Chavadej, S., Brisson, N., McNeil, J. N., & De Luca, V. (1994). Redirection of tryptophan leads to production of low indole glucosinolate canola. *Proceedings of the National Academy of Sciences*, 91(6), 2166-2170.

Charoonratana, T., Wungsintaweekul, J., Keawpradub, N., & Verpoorte, R. (2013). Molecular cloning and expression of tryptophan decarboxylase from *Mitragyna speciosa*. *Acta physiologiae plantarum*, 35(8), 2611-2621.

Choi, G. H., Lee, H. Y., & Back, K. (2017). Chloroplast overexpression of rice caffeic acid O-methyltransferase increases melatonin production in chloroplasts via the 5-methoxytryptamine pathway in transgenic rice plants. *Journal of pineal research*, 63(1), e12412.

Collier, H. O. J., & Chesher, G. B. (1956). Identification of 5-hydroxytryptamine in the sting of the nettle (Urtica dioica). *British journal of pharmacology and chemotherapy*, 11(2), 186.

Commisso, M., Negri, S., Bianconi, M., Gambini, S., Avesani, S., Ceoldo, S., ... & Guzzo, F. (2019). Untargeted and Targeted Metabolomics and Tryptophan Decarboxylase In Vivo Characterization Provide Novel Insight on the Development of Kiwifruits (*Actinidia deliciosa*). *International journal of molecular sciences*, 20(4), 897.

Dangol, A., Yaakov, B., Jander, G., Strickler, S. R., & Tzin, V. (2019). Characterizing the serotonin biosynthesis pathway upon aphid infestation in *Setaria viridis* leaves. *BioRxiv*, 642041.

Dastmalchi, M., & Facchini, P. J. (2016). Plant metabolons assembled on demand. *Science*, 354(6314), 829-830.

De Llano, D. G. (1998). Biogenic amine production by wild lactococcal and leuconostoc strains. *Letters in Applied Microbiology*, 26(4), 270-274.

De Luca, V., Marineau, C., & Brisson, N. (1989). Molecular cloning and analysis of cDNA encoding a plant tryptophan decarboxylase: comparison with animal dopa decarboxylases. *Proceedings of the National A cademy of Sciences*, 86(8), 2582-2586.

De Luca, V. (2000). Metabolic engineering of crops with the tryptophan decarboxylase of *Catharanthus roseus*. In Metabolic Engineering of Plant Secondary Metabolism (pp. 179-194). Springer, Dordrecht.

De Luca, V., Salim, V., Thamm, A., Masada, S. A., & Yu, F. (2014). Making iridoids/secoiridoids and monoterpenoid indole alkaloids: progress on pathway elucidation. *Current opinion in plant biology*, 19, 35-42.

De Masi, L., Castaldo, D., Pignone, D., Servillo, L., & Facchiano, A. (2017). Experimental evidence and in silico identification of tryptophan decarboxylase in *Citrus* genus. *Molecules*, 22(2), 272.

Delgoda, R., & Murray, J. E. (2017). Evolutionary perspectives on the role of plant secondary metabolites. In Pharmacognosy (pp. 93-100). Academic Press.

Delwiche, C. F., & Cooper, E. D. (2015). The evolutionary origin of a terrestrial flora. *Current Biology*, 25(19), R899-R910.

Di, D. W., Zhang, C., Luo, P., An, C. W., & Guo, G. Q. (2016). The biosynthesis of auxin: how many paths truly lead to IAA?. *Plant growth regulation*, 78(3), 275-285.

Diamante, M. S., Borges, C. V., da Silva, M. B., Minatel, I. O., Corrêa, C. R., Gomez Gomez, H. A., & Lima, G. P. P. (2019). Bioactive Amines Screening in Four Genotypes of Thermally Processed Cauliflower. *Antioxidants*, 8(8), 311.

Dos Santos, R. G., Bouso, J. C., & Hallak, J. E. (2017). Ayahuasca, dimethyltryptamine, and psychosis: a systematic review of human studies. *Therapeutic Advances in Psychopharmacology*, 7(4), 141-157.

Drăgoi, C. M., & Nicolae, A. C. (Eds.). (2018). Melatonin: Molecular Biology, Clinical and Pharmaceutical Approaches. BoD–Books on Demand.

Dubbels, R., Reiter, R. J., Klenke, E., Goebel, A., Schnakenberg, E., Ehlers, C., ... & Schloot, W. (1995). Melatonin in edible plants identified by radioimmunoassay and by high performance liquid chromatography-mass spectrometry. *Journal of pineal research*, 18(1), 28-31.

Ehmann, A. 1974. N-p-(Coumaroyl)tryptamine and N-feruloyltryptamine in kernels of *Zea* maize. *Phytochemistry*, 13:1979–1983.

Eklöf, S., Åstot, C., Moritz, T., Blackwell, J., Olsson, O., & Sandberg, G. (1996). Cytokinin metabolites and gradients in wild type and transgenic tobacco with moderate cytokinin over-production. *Physiologia Plantarum*, 98(2), 333-344.

Engström, K., Lundgren, L., & Samuelsson, G. (1992). Bioassay-guided isolation of serotonin from fruits of *Solanum tuberosum* L. *Acta pharmaceutica nordica*, 4(2), 91-92.

Erland, L. A., Murch, S. J., Reiter, R. J., & Saxena, P. K. (2015). A new balancing act: the many roles of melatonin and serotonin in plant growth and development. *Plant signaling & behavior*, 10(11), e1096469.

Erland, L. A., Turi, C. E., & Saxena, P. K. (2016). Serotonin: An ancient molecule and an important regulator of plant processes. *Biotechnology advances*, 34(8), 1347-1361.

Erland, L., & Saxena, P. K. (2017). Beyond a neurotransmitter: The role of serotonin in plants. *Neurotransmitter*, 4, e1538.

Erland, L. A., Shukla, M. R., Singh, A. S., Murch, S. J., & Saxena, P. K. (2018). Melatonin and serotonin: mediators in the symphony of plant morphogenesis. *Journal of pineal research*, 64(2), e12452.

Erland, L. A., Turi, C. E., & Saxena, P. K. (2019). Serotonin in Plants: Origin, Functions, and Implications. In Serotonin (pp. 23-46). *Academic Press*.

Erspamer, V., & Vialli, M. (1937). Ricerche sul secreto delle cellule enterocromaffini. Boll d Soc Med-chir Pavia, 51, 357-363.

Everat-Bourbouloux, A., & Charnay, D. (1982). Endogenous abscisic acid levels in stems and axillary buds of intact or decapitated broad-bean plants (Vicia faba L.). *Physiologia plantarum*, 54(4), 440-445.

Facchini, P. J., & De Luca, V. (1995). Expression in *Escherichia coli* and partial characterization of two tyrosine/dopa decarboxylases from opium poppy. *Phytochemistry*, 38(5), 1119-1126.

Facchini, P. J., Huber-Allanach, K. L., & Tari, L. W. (2000). Plant aromatic L-amino acid decarboxylases: evolution, biochemistry, regulation, and metabolic engineering applications. *Phytochemistry*, 54(2), 121-138.

Facchini, P. J., Hagel, J., & Zulak, K. G. (2002). Hydroxycinnamic acid amide metabolism: physiology and biochemistry. *Canadian Journal of Botany*, 80(6), 577-589.

Fawcett, C. H. (1961). Indole auxins. *Annual Review of Plant Physiology*, 12(1), 345-368.

Feldman, J. M., & Lee, E. M. (1985). Serotonin content of foods: effect on urinary excretion of 5-hydroxyindoleacetic acid. *The American journal of clinical nutrition*, 42(4), 639-643.

Fellows, L. E., & Bell, E. A. (1970). 5-Hydroxy-L-tryptophan, 5-hydroxytryptamine and L-tryptophan-5-hydroxylase in *Griffonia simplicifolia*. *Phytochemistry*, 9(11), 2389-2396.

Fellows, L. E., & Bell, E. A. (1971). Indole metabolism in Piptadenia peregrina. *Phytochemistry*, 10(9), 2083-2091.

Foy, J. M., & Parratt, J. R. (1960). A note on the presence of noradrenaline and 5-hydroxytryptamine in plantain (*Musa sapientum*). *Journal of Pharmacy and Pharmacology*, 12(1), 360-364.

Fricke, J., Blei, F., & Hoffmeister, D. (2017). Enzymatic synthesis of psilocybin. *Angewandte Chemie International Edition*, 56(40), 12352-12355.

Fujiwara, T., Maisonneuve, S., Isshiki, M., Mizutani, M., Chen, L., Wong, H. L., ... & Shimamoto, K. (2010). Sekiguchi lesion gene encodes a cytochrome P450 monooxygenase that catalyzes conversion of tryptamine to serotonin in rice. *Journal of Biological Chemistry*, 285(15), 11308-11313.

Gecchele, E., Merlin, M., Brozzetti, A., Falorni, A., Pezzotti, M., & Avesani, L. (2015). A comparative analysis of recombinant protein expression in different biofactories: bacteria, insect cells and plant systems. *Journal of Visualized Experiments*, (97), e52459.

Geerlings, A., Hallard, D., Caballero, A. M., Cardoso, I. L., Van der Heijden, R., & Verpoorte, R. (1999). Alkaloid production by a *Cinchona officinalis*' Ledgeriana'hairy root culture containing constitutive expression constructs of tryptophan decarboxylase and strictosidine synthase cDNAs from *Catharanthus roseus. Plant cell reports*, 19(2), 191-196.

Gill, R. I., Ellis, B. E., & Isman, M. B. (2003). Tryptamine-induced resistance in tryptophan decarboxylase transgenic poplar and tobacco plants against their specific herbivores. *Journal of chemical ecology*, 29(4), 779-793.

Gill, R. I., & Ellis, B. E. (2006). Over-expression of tryptophan decarboxylase gene in poplar and its possible role in resistance against *Malacosoma disstria*. *New forests*, 31(2), 195-209.

Giridhar, A. R. P., & Ravishankar, G. A. (2009). Indoleamines and calcium channels influence morphogenesis in in vitro cultures of *Mimosa pudica* L. *Plant signaling & behavior*, 4(12), 1136-1141.

Goddijn, O. J., Lohman, F. P., de Kam, R. J., & Hoge, J. H. C. (1994). Nucleotide sequence of the tryptophan decarboxylase gene of *Catharanthus roseus* and expression of tdc-gusA gene fusions in *Nicotiana tabacum*. *Molecular and General Genetics*, 242(2), 217-225.

Goddijn, O. J., Pennings, E. J., van der Helm, P., Schilperoort, R. A., Verpoorte, R., & Hoge, J. H. C. (1995). Overexpression of a tryptophan decarboxylase cDNA in *Catharanthus roseus* crown gall calluses results in increased tryptamine levels but not in increased terpenoid indole alkaloid production. *Transgenic research*, 4(5), 315-323.

González-Aguilera, K. L., Saad, C. F., Chávez Montes, R. A., Alves-Ferreira, M., & De Folter, S. (2016). Selection of reference genes for quantitative real-time RT-PCR studies in tomato fruit of the genotype MT-Rg1. *Frontiers in plant science*, 7, 1386.

Greene, S. L. (2013). Tryptamines. In Novel Psychoactive Substances (pp. 363-381). Academic press.

Grosse, W. (1982). Function of serotonin in seeds of walnuts. Phytochemistry, 21(4), 819-822.Hardeland, R. (2016). Melatonin in plants–diversity of levels and multiplicity of functions. *Frontiers in Plant Science*, 7, 198.

Guillet, G., Poupart, J., Basurco, J., & De Luca, V. (2000). Expression of tryptophan decarboxylase and tyrosine decarboxylase genes in tobacco results in altered biochemical and physiological phenotypes. *Plant Physiology*, 122(3), 933-944.

Hanahan, D. (1983). Studies on transformation of *Escherichia coli* with plasmids. *Journal of molecular biology*, 166(4), 557-580.

Hano, S., Shibuya, T., Imoto, N., Ito, A., Imanishi, S., Aso, H., & Kanayama, Y. (2017). Serotonin content in fresh and processed tomatoes and its accumulation during fruit development. *Scientia horticulturae*, 214, 107-113.

Hansen, R. L., & Lee, Y. J. (2018). High-Spatial Resolution Mass Spectrometry Imaging: Toward Single Cell Metabolomics in Plant Tissues. *The Chemical Record*, 18(1), 65-77.

Hartmann, T. (1996). Diversity and variability of plant secondary metabolism: a mechanistic view. In Proceedings of the 9th International Symposium on Insect-Plant Relationships (pp. 177-188). Springer, Dordrecht.

Hattori, A., Migitaka, H., Iigo, M., Itoh, M., Yamamoto, K., Ohtani-Kaneko, R., ... & Reiter, R. J. (1995). Identification of melatonin in plants and its effects on plasma melatonin levels and binding to melatonin receptors in vertebrates. *Biochemistry and molecular biology international*, 35(3), 627-634.

Hayashi, K., Fujita, Y., Ashizawa, T., Suzuki, F., Nagamura, Y., & Hayano-Saito, Y. (2016). Serotonin attenuates biotic stress and leads to lesion browning caused by a hypersensitive response to *Magnaporthe oryzae* penetration in rice. *The Plant Journal*, 85(1), 46-56.

Hellens, R. P., Edwards, E. A., Leyland, N. R., Bean, S., & Mullineaux, P. M. (2000). pGreen: a versatile and flexible binary Ti vector for *Agrobacterium*-mediated plant transformation. *Plant molecular biology*, 42(6), 819-832.

Hughes, E. H., Hong, S. B., Gibson, S. I., Shanks, J. V., & San, K. Y. (2004). Metabolic engineering of the indole pathway in *Catharanthus roseus* hairy roots and increased accumulation of tryptamine and serpentine. *Metabolic engineering*, 6(4), 268-276.

Isaacson, T., & Rose, J. K. (2018). Surveying the plant cell wall proteome, or secretome. *Annual Plant Reviews online*, 185-209.

Ishihara, A., Hashimoto, Y., Tanaka, C., Dubouzet, J. G., Nakao, T., Matsuda, F., ... & Wakasa, K. (2008). The tryptophan pathway is involved in the defense responses of rice against pathogenic infection via serotonin production. *The Plant Journal*, 54(3), 481-495.

Islam, J., Shirakawa, H., Nguyen, T. K., Aso, H., & Komai, M. (2016). Simultaneous analysis of serotonin, tryptophan and tryptamine levels in common fresh fruits and vegetables in Japan using fluorescence HPLC. *Food bioscience*, 13, 56-59.

Islas, I., Loyola-Vargas, V. M., & de Lourdes Miranda-Ham, M. (1994). Tryptophan decarboxylase activity in transformed roots from *Catharanthus roseus* and its relationship to tryptamine, ajmalicine, and catharanthine accumulation during the culture cycle. *In Vitro Cellular & Developmental Biology-Plant*, 30(1), 81-83.

Jadaun, J. S., Sangwan, N. S., Narnoliya, L. K., Tripathi, S., & Sangwan, R. S. (2017). *Withania coagulans* tryptophan decarboxylase gene cloning, heterologous expression, and catalytic characteristics of the recombinant enzyme. *Protoplasma*, 254(1), 181-192.

Jung, Y. J., Assefa, A. D., Lee, J. E., Lee, H. S., Rhee, J. H., & Sung, J. S. (2019). Analysis of Antioxidant Activity and Serotonin Derivatives in Safflower (*Carthamus tinctorius* L.) Germplasm Collected from Five Countries. *Korean Journal of Plant Resources*, 32(5), 423-432.

Kang, S., Kang, K., Lee, K., & Back, K. (2007_a). Characterization of tryptamine 5-hydroxylase and serotonin synthesis in rice plants. *Plant cell reports*, 26(11), 2009-2015.

Kang, S., Kang, K., Lee, K., & Back, K. (2007_b). Characterization of rice tryptophan decarboxylases and their direct involvement in serotonin biosynthesis in transgenic rice. *Planta*, 227(1), 263-272.

Kang, K., Kang, S., Lee, K., Park, M., & Back, K. (2008). Enzymatic features of serotonin biosynthetic enzymes and serotonin biosynthesis in plants. *Plant signaling & behavior*, 3(6), 389-390.

Kang, K., Park, S., Kim, Y. S., Lee, S., & Back, K. (2009_a). Biosynthesis and biotechnological production of serotonin derivatives. *Applied microbiology and biotechnology*, 83(1), 27-34.

Kang, K., Kim, Y. S., Park, S., & Back, K. (2009_b). Senescence-induced serotonin biosynthesis and its role in delaying senescence in rice leaves. *Plant physiology*, 150(3), 1380-1393.

Kang, K., Lee, K., Park, S., Byeon, Y., & Back, K. (2013). Molecular cloning of rice serotonin N-acetyltransferase, the penultimate gene in plant melatonin biosynthesis. *Journal of Pineal Research*, 55(1), 7-13.

Kanjanaphachoat, P., Wei, B. Y., Lo, S. F., Wang, I. W., Wang, C. S., Yu, S. M., ... & Chen, L. J. (2012). Serotonin accumulation in transgenic rice by over-expressing tryptophan decarboxlyase results in a dark brown phenotype and stunted growth. *Plant molecular biology*, 78(6), 525-543.

Karimi, M., Inzé, D., & Depicker, A. (2002). GATEWAY™ vectors for *Agrobacterium*-mediated plant transformation. *Trends in plant science*, 7(5), 193-195.

Kasahara, H. (2016). Current aspects of auxin biosynthesis in plants. *Bioscience, biotechnology, and biochemistry*, 80(1), 34-42.

Kawalleck, P., Keller, H., Hahlbrock, K., Scheel, D., & Somssich, I. E. (1993). A pathogen-responsive gene of parsley encodes tyrosine decarboxylase. *Journal of Biological Chemistry*, 268(3), 2189-2194.

Kersey, P. J. (2019). Plant genome sequences: past, present, future. *Current opinion in plant biology*, 48, 1-8.

Khan, M. Z., & Nawaz, W. (2016). The emerging roles of human trace amines and human trace amine-associated receptors (hTAARs) in central nervous system. *Biomedicine & pharmacotherapy*, 83, 439-449.

Kliebenstein, D. J., & Osbourn, A. (2012). Making new molecules–evolution of pathways for novel metabolites in plants. *Current opinion in plant biology*, 15(4), 415-423.

Koenig, D., Bayer, E., Kang, J., Kuhlemeier, C., & Sinha, N. (2009). Auxin patterns *Solanum lycopersicum* leaf morphogenesis. *Development*, 136(17), 2997-3006.

Kojima, K., Ohtake, E., & Yu, Z. (2002). Distribution and transport of IAA in tomato plants. *Plant growth regulation*, 37(3), 249-254.

Kousar, S., Noreen Anjuma, S., Jaleel, F., Khana, J., & Naseema, S. (2017). Biomedical significance of tryptamine: *A review. J. Pharmacovigil*, 5.

Koyanagi, T., Nakagawa, A., Sakurama, H., Yamamoto, K., Sakurai, N., Takagi, Y., ... & Kumagai, H. (2012). Eukaryotic-type aromatic amino acid decarboxylase from the root colonizer *Pseudomonas putida* is highly specific for 3, 4-dihydroxyphenyl-L-alanine, an allelochemical in the rhizosphere. *Microbiology*, 158(12), 2965-2974.

Kueger, S., Steinhauser, D., Willmitzer, L., & Giavalisco, P. (2012). High-resolution plant metabolomics: from mass spectral features to metabolites and from whole-cell analysis to subcellular metabolite distributions. *The Plant Journal*, 70(1), 39-50.

Kumar, R. (2016). Evolutionary trails of plant group II Pyridoxal phosphate-dependent decarboxylase genes. *Frontiers in plant science*, 7, 1268.

Kumar, V., Bhatt, V., & Kumar, N. (2018). Amides From Plants: Structures and Biological Importance. In Studies in Natural Products Chemistry (Vol. 56, pp. 287-333). Elsevier.

Kutchan, T. M. (1995). Alkaloid biosynthesis: the basis for metabolic engineering of medicinal plants. The plant cell, 7(7), 1059.

Lan, X., Chang, K., Zeng, L., Liu, X., Qiu, F., Zheng, W., ... & Liu, W. (2013). Engineering salidroside biosynthetic pathway in hairy root cultures of *Rhodiola crenulata* based on metabolic characterization of tyrosine decarboxylase. *PLoS One*, 8(10), e75459.

Lavizzari, T., Veciana-Nogués, M. T., Bover-Cid, S., Mariné-Font, A., & Vidal-Carou, M. C. (2006). Improved method for the determination of biogenic amines and polyamines in vegetable products by ion-pair high-performance liquid chromatography. *Journal of Chromatography A*, 1129(1), 67-72.

Lee, S. J., Sim, G. Y., Lee, Y., Kim, B. G., & Ahn, J. H. (2017). Engineering of *Escherichia coli* for the synthesis of N-hydroxycinnamoyl tryptamine and serotonin. *Journal of industrial microbiology & biotechnology*, 44(11), 1551-1560.

Lehmann, T., & Pollmann, S. (2009). Gene expression and characterization of a stress-induced tyrosine decarboxylase from *Arabidopsis thaliana*. *FEBS letters*, 583(12), 1895-1900.

Lei, Q., Wang, L., Tan, D. X., Zhao, Y., Zheng, X. D., Chen, H., ... & Kong, J. (2013). Identification of genes for melatonin synthetic enzymes in 'R ed F uji'apple (*Malus domestica* B orkh. cv. R ed) and their expression and melatonin production during fruit development. *Journal of Pineal Research*, 55(4), 443-451.

Li, L., Zheng, M., Long, H., Deng, G., Ishihara, A., Liu, F., ... & Yu, M. (2016). Molecular cloning and characterization of two genes encoding tryptophan decarboxylase from *Aegilops variabilis* with resistance to the cereal cyst nematode (*Heterodera avenae*) and root-knot nematode (*Meloidogyne naasi*). *Plant molecular biology reporter*, 34(1), 273-282.

Liu, W., Chen, R., Chen, M., Zhang, H., Peng, M., Yang, C., ... & Liao, Z. (2012). Tryptophan decarboxylase plays an important role in ajmalicine biosynthesis in *Rauvolfia verticillata*. *Planta*, 236(1), 239-250.

Ljung, K., Hull, A. K., Celenza, J., Yamada, M., Estelle, M., Normanly, J., & Sandberg, G. (2005). Sites and regulation of auxin biosynthesis in *Arabidopsis* roots. *The Plant Cell*, 17(4), 1090-1104.

Loonen, A. J. M., & Ivanova, S. A. (2016). Circuits regulating pleasure and happiness in major depression. Medical hypotheses, 87, 14-21.

López-Meyer, M., & Nessler, C. L. (1997). Tryptophan decarboxylase is encoded by two autonomously regulated genes in *Camptotheca acuminata* which are differentially expressed during development and stress. *The Plant Journal*, 11(6), 1167-1175.

Ly, D., Kang, K., Choi, J. Y., Ishihara, A., Back, K., & Lee, S. G. (2008). HPLC analysis of serotonin, tryptamine, tyramine, and the hydroxycinnamic acid amides of serotonin and tyramine in food vegetables. *Journal of medicinal food*, 11(2), 385-389.

Ma, Q., & Robert, S. (2014). Auxin biology revealed by small molecules. *Physiologia plantarum*, 151(1), 25-42.

Macoy, D. M., Kim, W. Y., Lee, S. Y., & Kim, M. G. (2015). Biosynthesis, physiology, and functions of hydroxycinnamic acid amides in plants. *Plant Biotechnology Reports*, 9(5), 269-278.

Manchester, L. C., Coto-Montes, A., Boga, J. A., Andersen, L. P. H., Zhou, Z., Galano, A., ... & Reiter, R. J. (2015). Melatonin: an ancient molecule that makes oxygen metabolically tolerable. *Journal of pineal research*, 59(4), 403-419.

Martínez-Esteso, M. J., Martínez-Márquez, A., Sellés-Marchart, S., Morante-Carriel, J. A., & Bru-Martínez, R. (2015). The role of proteomics in progressing insights into plant secondary metabolism. *Frontiers in plant science*, 6, 504.

McKenna, D. J. (1998). Ayahuasca: An ethnopharmacologic history.

Mérillon, J. M., Doireau, P., Guillot, A., Chénieux, J. C., & Rideau, M. (1986). Indole alkaloid accumulation and tryptophan decarboxylase activity in *Catharanthus roseus* cells cultured in three different media. *Plant cell reports*, 5(1), 23-26.

Mizoguchi, H., Oikawa, H., & Oguri, H. (2014). Biogenetically inspired synthesis and skeletal diversification of indole alkaloids. *Nature chemistry*, 6(1), 57.

Mohammad-Zadeh, L. F., Moses, L., & Gwaltney-Brant, S. M. (2008). Serotonin: a review. *Journal of veterinary pharmacology and therapeutics*, 31(3), 187-199.

Mohite, B. (2013). Isolation and characterization of indole acetic acid (IAA) producing bacteria from rhizospheric soil and its effect on plant growth. *Journal of soil science and plant nutrition*, 13(3), 638-649.

Møller, B. L. (2010). Dynamic metabolons. *Science*, 330(6009), 1328-1329.

Moore, B. D., Andrew, R. L., Külheim, C., & Foley, W. J. (2014). Explaining intraspecific diversity in plant secondary metabolites in an ecological context. *New Phytologist*, 201(3), 733-750.

Mujib, A., Ilah, A., Aslam, J., Fatima, S., Siddiqui, Z. H., & Maqsood, M. (2012). *Catharanthus roseus* alkaloids: application of biotechnology for improving yield. *Plant growth regulation*, 68(2), 111-127.

Mukherjee, S., David, A., Yadav, S., Baluška, F., & Bhatla, S. C. (2014). Salt stress-induced seedling growth inhibition coincides with differential distribution of serotonin and melatonin in sunflower seedling roots and cotyledons. *Physiologia plantarum*, 152(4), 714-728.

Mukherjee, S. (2018). Novel perspectives on the molecular crosstalk mechanisms of serotonin and melatonin in plants. *Plant Physiology and Biochemistry*, 132, 33-45.

Muller, P. Y., Janovjak, H., Miserez, A. R., & Dobbie, Z. (2002). Short technical report processing of gene expression data generated by quantitative real-time RT-PCR. *Biotechniques*, 32(6), 1372-1379.

Murch, S. J., Simmons, C. B., & Saxena, P. K. (1997). Melatonin in feverfew and other medicinal plants. *The Lancet*, 350(9091), 1598-1599.

Murch, S. J., KrishnaRaj, S., & Saxena, P. K. (2000). Tryptophan is a precursor for melatonin and serotonin biosynthesis in in vitro regenerated St. John's wort (*Hypericum perforatum* L. cv. Anthos) plants. *Plant Cell Reports*, 19(7), 698-704.

Murch, S. J., Campbell, S. S., & Saxena, P. K. (2001). The role of serotonin and melatonin in plant morphogenesis: regulation of auxin-induced root organogenesis in in vitro-cultured explants of St. John's wort (*Hypericum perforatu*m L.). In Vitro Cellular & Developmental Biology-Plant, 37(6), 786-793.

Murch, S. J., Alan, A. R., Cao, J., & Saxena, P. K. (2009). Melatonin and serotonin in flowers and fruits of *Datura metel* L. *Journal of Pineal Research*, 47(3), 277-283.

Murch, S. J., Hall, B. A., Le, C. H., & Saxena, P. K. (2010). Changes in the levels of indoleamine phytochemicals during véraison and ripening of wine grapes. *Journal of pineal research*, 49(1), 95-100.

Muszyńska, B., Sułkowska-Ziaja, K., & Ekiert, H. (2011). Indole compounds in fruiting bodies of some edible Basidiomycota species. *Food Chemistry*, 125(4), 1306-1308.

Nakazawa, H., Kumagai, H., & Yamada, H. (1974). Constitutive aromatic L-amino acid decarboxylase from *Micrococcus percitreus*. *Biochemical and biophysical research communications*, 61(1), 75-82.

Nascimento, N. C., & Fett-Neto, A. G. (2010). Plant secondary metabolism and challenges in modifying its operation: an overview. In Plant Secondary Metabolism Engineering (pp. 1-13). Humana Press, Totowa, NJ.

Nawaz, M. A., Huang, Y., Bie, Z., Ahmed, W., Reiter, R. J., Niu, M., & Hameed, S. (2016). Melatonin: current status and future perspectives in plant science. *Frontiers in plant science*, 6, 1230.

Negi, A., Singla, R., & Singh, V. (2014). Indole based alkaloid in cancer: an overview. PharmaTutor, 2(1), 76-82.

Noda, S., Shirai, T., Mochida, K., Matsuda, F., Oyama, S., Okamoto, M., & Kondo, A. (2015). Evaluation of *Brachypodium distachyon* L-tyrosine decarboxylase using L-tyrosine over-producing Saccharomyces cerevisiae. *PloS one*, 10(5), e0125488.

Nordström, A., O'Maille, G., Qin, C., & Siuzdak, G. (2006). Nonlinear data alignment for UPLC− MS and HPLC− MS based metabolomics: quantitative analysis of endogenous and exogenous metabolites in human serum. *Analytical chemistry*, 78(10), 3289-3295.

Novello, C. R., Marques, L. C., Pires, M. E., Kutschenco, A. P., Nakamura, C. V., Nocchi, S., ... & Mello, J. C. (2016). Bioactive indole alkaloids from *Croton echioides*. *Journal of the Brazilian Chemical Society*, 27(12), 2203-2209.

O'Connor, S. E., & Maresh, J. J. (2006). Chemistry and biology of monoterpene indole alkaloid biosynthesis. *Natural product reports*, 23(4), 532-547.

Oksman-Caldentey, K. M., Inzé, D., & Orešič, M. (2004). Connecting genes to metabolites by a systems biology approach. *Proceedings of the National Academy of Sciences*, 101(27), 9949-9950.

Oliver, S. G., Winson, M. K., Kell, D. B., & Baganz, F. (1998). Systematic functional analysis of the yeast genome. *Trends in biotechnology*, 16(9), 373-378.

Olivier, B. (2015). Serotonin: a never-ending story. *European journal of pharmacology*, 753, 2-18.

Olmedo, G. M., Cerioni, L., González, M. M., Cabrerizo, F. M., Rapisarda, V. A., & Volentini, S. I. (2017). Antifungal activity of β-carbolines on *Penicillium digitatum* and *Botrytis cinerea*. *Food microbiology*, 62, 9-14.

Ouwerkerk, P. B. F., Trimborn, T. O., Hilliou, F., & Memelink, J. (1999). Nuclear factors GT-1 and 3AF1 interact with multiple sequences within the promoter of the Tdc gene from Madagascar periwinkle: GT-1 is involved in UV light-induced expression. *Molecular and General Genetics*, 261(4-5), 610-622.

Pan, Q., Mustafa, N. R., Tang, K., Choi, Y. H., & Verpoorte, R. (2016_a). Monoterpenoid indole alkaloids biosynthesis and its regulation in *Catharanthus roseus*: a literature review from genes to metabolites. *Phytochemistry reviews*, 15(2), 221-250.

Pan, C., Ye, L., Qin, L., Liu, X., He, Y., Wang, J., ... & Lu, G. (2016_b). CRISPR/Cas9-mediated efficient and heritable targeted mutagenesis in tomato plants in the first and later generations. *Scientific reports*, 6, 24765.

Pang, X., Wei, Y., Cheng, Y., Pan, L., Ye, Q., Wang, R., ... & Yang, Y. (2018). The Tryptophan Decarboxylase in *Solanum lycopersicum*. *Molecules*, 23(5), 998.

Park, M., Kang, K., Park, S., Kim, Y. S., Ha, S. H., Lee, S. W., ... & Back, K. (2008). Expression of serotonin derivative synthetic genes on a single self-processing polypeptide and the production of serotonin derivatives in microbes. *Applied microbiology and biotechnology*, 81(1), 43-49.

Park, S., Kang, K., Lee, K., Choi, D., Kim, Y. S., & Back, K. (2009). Induction of serotonin biosynthesis is uncoupled from the coordinated induction of tryptophan biosynthesis in pepper fruits (*Capsicum annuum*) upon pathogen infection. *Planta*, 230(6), 1197.

Park, S., Lee, K., Kim, Y. S., Chi, Y. T., Shin, J. S., & Back, K. (2012). Induced tyramine overproduction in transgenic rice plants expressing a rice tyrosine decarboxylase under the control of methanol-inducible rice tryptophan decarboxylase promoter. *Bioprocess and biosystems engineering*, 35(1-2), 205-210.

Pasquali, G., Porto, D. D., & Fett-Neto, A. G. (2006). Metabolic engineering of cell cultures versus whole plant complexity in production of bioactive monoterpene indole alkaloids: recent progress related to old dilemma. *Journal of Bioscience and Bioengineering*, 101(4), 287-296.

Pelagio-Flores, R., Ortíz-Castro, R., Méndez-Bravo, A., Macías-Rodríguez, L., & López-Bucio, J. (2011). Serotonin, a tryptophan-derived signal conserved in plants and animals, regulates root system architecture probably acting as a natural auxin inhibitor in *Arabidopsis thaliana*. *Plant and Cell Physiology*, 52(3), 490-508.

Pelagio-Flores, R., López-Bucio, J. S., & López-Bucio, J. (2018). 6 Serotonin and Melatonin. Neurotransmitters in Plants: Perspectives and Applications, 103.

Perley, J. E., & Stowe, B. B. (1966). The production of tryptamine from tryptophan by Bacillus cereus (KVT). *Biochemical Journal*, 100(1), 169.

Petersson, S. V., Johansson, A. I., Kowalczyk, M., Makoveychuk, A., Wang, J. Y., Moritz, T., ... & Ljung, K. (2009). An auxin gradient and maximum in the *Arabidopsis* root apex shown by high-resolution cell-specific analysis of IAA distribution and synthesis. *The Plant Cell*, 21(6), 1659-1668.

Pichersky, E., & Lewinsohn, E. (2011). Convergent evolution in plant specialized metabolism. *Annual review of plant biology*, 62, 549-566.

Piechowska, P., Zawirska-Wojtasiak, R., & Mildner-Szkudlarz, S. (2019). Bioactive β-Carbolines in Food: A Review. *Nutrients*, 11(4), 814.

Poulsen, C., Goddijn, O. J., Hoge, J. H. C., & Verpoorte, R. (1994). Anthranilate synthase and chorismate mutase activities in transgenic tobacco plants overexpressing tryptophan decarboxylase from *Catharanthus roseus*. *Transgenic research*, 3(1), 43-49.

Quittenden, L. J., Davies, N. W., Smith, J. A., Molesworth, P. P., Tivendale, N. D., & Ross, J. J. (2009). Auxin biosynthesis in pea: characterization of the tryptamine pathway. *Plant Physiology*, 151(3), 1130-1138.

Rai, A., Saito, K., & Yamazaki, M. (2017). Integrated omics analysis of specialized metabolism in medicinal plants. *The Plant Journal*, 90(4), 764-787.

Ramakrishna, A., Giridhar, P., & Ravishankar, G. A. (2011). Phytoserotonin: a review. *Plant signaling & behavior*, 6(6), 800.

Ramakrishna, A., Giridhar, P., Sankar, K. U., & Ravishankar, G. A. (2012). Melatonin and serotonin profiles in beans of *Coffea* species. *Journal of pineal research*, 52(4), 470-476.

Ramakrishna, A., Gill, S. S., Sharma, K. K., Tuteja, N., & Ravishankar, G. A. (2016). Indoleamines (Serotonin and Melatonin) and Calcium-Mediated Signaling in Plants. In Serotonin and Melatonin (pp. 107-118). CRC Press.

Ran, X., Zhao, F., Wang, Y., Liu, J., Zhuang, Y., Ye, L., ... & Zhang, Y. (2019). Plant Regulomics: a data-driven interface for retrieving upstream regulators from plant multi-omics data. *The Plant Journal*.

Ravishankar, G. A., & Ramakrishna, A. (Eds.). (2016). Serotonin and Melatonin: Their Functional Role in Plants, Food, Phytomedicine, and Human Health. CRC Press.

Rayne, S. (2010). Concentrations and profiles of melatonin and serotonin in fruits and vegetables during ripening: a mini-review.

Reem, N. T., & Van Eck, J. (2019). Application of CRISPR/Cas9-mediated gene editing in tomato. In Plant Genome Editing with CRISPR Systems (pp. 171-182). Humana Press, New York, NY.

Reiter, R. J., Tan, D. X., & Fuentes-Broto, L. (2010). Melatonin: a multitasking molecule. In Progress in brain research (Vol. 181, pp. 127-151). Elsevier.

Rensing, S. A. (2018). Great moments in evolution: the conquest of land by plants. *Current opinion in plant biology*, 42, 49-54.

Rodrigues, D. A., & Casal, S. (2019). β-Carbolines. In Coffee (pp. 697-704).

Roshchina, V. V. (2010). Evolutionary considerations of neurotransmitters in microbial, plant, and animal cells. In Microbial endocrinology (pp. 17-52). Springer, New York, NY.

Sáenz-de-Miera, L. E., & Ayala, F. J. (2004). Complex evolution of orthologous and paralogous decarboxylase genes. *Journal of evolutionary biology*, 17(1), 55-66.

Sakamura, S., Terayama, Y., Kawakatsu, S., Ichihara, A., & Saito, H. (1978). Conjugated serotonins related to cathartic activity in safflower seeds (Carthamus tinctorius L.). *Agricultural and Biological Chemistry*, 42(9), 1805-1806.

Sakarkar, D. M., & Deshmukh, V. N. (2011). Ethnopharmacological review of traditional medicinal plants for anticancer activity. Int J Pharm Tech Res, 3(1), 298-308.

Sandmeier, E., Hale, T. I., & Christen, P. (1994). Multiple evolutionary origin of pyridoxal-5'-phosphate-dependent amino acid decarboxylases. *European journal of biochemistry*, 221(3), 997-1002.

Sarrion-Perdigones, A., Falconi, E. E., Zandalinas, S. I., Juárez, P., Fernández-del-Carmen, A., Granell, A., & Orzaez, D. (2011). GoldenBraid: an iterative cloning system for standardized assembly of reusable genetic modules. *PloS one*, 6(7), e21622.

Sarrion-Perdigones, A., Vazquez-Vilar, M., Palací, J., Castelijns, B., Forment, J., Ziarsolo, P., ... & Orzaez, D. (2013). GoldenBraid 2.0: a comprehensive DNA assembly framework for plant synthetic biology. *Plant physiology*, 162(3), 1618-1631.

Schwab, W. (2003). Metabolome diversity: too few genes, too many metabolites?. *Phytochemistry*, 62(6), 837-849.

Servillo, L., Giovane, A., Balestrieri, M. L., Cautela, D., & Castaldo, D. (2012). N-Methylated tryptamine derivatives in *Citrus* genus plants: identification of N, N, N-trimethyltryptamine in bergamot. Journal of agricultural and food chemistry, 60(37), 9512-9518.

Servillo, L., Giovane, A., Balestrieri, M. L., Casale, R., Cautela, D., & Castaldo, D. (2013). *Citrus* genus plants contain N-methylated tryptamine derivatives and their 5-hydroxylated forms. *Journal of agricultural and food chemistry*, 61(21), 5156-5162.

Servillo, L., Giovane, A., Casale, R., D'Onofrio, N., Ferrari, G., Cautela, D., ... & Castaldo, D. (2015). Serotonin 5-O-β-glucoside and its N-methylated forms in Citrus genus plants. *Journal of agricultural and food chemistry*, 63(16), 4220-4227.

Servillo, L., Giovane, A., Casale, R., Cautela, D., D'Onofrio, N., Balestrieri, M. L., & Castaldo, D. (2016). Glucosylated forms of serotonin and tryptophan in green coffee beans. *LWT*, 73, 117-122.

Sharma, A., Verma, P., Mathur, A., & Mathur, A. K. (2018). Overexpression of tryptophan decarboxylase and strictosidine synthase enhanced terpenoid indole alkaloid pathway activity and antineoplastic vinblastine biosynthesis in *Catharanthus roseus*. *Protoplasma*, 255(5), 1281-1294.

Sirek, A., & Sirek, O. V. (1970). Serotonin: a review. Canadian Medical Association Journal, 102(8), 846.

Songstad, D. D., De Luca, V., Brisson, N., Kurz, W. G., & Nessler, C. L. (1990). High levels of tryptamine accumulation in transgenic tobacco expressing tryptophan decarboxylase*. Plant physiology*, 94(3), 1410-1413.

Spiering, M. J., Urban, L. A., Nuss, D. L., Gopalan, V., Stoltzfus, A., & Eisenstein, E. (2011). Gene identification in black cohosh (*Actaea racemosa* L.): expressed sequence tag profiling and genetic screening yields candidate genes for production of bioactive secondary metabolites. *Plant cell reports*, 30(4), 613-629.

Sprenger, J., Hardeland, R., Fuhrberg, B., & Han, S. Z. (1999). Melatonin and other 5-methoxylated indoles in yeast: presence in high concentrations and dependence on tryptophan availability. *Cytologia*, 64(2), 209-213.

Stowe, B. B. (1959). Occurrence and metabolism of simple indoles in plants. *Progress in the Chemistry of Organic Natural Products* (pp. 248-297). Springer, Vienna.

Takahashi, T., & Miyazawa, M. (2012). Synthesis and structure–activity relationships of serotonin derivatives effect on α-glucosidase inhibition. *Medicinal Chemistry Research*, 21(8), 1762-1770.

Tan, D. X., Hardeland, R., Manchester, L. C., Korkmaz, A., Ma, S., Rosales-Corral, S., & Reiter, R. J. (2011). Functional roles of melatonin in plants, and perspectives in nutritional and agricultural science. *Journal of experimental botany*, 63(2), 577-597.

Tan, D. X., Zheng, X., Kong, J., Manchester, L. C., Hardeland, R., Kim, S. J., ... & Reiter, R. J. (2014). Fundamental issues related to the origin of melatonin and melatonin isomers during evolution: relation to their biological functions. *International Journal of Molecular Sciences*, 15(9), 15858-15890.

Theis, N., & Lerdau, M. (2003). The evolution of function in plant secondary metabolites. *International Journal of Plant Sciences*, 164(S3), S93-S102.

Thomas J.C., Adams D.G., Nessler C.L., Brown J.K. and Bohnert H.J. 1995. Tryptophan decarboxylase, tryptamine and reproduction of the whitefly (*Bemisia tabaci*). *Plant Physiology,* 109: 717–720.

Thomas, J. C., Saleh, E. F., Alammar, N., & Akroush, A. M. (1998). The indole alkaloid tryptamine impairs reproduction in *Drosophila melanogaster*. *Journal of economic entomology*, 91(4), 841-846.

Thomas, J. C., Akroush, A. M., & Adamus, G. (1999). The indole alkaloid tryptamine produced in transgenic *Petunia hybrida*. *Plant Physiology and Biochemistry*, 37(9), 665-670.

Tivendale, N. D., Davies, N. W., Molesworth, P. P., Davidson, S. E., Smith, J. A., Lowe, E. K., ... & Ross, J. J. (2010). Reassessing the role of N-hydroxytryptamine in auxin biosynthesis. *Plant physiology*, 154(4), 1957-1965.

Tivendale, N. D., Ross, J. J., & Cohen, J. D. (2014). The shifting paradigms of auxin biosynthesis. *Trends in plant science*, 19(1), 44-51.

Tomato Genome Consortium. (2012). The tomato genome sequence provides insights into fleshy fruit evolution. *Nature*, 485(7400), 635.

Torrens-Spence, M. P., Liu, P., Ding, H., Harich, K., Gillaspy, G., & Li, J. (2013). Biochemical evaluation of the decarboxylation and decarboxylation-deamination activities of plant aromatic amino acid decarboxylases. *Journal of Biological Chemistry*, 288(4), 2376-2387.

Torrens-Spence, M. P., Lazear, M., von Guggenberg, R., Ding, H., & Li, J. (2014). Investigation of a substrate-specifying residue within *Papaver somniferum* and *Catharanthus roseus* aromatic amino acid decarboxylases. *Phytochemistry*, 106, 37-43.

Torrens-Spence, M. P., Chiang, Y. C., Smith, T., Vicent, M. A., Wang, Y., & Weng, J. K. (2018). Structural basis for independent origins of new catalytic machineries in plant AAAD proteins. *bioRxiv*, 404970.

Ueno, M., Shibata, H., Kihara, J., Honda, Y., & Arase, S. (2003). Increased tryptophan decarboxylase and monoamine oxidase activities induce Sekiguchi lesion formation in rice infected with *Magnaporthe grisea*. *The Plant Journal*, 36(2), 215-228.

Udenfriend, S., Lovenberg, W., & Sjoerdsma, A. (1959). Physiologically active amines in common fruits and vegetables. *Archives of Biochemistry and Biophysics*, 85(2), 487-490.

Vazquez-Vilar, M., Bernabé-Orts, J. M., Fernandez-del-Carmen, A., Ziarsolo, P., Blanca, J., Granell, A., & Orzaez, D. (2016). A modular toolbox for gRNA–Cas9 genome engineering in plants based on the GoldenBraid standard. *Plant Methods*, 12(1), 10.

Veenstra-VanderWeele, J., Anderson, G. M., & Cook Jr, E. H. (2000). Pharmacogenetics and the serotonin system: initial studies and future directions. *European journal of pharmacology*, 410(2-3), 165-181.

Wang, X. J., Ren, J. L., Zhang, A. H., Sun, H., Yan, G. L., Han, Y., & Liu, L. (2019_a). Novel applications of mass spectrometry-based metabolomics in herbal medicines and its active ingredients: Current evidence. *Mass spectrometry reviews*.

Wang, T., Zhang, H., & Zhu, H. (2019_b). CRISPR technology is revolutionizing the improvement of tomato and other fruit crops. *Horticulture research*, 6(1), 1-13.

Weng, J. K., Philippe, R. N., & Noel, J. P. (2012). The rise of chemodiversity in plants. *Science*, 336(6089), 1667-1670.

West, G. B. (1959). Tryptamines in tomatoes. *The Journal of pharmacy and pharmacology*, 11(5), 319-320.

West, C. A. (1960). Gibberellins as native plant growth regulators. *Annual Review of Plant Physiology*, 11(1), 411-436.

White, E. P. (1944). Part XIII. Isolation of Tryptamine from some *Acacia* species. *New Zealand Journal of Science and Technology*, 25, 157-162.

Whitmer, S., van der Heijden, R., & Verpoorte, R. (2002). Effect of precursor feeding on alkaloid accumulation by a tryptophan decarboxylase over-expressing transgenic cell line T22 of *Catharanthus roseus*. *Journal of biotechnology*, 96(2), 193-203.

Williams, B. B., Van Benschoten, A. H., Cimermancic, P., Donia, M. S., Zimmermann, M., Taketani, M., ... & Fischbach, M. A. (2014). Discovery and characterization of gut microbiota decarboxylases that can produce the neurotransmitter tryptamine. *Cell host & microbe*, 16(4), 495-503.

Wink, M. (2003). Evolution of secondary metabolites from an ecological and molecular phylogenetic perspective. *Phytochemistry*, 64(1), 3-19.

Wink MWink M (1999) Introduction: biochemistry, role and biotechnology of secondary products. In Biochemistry of Secondary Product Metabolism. ed Wink M (CRC Press, Boca Raton, FL), pp 1–16.

Wink, M. (2010). Introduction: biochemistry, physiology and ecological functions of secondary metabolites. *Annual plant reviews volume 40: Biochemistry of plant secondary metabolism*, 1-19.

Wise, A. A., Liu, Z., & Binns, A. N. (2006). Three methods for the introduction of foreign DNA into *Agrobacterium*. In *Agrobacterium* protocols (pp. 43-54). Humana Press.

Yadav, C. B., Pandey, G., Muthamilarasan, M., & Prasad, M. (2018). Epigenetics and epigenomics of plants. *Plant Genetics and Molecular Biology* (pp. 237-261). Springer, Cham.

Yamazaki, Y., Sudo, H., Yamazaki, M., Aimi, N., & Saito, K. (2003). Camptothecin biosynthetic genes in hairy roots of *Ophiorrhiza pumila*: cloning, characterization and differential expression in tissues and by stress compounds. *Plant and Cell Physiology*, 44(4), 395-403.

Yao, K., De Luca, V., & Brisson, N. (1995). Creation of a metabolic sink for tryptophan alters the phenylpropanoid pathway and the susceptibility of potato to *Phytophthora infestans*. *The Plant Cell*, 7(11), 1787-1799

Yin, J., Li, G., Ren, X., & Herrler, G. (2007). Select what you need: a comparative evaluation of the advantages and limitations of frequently used expression systems for foreign genes. *Journal of biotechnology*, 127(3), 335-347.

Yonekura-Sakakibara, K., & Saito, K. (2009). Functional genomics for plant natural product biosynthesis. *Natural product reports*, 26(11), 1466-1487.

Zhang, J. (2003). Evolution by gene duplication: an update. *Trends in ecology & evolution*, 18(6), 292-298.

Zhang, J. X., Ma, L. Q., Yu, H. S., Zhang, H., Wang, H. T., Qin, Y. F., ... & Wang, Y. N. (2011). A tyrosine decarboxylase catalyzes the initial reaction of the salidroside biosynthesis pathway in *Rhodiola sachalinensis*. *Plant cell reports*, 30(8), 1443-1453.

Zhao, Y. (2018). Essential roles of local auxin biosynthesis in plant development and in adaptation to environmental changes. *Annual review of plant biology*, 69, 417-435.

Zhao, D., Wang, R., Liu, D., Wu, Y., Sun, J., & Tao, J. (2018). Melatonin and expression of tryptophan decarboxylase Gene (TDC) in Herbaceous Peony (*Paeonia lactiflora* Pall.) Flowers. *Molecules*, 23(5), 1164.

Zhu, T., & Niu, D. K. (2013). Frequency of intron loss correlates with processed pseudogene abundance: a novel strategy to test the reverse transcriptase model of intron loss. *BMC biology*, 11(1), 23.

Zhu, J., Wang, M., Wen, W., & Yu, R. (2015). Biosynthesis and regulation of terpenoid indole alkaloids in Catharanthus roseus. *Pharmacognosy reviews*, 9(17), 24.

Appendice

Products of the research

Oral communications presented at international congresses

- "From kiwifruit to tomato: Looking for a biological role of fruit serotonin" presented at the "Winter School in Plant Biotechnology & Environmental sustainability" that was held in Canazei (Trento, Italy) on January 15-20, 2017
  Authors: *Stefano Negri, Mauro Commisso, Linda Avesani, Flavia Guzzo*
- "The tomato serotonin pathway: in search of biological roles for fruit indolamines" presented at the "XVI Solanaceae conference (SOL 2019) - Yield and nutrition" that was held in Jerusalem (Israel) on September 15-19, 2019
  Authors: *Stefano Negri, Mauro Commisso, Elisa Gecchele, Massimiliano Perduca, Julien Pirrello, Linda Avesani, Flavia Guzzo*

Posters presented at international congresses

- "Plant tryptamine and serotonin: in search of their biological role in the fruit" presented at the "113th Congress of the Società Botanica Italiana Onlus" that was held in Fisciano (Salerno, Italy) on September 12-15, 2018, Fisciano (SA)
  Authors: *Stefano Negri, Mauro Commisso, Matilde Merlin, Elisa Gecchele, Massimiliano Perduca, Sara Zenoni, Linda Avesani, Flavia Guzzo*
  This poster was honoured with the "Best poster award" by Aboca.
- "The tomato serotonin pathway: in search of biological roles for fruit indolamines" presented at the "63rd Congress of the Italian Society of Agricultural Genetics" that was held in Napoli (Italy) on September 10-13, 2019
  Authors: *Stefano Negri, Mauro Commisso, Matilde Merlin, Elisa Gecchele, Massimiliano Perduca, Nicola Vitulo, Sara Zenoni, Julien Pirrello, Linda Avesani, Flavia Guzzo*

All authors are currently affiliated to the Department of Biotechnology of the University of Verona except for Prof. Pirrello (Institut National Polytechnique/INRA of Toulouse, France) and Dr. Merlin (Demethra Biotech, Camisano Vicentino).

Publications in the pipeline

- The content of Chapter 1 reporting the state of the art on plant indolamines research is currently being used to write a review article discussing the biosynthesis and the roles of tryptamine and of its direct offspring, serotonin, in plants.
- The content of Chapter 2 and Chapter 3 is currently being used as a draft for a research article that will present the tomato serotonin pathway together with accumulation data of tryptamine and serotonin and the expression of their biosynthetic genes in this model plant. Information about promoter analysis and co-expression data related to these genes will also be added.
- The content of Chapter 4 together with further experimental evidences related to the metabolic engineering of all the *SlTDC* genes and of *SlT5H*, which is currently an ongoing project, will be the object of a future publication.

Authors contributions

Major contributing authors:

Dr. Mauro Commisso – Supervisor of transient expression experiments and *SlTDCs*/*SlT5H* functional characterization (Chapter 2)

Dr. Elisa Gecchele – Supervisor of expression analysis experiments (Chapter 3)

Prof. Linda Avesani – Supervisor of molecular biology techniques and metabolic engineering strategies

Prof. Flavia Guzzo – PhD tutor and supervisor of the metabolomics analyses

Side contributing authors:

Dr. Matilde Merlin – Advisor in CRISPR/Cas9 experimental design (Chapter 4)

Prof. Julien Pirrello – Advisor in Micro-Tom genetic transformation and regeneration (Chapter 4)

Prof. Massimiliano Perduca – Supervisor of *SlTDCs* heterlogous expression in *Escherichia coli* and enzyme structure elucidation (not carried out by the Phd candidate and not shown in this thesis)

Prof Nicola Vitulo and Prof. Sara Zenoni – Advisors in *SlTDCs*/*SlT5H* promoter analysis and gene co-expression analysis (partially carried out by the Phd candidate but not shown in this thesis)

Acknowledgements

My greatest gratitude goes to Prof. Flavia Guzzo who supervised this PhD thesis and, since the beginning of my working experience in her research group, through her deep inspiring and fascinating vision of the plant world, raised in me a great interest and passion towards the botanical sciences, finally convincing me to undertake this PhD project. Her precious scientific advice has been crucial to the success of this work.

I express sincere and special thanks to Dr. Mauro Commisso for his constant presence and help in solving critical points in this PhD work and for his active participation in both gene functional characterization and metabolomics experiments.

My heartfel special thanks go to Dr. Linda Avesani, Dr. Matilde Merlin and Stefania Ceoldo whose scientific recommendations have been an essential support in the exploitation of metabolic engineering techniques and *in-vitro* plant cultures, as well as their never-missing encouragements during the writing of this thesis.

I am very grateful to Prof. Mondher Bouzayen, Prof. Julien Pirrello and Lydie Tessarotto for hosting me in their laboratory at the Institut National Polytechnique/INRA of Toulouse (France) and for supervising the generation of the transgenic tomato lines used in this project.

Finally, I would thank all the people which whom I share very special connections in my everyday life and my parents, above all, for their never-ending trust in me.